

**PROBABILISTIC ANALYSIS OF DIVERTOR PLATE  
LIFETIME IN TOKAMAK REACTORS**

by

**Ruxandra Paula Golinescu**

S.M., Polytechnic Institute of Bucharest, Romania (1988)

Submitted to the Department of Nuclear Engineering  
in partial fulfillment of the requirements for the degree of

Master of Science


at the

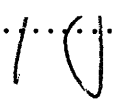
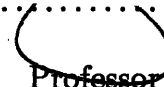
**MASSACHUSETTS INSTITUTE OF TECHNOLOGY**

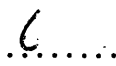
January 1994

© 1994 Ruxandra Paula Golinescu  
All rights reserved

The author hereby grants to Massachusetts Institute of Technology permission to  
reproduce and  
to distribute copies of this thesis document in whole or in part.

Signature of Author.....  
Department of Nuclear Engineering  
January 14, 1994

Certified by..........  
Mujid S. Kazimi  
Professor of Nuclear Engineering  
Thesis Advisor

Accepted by..........  
Allan F. Henry  
Chairman, Department Committee on Graduate Students

MASSACHUSETTS INSTITUTE  
OF TECHNOLOGY

Science

**JUN 30 1994**

# PROBABILISTIC ANALYSIS OF DIVERTOR PLATE LIFETIME IN TOKAMAK REACTORS

by

Ruxandra Paula Golinescu

Submitted to the Department of Nuclear Engineering  
on January 14, 1994, in partial fulfillment of the  
requirements for the degree of  
Master of Science

## Abstract

Probabilistic methods have been successfully used to analyze the risk associated with different existing nuclear power plant designs. Such tools can be also used at earlier stages in the design process. Defining a methodology for generation of the probabilistic lifetime reliability for a specific tokamak in-vessel component, the divertor, is the objective of this thesis. The divertor plates establish an interface between the plasma and the material surface of the tokamak device. The design of the divertor cooling system is a most demanding task since it endures the largest power density during operation. Even more severe consequences would appear under some transient conditions.

In the present analysis, the divertor conditions for the technology phase of operation of the International Thermonuclear Experimental Reactor (ITER) as specified at the conceptual design stage are used as the reference design. The methodology developed to analyze the ITER divertor reliability consists of the following steps:

1. description of normal operating conditions;
2. thermal-hydraulic analysis for normal operation;
3. identification and classification of transient events;
4. estimation of frequency of occurrence of transient events;
5. thermal analysis for transient event conditions;
6. defining the failure modes / failure criteria models;
7. assessment and propagation of uncertainties;
8. evaluation of the probability of avoiding failure of the divertor plate.

The transient events considered in this work are grouped in two categories as follows:

- transients that do not affect the divertor temperature distribution prior to shutdown, such as: auxiliary heating system disturbances, magnet system disturbances, main coolant disturbances, balance of plant disturbances, internal plasma disturbances;

- transients that affect the divertor temperature distribution prior to shutdown, such as those on the coolant side: Loss of Coolant Accident (LOCA), Loss of Flow Accident (LOFA), and Loss of Heat Sink (LHS), and overpower (OP) transient on the plasma side.

In applying this methodology, one failure mode is assumed to be the predominant failure mode: that of surface material loss due to sputtering, melting and evaporation. Taking no credit for redeposition of that material partially balances the fact that other failure modes are not accounted for.

The heat conduction computer code HEATING 7.2 is used for the steady-state and transient thermohydraulic analyses as well as for estimating the material loss during transients. The development of a reliability function requires defining a probability distribution function for the material loss during transients. A second order response surface (Response Surface Methodology) is derived for the material loss as a function of the uncertain parameters. The uncertainties of the frequency of occurrence of transients and material loss parameters are propagated through the reliability function by a Monte Carlo simulation.

Using the limited data available leads to the conclusion that there is a high probability that the divertor plate (tungsten surface but niobium based structure) will reliably withstand a peak heat flux of  $11 \text{ MW/m}^2$ . However, transient events will lead to a much shorter lifetime than desirable for the divertor plates, mainly due to the severe effects of plasma disruptions assumed. Though, improved characterization of the disruption conditions, and enlarged scope of failure mode consideration should be pursued to gain confidence in the conclusions.

Thesis Advisor: Mujid S. Kazimi

Title: Professor of Nuclear Engineering

## **Acknowledgements**

My deepest appreciation is given to my thesis supervisor, Professor Mujid S. Kazimi. Without his instruction and scientific advising, this work would not have been possible. I wish to express my gratitude to Professor John Meyer and to my colleagues in the fusion group, Boris Lekakh, Mitch Crosswait, and Tony Hechanova, for their interest and suggestions during our meetings. Thanks are also due to my husband, Nick, for his ever-present support and understanding, to my parents for their steady love and help, and, last but not least, to my friend Florinel Morosan for his invaluable advise and encouragement.

# Contents

<b>1</b>	<b>Introduction</b>	<b>9</b>
1.1	Objective . . . . .	9
1.2	Background . . . . .	10
1.3	Scope . . . . .	11
<b>2</b>	<b>Method of Reliability Estimate</b>	<b>13</b>
2.1	Introduction . . . . .	13
2.2	Description of normal operating conditions and divertor design . . . . .	15
2.3	Identification and Classification of the Transient Events . . . . .	15
2.4	Identification of Failure Modes . . . . .	18
2.5	Steps Required to Assess Reliability . . . . .	19
2.5.1	Thermal Analysis . . . . .	19
2.5.2	Assessment of Uncertainties . . . . .	20
2.5.3	Generation of Reliability Curves . . . . .	20
<b>3</b>	<b>Description of Reference Design</b>	<b>23</b>
3.1	Divertor Plate Design and Normal Operation Conditions . . . . .	23
3.2	Material Properties . . . . .	28
3.3	Divertor Cooling Circuit Design . . . . .	31
3.4	Steady-State Thermohydraulic Analysis . . . . .	31
<b>4</b>	<b>Effects of Transients and Associated Uncertainties</b>	<b>39</b>
4.1	Identification of transients and their frequencies of occurrence . . . . .	39

4.1.1	Category 1 Transients . . . . .	40
4.1.2	Category 2 Transients . . . . .	41
4.2	Thermal Analysis of the Transients . . . . .	48
4.3	Uncertainties in the Frequencies of Occurrence of Transients . . . . .	51
4.3.1	Category 1 Transients . . . . .	51
4.3.2	Category 2 Transients . . . . .	53
4.3.3	Catastrophic and non-catastrophic transients . . . . .	53
4.4	Parameters affecting Material Loss . . . . .	55
4.4.1	Uncertainties in the parameters affecting the material loss . . . . .	56
4.4.2	Uncertainty of the Material Loss . . . . .	57
<b>5</b>	<b>Generation of Reliability Function</b>	<b>63</b>
5.1	Development of a stochastic reliability function . . . . .	63
5.2	Propagation of Uncertainties . . . . .	67
<b>6</b>	<b>Summary, Conclusions and Recommendations for Future Work</b>	<b>73</b>
6.1	Summary . . . . .	73
6.2	Recommendations . . . . .	74
6.2.1	Extension to other failure modes . . . . .	74
6.2.2	Improvement in the limiting rules . . . . .	74
6.2.3	Providing the appropriate model geometry selection . . . . .	74
6.2.4	Modeling of the material losses . . . . .	74
6.2.5	Improving the calculational tools . . . . .	75
<b>A</b>	<b>HEATING 7.2 input file for steady-state problem</b>	<b>76</b>
<b>B</b>	<b>MATHCAD heat transfer coefficient calculations</b>	<b>79</b>
<b>C</b>	<b>HEATING 7.2 input files for problems 2 (LOCA and OP) and 3 (OP); output file for problem 2 (OP)</b>	<b>85</b>
<b>D</b>	<b>MATHCAD calculations of the parameters uncertainties</b>	<b>101</b>

<b>E MATHCAD program for response surface coefficients calculation</b>	<b>107</b>
<b>F MATHCAD program for propagation of the parameters uncertainties through the reliability function</b>	<b>111</b>
<b>G HEATING 7.2 thermal analyses results</b>	<b>113</b>
<b>Bibliography</b>	<b>125</b>

# List of Tables

- 2.1 Categories of Transients considered in this study . . . . . 17
  
- 3.1 Main Operating Conditions for the ITER divertor technology phase [3] . . . . . 27
- 3.2 Properties of divertor plate materials [18-20] . . . . . 30
- 3.3 Major parameters of the primary cooling system of ITER divertor [15] . . . . . 34
  
- 4.1 Mean frequencies of occurrence of category 1 transients [1] . . . . . 40
- 4.2 Mean frequencies of occurrence of category 2 transients . . . . . 41
- 4.3 Mean failure rates of components and mean beata factor [9] . . . . . 46
- 4.4 Estimates of frequencies of occurrence of category 1 transients [1] . . . . . 52
- 4.5 Probability distributions for frequencies of occurrence of category 1 transients . . 52
- 4.6 Component failure rates [9,15] . . . . . 54
- 4.7 Probability distributions for frequencies of occurrence of category 2 transients . . 55
- 4.8 Probability distributions of the frequencies of occurrence for catastrophic and  
non-catastophic transients . . . . . 56
- 4.9 Probability distributions for the parameters affecting the material loss . . . . . 58



# List of Figures

2-1	Methodology for Analyzing IVC Reliability [1]	14
2-2	Propagation of uncertainties	22
3-1	Layout of an ITER cross section, dimensions in millimeters [44]	25
3-2	ITER divertor module [14]	26
3-3	Coolant channel configuration for technology phase divertor [3]	26
3-4	Divertor plate and typical surface heat flux distribution [5]	28
3-5	Divertor materials thermal conductivity [18]	30
3-6	Typical cooling loop configuration for divertor [15]	32
3-7	Primary loop for divertor [15]	33
3-8	Divertor submodule regions as used for the thermal analysis	37
4-1	Fault Tree for Loss of Flow in divertor coolant loop	44
4-2	Knot-points for single quadrant response surface	61
4-3	Knot-points for multi quadrant response surface	61
5-1	(k,n) plane	68
5-2	Divertor reliability versus time	71
5-3	Divertor reliability versus the number of cycles	72

# Chapter 1

## Introduction

### 1.1 Objective

The objective of the present study is to develop a methodology for obtaining a reliability estimate of the International Tokamak Experimental Reactor (ITER) divertor plate. The occurrence of several transient events would have the most important contribution to the expected divertor failure rate. Some of them would cause the temperature in the divertor plate (DP) to rise; if these temperatures get too high, the structural elements in the DP will weaken and subsequently suffer structural failure or even possibly reach the melting temperature. Therefore, quick plasma shutdown is desired in order to protect the reactor from damage. It is generally assumed that the shutdown mechanism response time can be of the order of seconds, and that the shutdown is terminated via a disruption phenomenon, in which the plasma is dumped on the plate in a very short time.

As previous studies [1] reveal, the dominant failure modes are material loss and cumulative cyclic damage, depending on the type of reactor. The current study considers only the material loss as a failure mode. However, once the method of solution is completed for one failure mode, it is easy to integrate other failure modes into the problem.

## 1.2 Background

Fusion reactions between light hydrogen isotopes appear to be an immense energy resource that could offer significant safety and environmental advantages over alternative sources of energy. Although it remains to be seen if fusion can become an attractive energy source, it is important that the safety concerns be included in the early design processes.

Large uncertainties exist in a fusion tokamak reactor conditions regarding several parameters characterizing plasma disruptions or even operating parameters. Furthermore, the occurrence of transients is a random phenomenon in time, and it is not easily included in a deterministic analysis. As a consequence, a probabilistic approach seems to be more suitable for a lifetime analysis of a tokamak in-vessel component.

Reliability is an approach for engineering uncertainty estimate. Whether an item works for a particular period is a question which can be answered as a probability. Therefore, an engineering definition of reliability is: the probability that an item will perform a required function without failure under stated conditions for a stated period of time. Since reliability is a key factor in determining the ultimate success of any fusion facility, substantial effort has been expended to acquire the information needed to assess the reliability of fusion reactor components and systems. Most of the previous efforts do not combine normal operating and transient conditions when calculating the component lifetime. However, reference [1] was the first to provide a framework that allows these conditions to be combined along with their attendant uncertainties, so that reliability can be assessed. Their approach was to develop analytical models for the thermal analyses of steady state and transient conditions, as well as for the failure modes considered. While an analytical approach lends insight into the parameters affecting the physics of the process, several simplifying assumptions are necessary in order to facilitate analytic solutions.

In the present paper, the computer code HEATING7.2 has been used for the thermal analyses, which allows the usage of more realistic conditions such as the real geometry, and temperature dependant properties. Probability distributions are assigned to the input parameters with uncertainties. The consequences of interest (melted and evaporated thickness) are modeled as a function of the input parameters using Response Surface Methodology (RSM). RSM involves the approximation of the consequence as a quadratic function of a specified set of input

parameters. The RSM is used to minimize computational time by providing a quick, but accurate, value of the consequence for each Monte Carlo sampling of the input parameters. Then, a methodology for assessing the reliability is developed. We choose the divertor for analysis because of its considerable importance for impurity control in a tokamak fusion reactor, while subject to high heat loads.

### **1.3 Scope**

In order to clearly define a solvable engineering problem, the parameters and the design proposed by the International Thermonuclear Experimental Reactor (ITER) team for the technology phase will be used as the basis for this analysis.

ITER is a joint design, research and development effort involving the European Community, Japan, the Soviet Union and the United States. Joint work on ITER Conceptual Design Activities (CDA), under the auspices of the International Atomic Energy Agency (IAEA), began in April 1988 with the overall objective to "demonstrate the scientific and technological feasibility of fusion energy for peaceful purposes" [2]. The ITER CDA for the Plasma Facing Components (PFC) led to the definition of the basic design concepts and of the research and development plans to support the Engineering Design Activity (EDA) in preparation for construction.

In the ITER geometry, the magnetic field is opened at two points so that the charged heavy particles are forced by the magnetic field to escape from the plasma in these regions. The components facing these regions are the divertor plates, the basic elements of the plasma impurity control system, whose main functions are as follows:

1. removal of a sizable fraction of the total heat power transferred from the plasma to the plate;
2. exhaustion of the gaseous products from the fusion process;
3. minimization of the level of impurities entering the plasma core produced by plasma/wall interactions.

The divertor of ITER is the focus of the present study, because it is one of the most difficult design tasks for the reactor. The main design parameters are those released as a result of the

CDA technology phase. We should note that "a fully coherent and robust divertor does not exist and is one of the most difficult challenges of the ITER EDA" [2]. The design parameters used in that paper might not be the present choice of interest, but the methodology developed here could be easily applied to a variety of designs with appropriate modifications.

The severe working conditions of the components strongly limit their lifetime. The most limiting factors are the following:

1. high surface erosion due to sputtering and disruptions;
2. embrittlement and unfavorable changes in the material properties;
3. thermal fatigue due to cyclical working conditions;
4. neutron damage.

Replacing or repairing the divertor involves removing an irradiated sector of the reactor, a time - consuming event which affects overall plant availability and economics. Therefore, it is highly desirable to design the divertor to be highly reliable over a long period of operating life.

## Chapter 2

# Method of Reliability Estimate

### 2.1 Introduction

PRA is an analysis process that quantifies the likelihood and the consequences of the potential outcomes of postulated events.

In his Ph.D. thesis, Sanzo used a methodology with the block diagram shown in Figure 2-1. He specifies that this methodology is broadly used on techniques developed to perform Probabilistic Risk Assessments (PRA) of fission nuclear power plants.

A PRA analysis should follow three steps:

1. identify and delineate the combination of events (scenarios) that, if they occur, will lead to a severe accident;
2. estimate the frequency of occurrence for each scenario;
3. estimate the consequences.

An integral part of the PRA process is an uncertainty analysis. Uncertainties in the data and uncertainties arising from modeling assumptions are propagated through the analysis to estimate the uncertainties in the PRA results.

This chapter contains a discussion of the steps required to implement the methodology for assessing the divertor plate reliability.

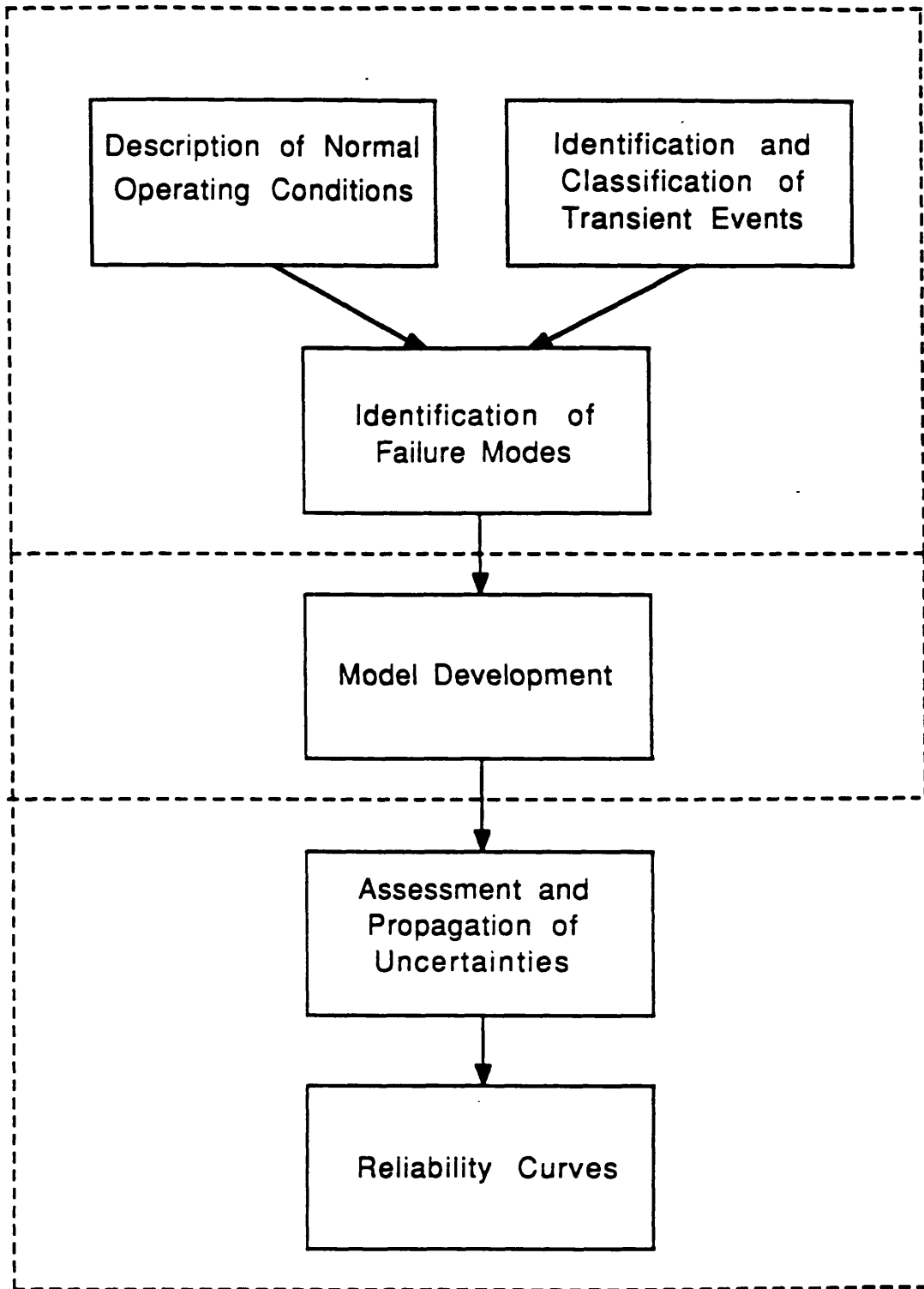


Figure 2-1: Methodology for Analyzing IVC Reliability [1]

## **2.2 Description of normal operating conditions and divertor design**

The first step in a PRA process is the initial information collection; that includes a thorough understanding of the plant analyzed and the initiator selection.

For the present work, the normal operating conditions used as a baseline are those of the ITER for technology phase of the CDA as specified in reference [3]. During the CDA phase, the reactor is supposed to operate in pulses each lasting about 2000 seconds. The integrated burn time should be at least one year. The operating conditions also depend on the materials used.

The divertor design depends critically on the operating conditions which currently can only be predicted with some uncertainty. Major design requirements are as follows:

- the divertor plate peak surface heat fluxes are up to  $30 \text{ MW/m}^2$ , and the peak disruption energy deposition is up to  $20 \text{ MJ/m}^2$  with the possibility for run-away electron incidence;
- the need for remote maintenance leads to divertor plate segmentation;
- water is the coolant choice, because it allows a compact design, low temperature and low pressure in normal operation, and because of its passive safety features such as natural convection after shutdown.

## **2.3 Identification and Classification of the Transient Events**

In preparing a PRA, a methodology is needed to assure that all significant accidents will be considered by preparing a list of accident initiators. A method of selecting the initiating events is the Master Logic Diagram (MLD), which uses a deductive logic. The MLD is similar in nature with a fault-tree approach; it starts with a top event that is the undesirable consequence and ends with a list of possible initiating events. Reference [4] identifies a set of initiating events and the associated accident sequences for impurity control systems in tokamak fusion reactors. The authors used International Tokamak Reactor (INTOR) as a baseline, but the similar nature of all tokamak designs allows their results to be used for any tokamak machine via extrapolation to generic component groups.



We define the transients as being all events which are not part of normal operation, including start-up, steady state operation or shutdown.

The following assumptions are crucial for the developing a method to estimate the reliability of the ITER divertor:

1. all transients constitute events which require immediate shutdown in order to minimize potential reactor damage;
2. each shutdown ends with an induced disruption, irrespective of the shutdown mechanism.

These are conservative assumptions, since there might be transients that do not have such a major effect to require shutdown. Other papers (e. g. [5]) have studied the thermal-hydraulic behavior of the NET/ITER divertor cooling system during a Loss of Flow Accident simulating the plasma shutdown by a linearly decreasing power from the nominal value to the decay heat power during a specified time interval. However, although a disruption is a shorter event (milliseconds), the heat loads are considerably higher, and effects such as melting and vaporization, thermally induced stresses, and electromagnetically induced stresses might impact the divertor lifetime.

Previous studies [6] have shown that the parameter most likely to be affected by a transient event is the temperature of the material at the time a disruption occurs. As a consequence, this parameter might be used as a criterion for classifying the transient events into two categories:

**Category 1:** transients causing no impact on divertor temperature prior to a disruption;

**Category 2:** transients causing an impact on divertor temperature prior to a disruption.

Category 1 transients refer to those transients initiated in the reactor that may cause a disruptive shutdown, but have no effect on the divertor's temperature prior to the disruption. These transients, as described in references [4] and [1], are included in the reliability function developed in the present work.

Category 2 transients include those affecting the coolant and the plasma side of the divertor. The coolant side transients are the Loss of Coolant Accident (LOCA), the Loss of Flow Accident (LOFA), and the Loss of Heat Sink (LHS). The plasma side transients refer to the overpower transients (OP), which for this work will be modeled as a linear increase in power.

Table 2.1 contains a list of the transients included in our reliability function.

**Category 1 Transients: Transients not affecting Divertor Temperature prior to Disruption**

---

1. Auxiliary Heating System Disturbances
2. Magnet Systems Disturbances
3. Main Coolant Disturbances
4. Balance of Plant Disturbances
5. Internal Plasma Disturbances

**Category 2 Transients: Transients affecting Divertor Temperature prior to Disruption**

---

1. Loss of Coolant (LOCA)
2. Loss of Flow (LOFA)
3. Loss of Heat Sink (LHS)
4. Overpower Transient (OP)

Table 2.1: Categories of Transients considered in this study

Once the transients are classified, their frequency of occurrence need to be calculated. The frequencies of occurrence of Category 1 transients are taken from reference [1] for a pulsed machine. They are actually the results of two other studies: [7] and [8], which, although based on another tokamak machine and a Tandem Mirror Reactor in [8] as baseline, give reasonable estimates for similar components of ITER. For Category 2 transients, we perform a system analysis described in the following sections. The component failure rates have basically been extracted from reference [9], which contains failure rate screening data for application to fusion components. Where similarities exist between fusion plant components and fission plant components, the available fission power plant data base is exploited [10].

## 2.4 Identification of Failure Modes

Since there is no specific design code for fusion components at this time, Section III, Division 1 of the ASME Boiler and Pressure Vessel Code and Code Case N47 [11, 12] for Class 1 Components in Elevated Temperature Service have been used as guides in identifying potential failure modes (FM's) and associated failure criteria (FC).

Previous fusion component design studies have identified the following modes of failure:

1. **Erosion:** the loss of material due to sputtering during normal operation and the loss of material during transients due to melting and evaporation;
2. **Deformation:** structural material exceeds a total allowable strain following thermal expansion and irradiation effects;
3. **Instability:** general instability or buckling of structural components, local buckling, or wrinkling of structural members;
4. **Leaks:** minor cracks resulting in coolant penetration into the plasma which introduces excessive impurities into the plasma;
5. **Fracture:** gross rupture of the wall producing loss of vacuum, or flow of coolant into adjacent areas.

For example, reference [1] has particularly paid attention to those failure modes that are affected by transient events, like erosion of the limiter coating, failure of the limiter substrate

caused by cumulative cyclic damage due to fatigue and creep, limits on the amounts of swelling strain and creep irradiation strain.

Rather than obtaining the total reliability curves for the ITER divertor, the emphasis in the present work has been placed on the methodology for obtaining the curves, quantifying only the impact of one failure mode; that is the erosion of the divertor coating. The amount of material lost during transients due to melting and vaporization can be large, and that loss is in addition to the material lost during normal operation due to sputtering.

## **2.5 Steps Required to Assess Reliability**

The term 'reliability', as defined by the International Electrotechnical Commission [42], is "the ability of an item to perform a required function, under stated conditions, for a stated period of time. The term reliability is also used as a reliability characteristic denoting a probability of success or a success ratio." At the design stage, it is essential to have methods of predicting reliability in order to meet a specification, to achieve consistency, and to realize an objective at minimum cost (improved reliability usually increases construction cost, but reduces operating expenses).

### **2.5.1 Thermal Analysis**

For a reactor in the pulsed mode of operation, the duration of the 'on' portion of the cycle is on the order of hundreds of seconds, while the duration of the 'off' portion of the cycle is on the order of tens of seconds. This sets up a cyclical temperature distribution through the divertor.

Depending on its category, a transient might or might not cause an increase in temperature prior to the shutdown by disruption, so the temperature distribution through the component would depend on the model associated with each transient.

The disruption is an extremely fast transient on the order of milliseconds during which the plasma energy is deposited; this causes a temperature increase in the divertor on the order of hundreds of degrees Celsius, which may lead to surface melting and evaporation.

We perform the thermal analyses using the HEATING 7.2 program [12], which can solve steady state and/or transient heat conduction problems. A model in HEATING 7.2 allows for

multiple materials with time- and temperature- dependent properties. Materials may undergo change of phase. The melt and evaporated material can be estimated.

### **2.5.2 Assessment of Uncertainties**

Reliability is a probabilistic concept. That makes possible the consideration of both the effects of transient events, which occur randomly in time, and the effects of normal operation impacting reliability.

Quantifying reliability involves calculating the minimum time to failure under the failure criteria (FC) associated to the failure modes (FM's) considered. The time to failure is uncertain due to the presence of uncertainties in both operating conditions and transients. The sources of uncertainty generally are as follows [11]:

- **statistical or stochastic uncertainty:** a particular phenomenon is random in nature, and the uncertainty associated with its occurrence can not be reduced by collection of data;
- **parameter uncertainty:** is a state-of-knowledge uncertainty, and refers to the values of the input parameters; they could be reduced by collection of data;
- **model uncertainty:** is also a state-of-knowledge uncertainty, but more difficult to quantify; we distinguish uncertainties in our physical modeling, and uncertainties in the numerical implementation of our model.

Once the uncertain parameters included in a particular model have been determined, probability distribution functions are to be associated with them according to the existing information in data bases.

### **2.5.3 Generation of Reliability Curves**

There are several steps required to assess the reliability curves as follows:

1. development of the reliability function  $R(t|\bar{v})$ , where  $\bar{v}$  is a vector whose elements are the parameters with uncertainties;
2. development of the probability distributions for the vector  $\bar{v}$ 's elements;

3. choosing a method for propagating the uncertainties in  $\bar{v}$  through the reliability function in order to obtain a probability distribution of the reliability at any time point of interest.

The Monte Carlo method is a powerful mathematical tool for propagating the uncertainties through a model. The method consists of picking a random value for each of the variables from their probability distributions, and repeating this process for many trials at each time  $t$  of interest. Probability distribution functions (pdf's) are obtained for  $R(t)$  at each  $t$ . The percentiles of these distributions represent our confidence that the reliability is greater than a certain value at a particular time. The procedure is shown in Figure 2-2.

The problem with the Monte Carlo method is that the accuracy of the final result depends on the number of trials, which makes it computationally demanding. Each Monte Carlo sample of the input parameters requires a separate computer run, and the Monte Carlo approach will require thousands of runs to determine a statistically meaningful output pdf.

To minimize computer time, a simplified but accurate approximation to the output of the HEATING computer program is required. The Response Surface Method (RSM) involves the approximation of the consequence as a quadratic function of a specified set of input parameters. Thus, the sensitivity of the consequence to the various input parameters can readily be found.

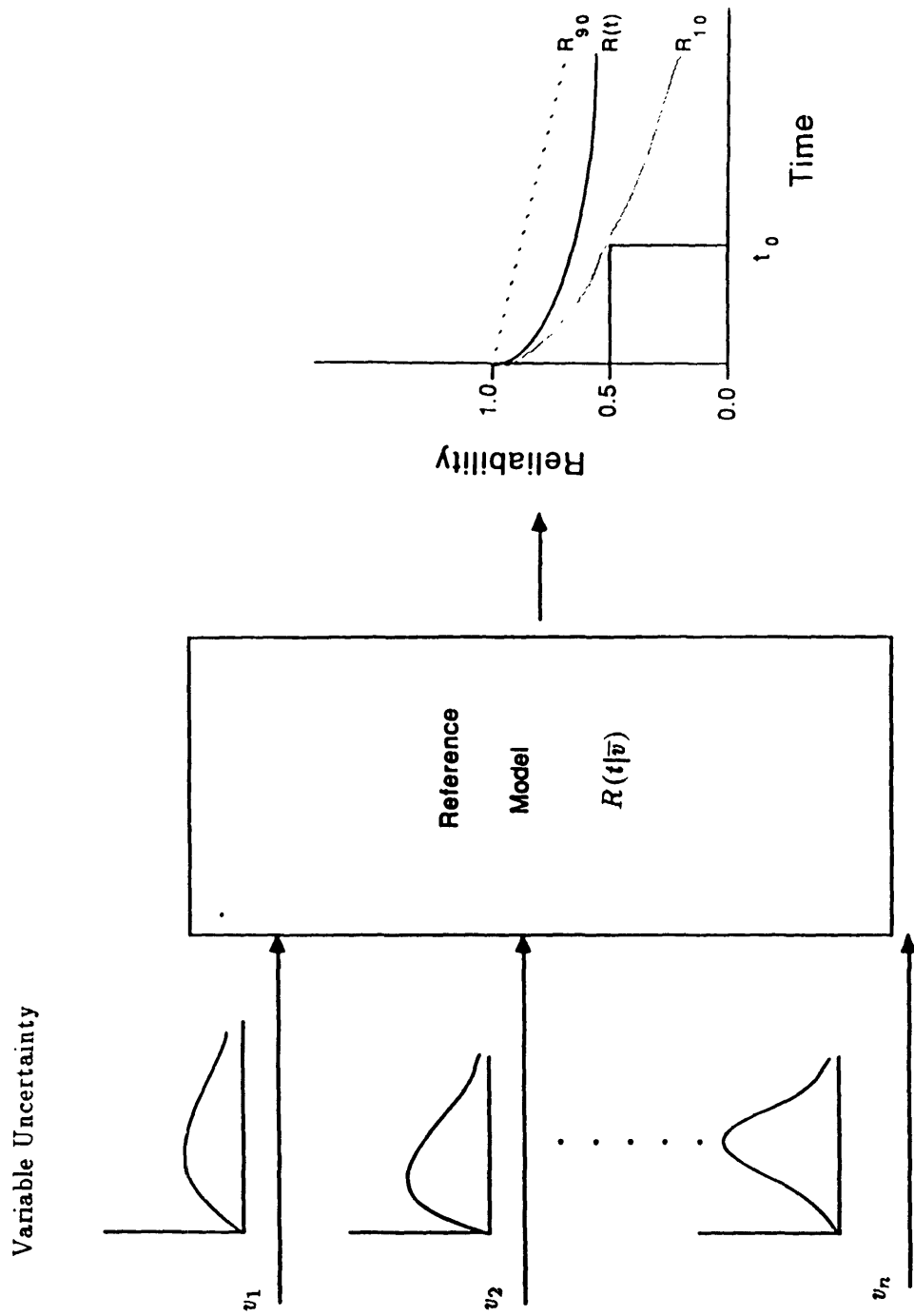


Figure 2-2: Propagation of uncertainties

## Chapter 3

# Description of Reference Design

The programmatic objective of ITER is to demonstrate the scientific and technological feasibility of fusion energy for peaceful purposes [13]. ITER is currently envisioned as a large, superconducting, ignited tokamak fusion reactor. The tokamak concept uses doughnut-shaped magnetic fields to confine a hot plasma. The requirement for energy confinement is the major factor determining the size of the machine. Today's design has a major radius of 7.75 meters and a minor radius of 2.8 meters. This design is expected to generate 1000 MW of total fusion power, when pulsed at the peak conditioned during the technology phase. The technology phase of the testing program will follow an initial phase to test the physics of ignited plasmas.

### 3.1 Divertor Plate Design and Normal Operation Conditions

Joint work on ITER Conceptual Design Activities (CDA), under the auspices of the International Atomic Energy Agency (IAEA), began in April 1988. The plan included two phases: the definition phase and the design phase. The design phase produced a conceptual design, which is to be used as a baseline for the present work.

The divertor plates (DP's), located above and below the plasma region within the torus vacuum vessel, establish the interface between the plasma and the material surface of the tokamak device. Figure 3.1 shows the layout of a cross section in the ITER tokamak. Figures 3.2 and 3.3 show a typical ITER divertor module designed at the Fusion Energy Design Center for the technology phase, as described in references [3] and [14]. For this particular double null



design, there are 48 such modules, 24 each at the top and bottom of the machine. Each module has its own inlet and exit manifold, and is meant to be removed and replaced with remote handling techniques if necessary. During normal operation, the plates, with a total area of 200 m<sup>2</sup>, must withstand and allow removal of at least 100 MW of heat conducted to them from the plasma boundary. Here also the plasma impurities are neutralized for subsequent exhaust by the torus vacuum pumping system.

The divertor system represents one of the most difficult design tasks for ITER. Physics reference scenarios used for its design predict static peak power loads in the range of 10-20 MW/m<sup>2</sup>. With 'engineering' peaking factors, this results in peak heat loads of up to 30-50 MW/m<sup>2</sup> to the DP. These design requirements are characterized by considerable uncertainty, which will be reduced as the understanding of plasma edge conditions improves during the course of the EDA research and development (R&D) effort. In light of this uncertainty and of the importance of the divertor to overall machine performance, the approach has been to design as high a performance system as possible under the constraints presented by the machine. The result is a system capable of operating with static peak thermal loads on the divertor plate of about 15 MW/m<sup>2</sup> in steady-state. With "sweeping" of the heat loads across the face of the divertor, effective peak loads approaching 30 MW/m<sup>2</sup> appear possible. The lifetime of the divertor plate is a sensitive function of such factors like plasma edge temperature, choice of material, and the frequency and nature of plasma disruptions.

Table 3.1 summarizes the main operating requirements for the system. The peak heat fluxes in normal operation on the inclined DP's include estimated physics and engineering peaking factors for uncertainties in the scrape-off layer width or geometrical alignment. For the ignition and long pulse scenarios with high peak powers the power deposition profile becomes highly peaked, with a width at half height of only 5-6 cm, as shown in Figure 3-4. During the initial thermal quench in disruptions, about 80 % of the plasma thermal energy (about 600 MJ) is estimated to be deposited equally on the first wall and divertor plates.

It should be noted that the DP operating requirements are among the most challenging of the ITER design. The edge plasma parameters are rather uncertain and can only be fully understood from the operation of the ITER itself.

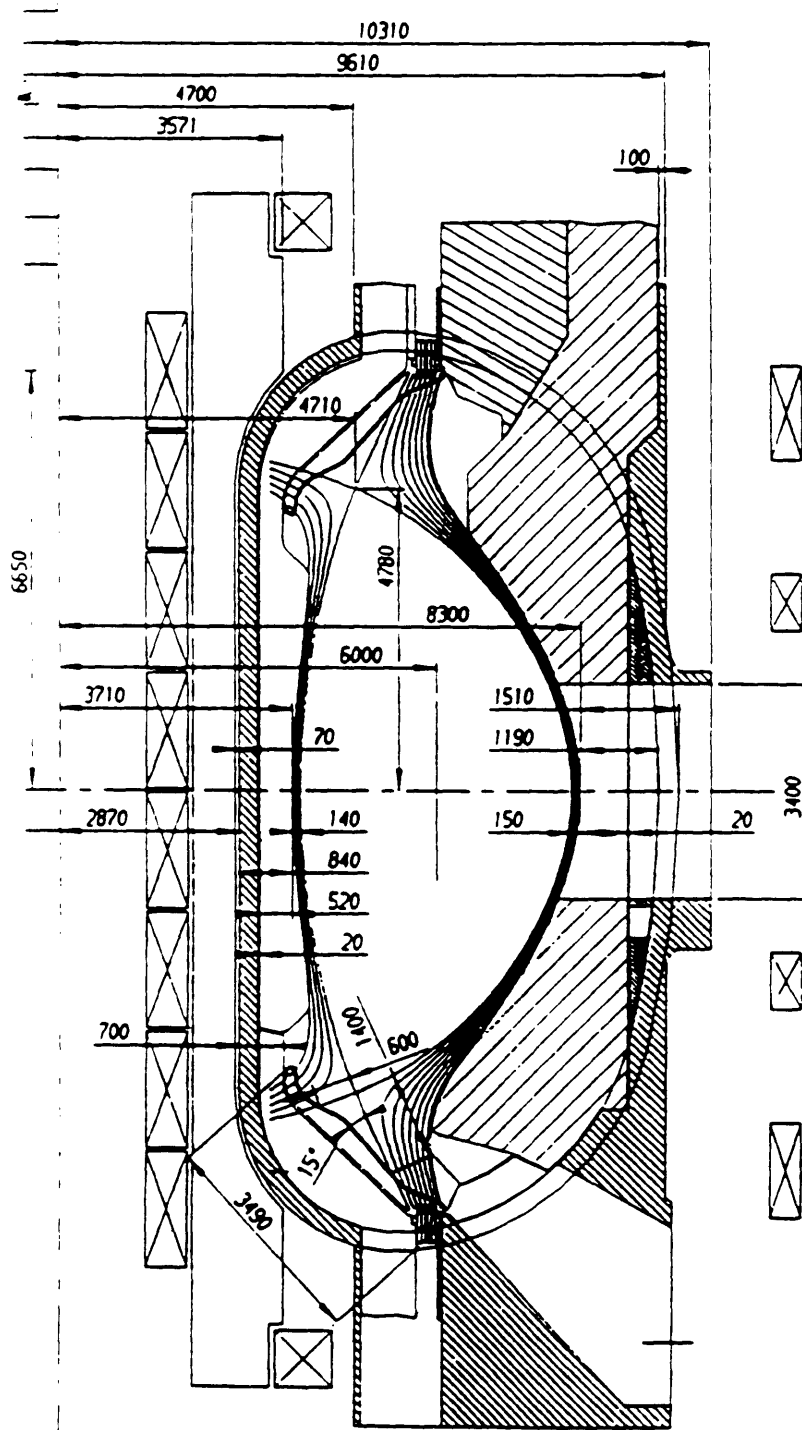


Figure 3-1: Layout of an ITER cross section, dimensions in millimeters [44]

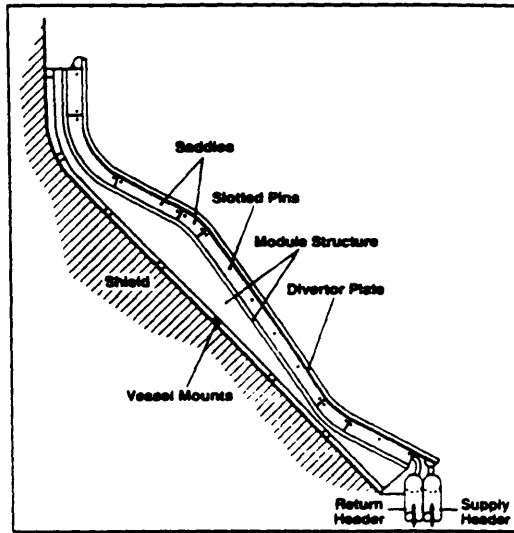


Figure 3-2: ITER divertor module [14]

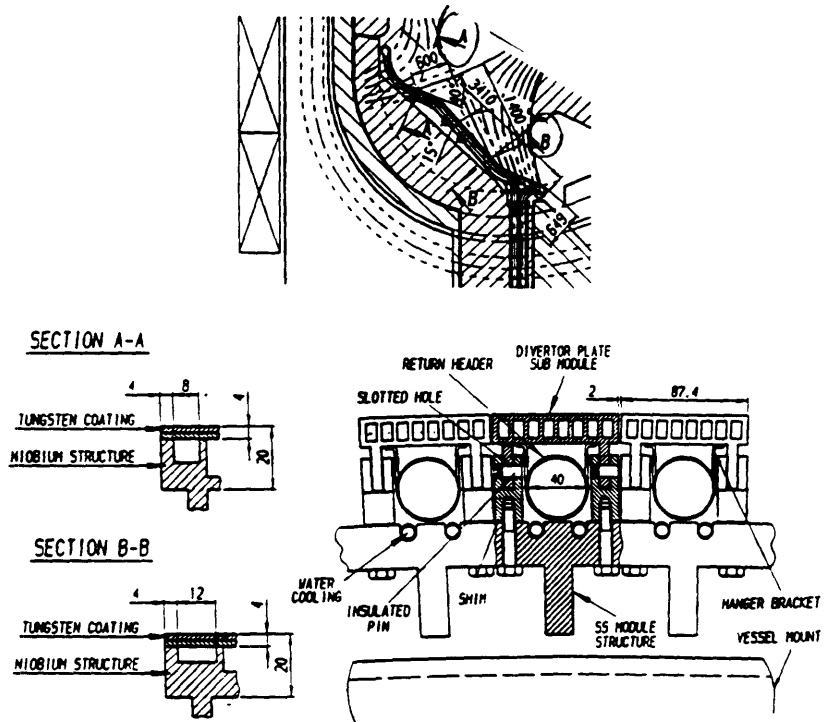


Figure 3-3: Coolant channel configuration for technology phase divertor [3]

### **Normal Operation**

---

Ave. neutron wall load	0.4 MW/m <sup>2</sup>
Peak/ave. surface heat flux	15-30/0.6 MW/m <sup>2</sup>
Peak volum. heat load in structure	4 MW/m <sup>3</sup>
Number of pulses (full load)	2·10 <sup>4</sup> - 5·10 <sup>4</sup>
Total burn time	1·10 <sup>4</sup> - 3·10 <sup>4</sup> h
Pulse length	2000 s
Min. dwell time	200 s
Incident DT ions:	
-peak flux	4·10 <sup>23</sup> ions/m <sup>2</sup> s
-energy	60-200 eV

### **Disruptions**

---

Number (at full load)	200-500
Thermal quench:	
-time	0.1-3 ms
-peak energy deposition	5-20 MJ/m <sup>2</sup>
Current quench:	
-time	5-100 ms
-radiative energy deposition	2 MJ/m <sup>2</sup>
-run-away electron energy depos.	30 MJ/m <sup>2</sup>

Table 3.1: Main Operating Conditions for the ITER divertor technology phase [3]

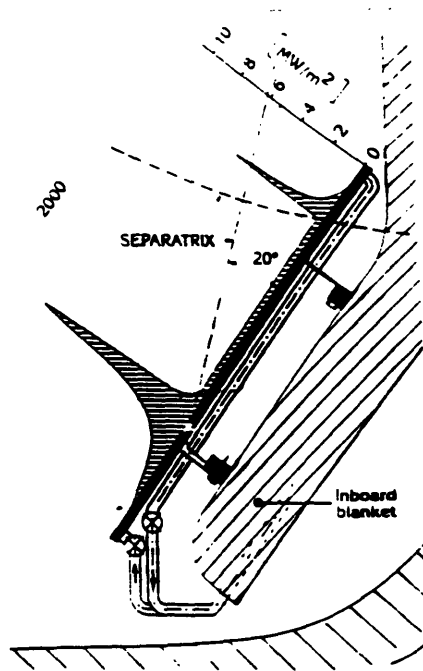


Figure 3-4: Divertor plate and typical surface heat flux distribution [5]

### 3.2 Material Properties

As DP armor for the technology phase, tungsten is considered an alternative to carbon mainly due to prospects for significantly lower sputtering erosion rates, better neutron irradiation resistance, potential for in-situ repair by plasma spray, lower bake-out and conditioning temperatures, and better protection of the heat sink against run-away electrons.

The DP concept for the technology phase consists of a two millimeters thick tungsten coating diffusion bonded onto a niobium alloy heat sink with rectangular channels. Critical issues with this tungsten DP concept include:

- extremely low allowable tungsten concentrations in the plasma;
- neutron activation, volatilization of oxides due to reactions with steam and air above 600 degrees Celsius, and the indication of potentially high tritium inventories;
- tungsten peak temperatures of up to 1500 degrees Celsius with the W coating and Nb substrate at the required heat loads;
- the need for experimental verification of the critical heat flux limits for the rectangular

geometry with thin armor and sweeping;

- thermal shock and fatigue damage of the heat sink.

R. F. Mattas has studied divertor performance and lifetime analysis for U. S. ITER design [16] by comparing different material choices. He concludes that Nb-1Zr is recommended as the best option for divertor structural material, and pure tungsten is recommended as plasma facing material.

The heat flux limits for the technology phase based upon fatigue damage considerations indicate that the materials will be pushed to their performance limits. For duplex structures, the maximum allowable heat flux is estimated to be 10-12 MW/m<sup>2</sup> for a plate that is allowed to expand but not bend without fatigue safety factors. This limit is likely to be reduced when additional stress constraints and safety factors are imposed [16]. Hence, the application of tungsten will be more viable if a gas target divertor configuration which reduces the heat load to the plate is implemented.

Reference [17] also concludes that tungsten is a possible choice when taking into considerations criteria like high thermal conductivity at high temperatures, minimal erosion due to sputtering and evaporation, minimized surface erosion due to melting, minimal tritium retention, low outgassing material. However, tungsten is not a very practical engineering material because machining and welding of it is generally difficult.

A summary of the properties of interest is presented in Table 3.2. The use of HEATING 7.2 program for performing the thermo-hydraulic analysis allows for temperature dependant properties; so the thermal conductivity is defined as temperature dependant for both W and Nb-1Zr as in Figure 3-5 [18]. The density is taken constant for both of materials (otherwise, the mass is not conserved when a time- or temperature- dependent density is specified). The specific heat of tungsten is specified as temperature dependent, especially because this material might undergo a change of phase during disruption transients. References [19] and [20] have also been used for choosing the material properties.

Property	Tungsten	Nb-1Zr
Melting point (°C)	3410	2407
Boiling point (°C)	5660	4700
Density (g/cm <sup>3</sup> )	19.3	8.59
Specific heat (J/kgK)	132 at 25°C 360 at 3410°C-solid 193 at 3410°C-liquid	270
Thermal conductivity (W/mK)	174 at 27°C 90 at 2500°C	48 at 27°C 60 at 1000°C

Table 3.2: Properties of divertor plate materials [18-20]

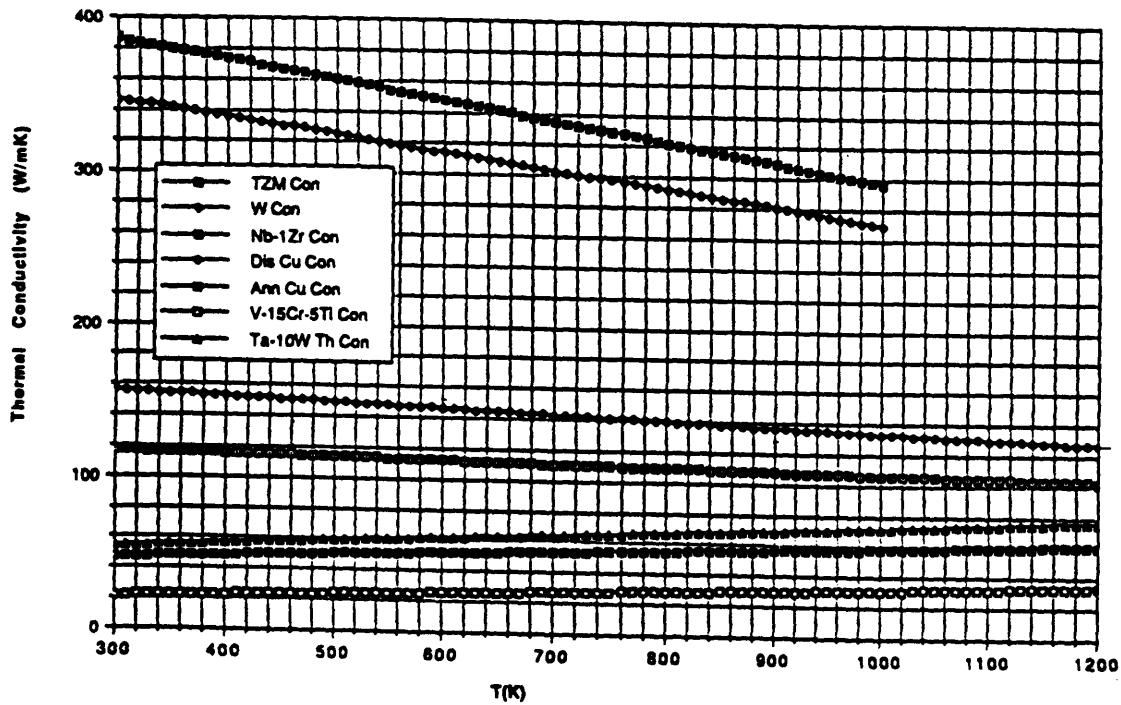


Figure 3-5: Divertor materials thermal conductivity [18]

### 3.3 Divertor Cooling Circuit Design

In some components to be cooled, heat is released mainly during pulses. Up to 680 MW of heat will be released in the first wall and divertors during pulses, and about 11MW in the primary circuit pumps. However, afterheat will continue to be released after reactor shutdown and must be removed as well.

The coolant of choice for ITER divertor technology phase is water under a pressure of 3.5 MPA, with a velocity of 10 m/s.

The cooling of components where the coolant may be contaminated with radioactive materials, especially tritium and corrosion products, requires intermediate (secondary) circuits between the primary cooling circuits and an ultimate heat sink.

The layout of the divertor cooling loop is the following: one cooling loop for both the upper and lower divertor targets which are connected respectively to the upper and lower access ports; each divertor target (upper and lower) is connected by inlet and outlet feeders to manifolds, per sector, connecting to two upper and two lower ring headers; the upper and lower ring header system are connected by piping through a risershaft and then connected to one primary loop.

Typical flow diagrams of the primary cooling circuits for the divertors are shown in Figures 3-6 and 3-7. The major parameters of these circuits are given in Table 3.3.

According to CDA phase estimations [15], the tritium concentration in the first wall and divertor coolants will be about 1 Ci/l (40 GBq/l). Therefore, for safety reasons, the primary cooling circuits for the first wall and divertors are divided into four separate loops each.

In the heat exchangers, the primary water flowing inside the tubes will transfer heat to the water of the secondary circuits equipped with pumps, buffer tanks, pressurizers, filters, and chemical purification facilities.

### 3.4 Steady-State Thermohydraulic Analysis

In order to calculate the divertor reliability, we need to calculate the extent of material melting and vaporization during disruptions. Instead of developing analytical thermal models for the temperature profile through the divertor at the onset of disruption and for melting and vaporization thickness, as in reference [1], we prefer to use the HEATING 7.2 program [12].



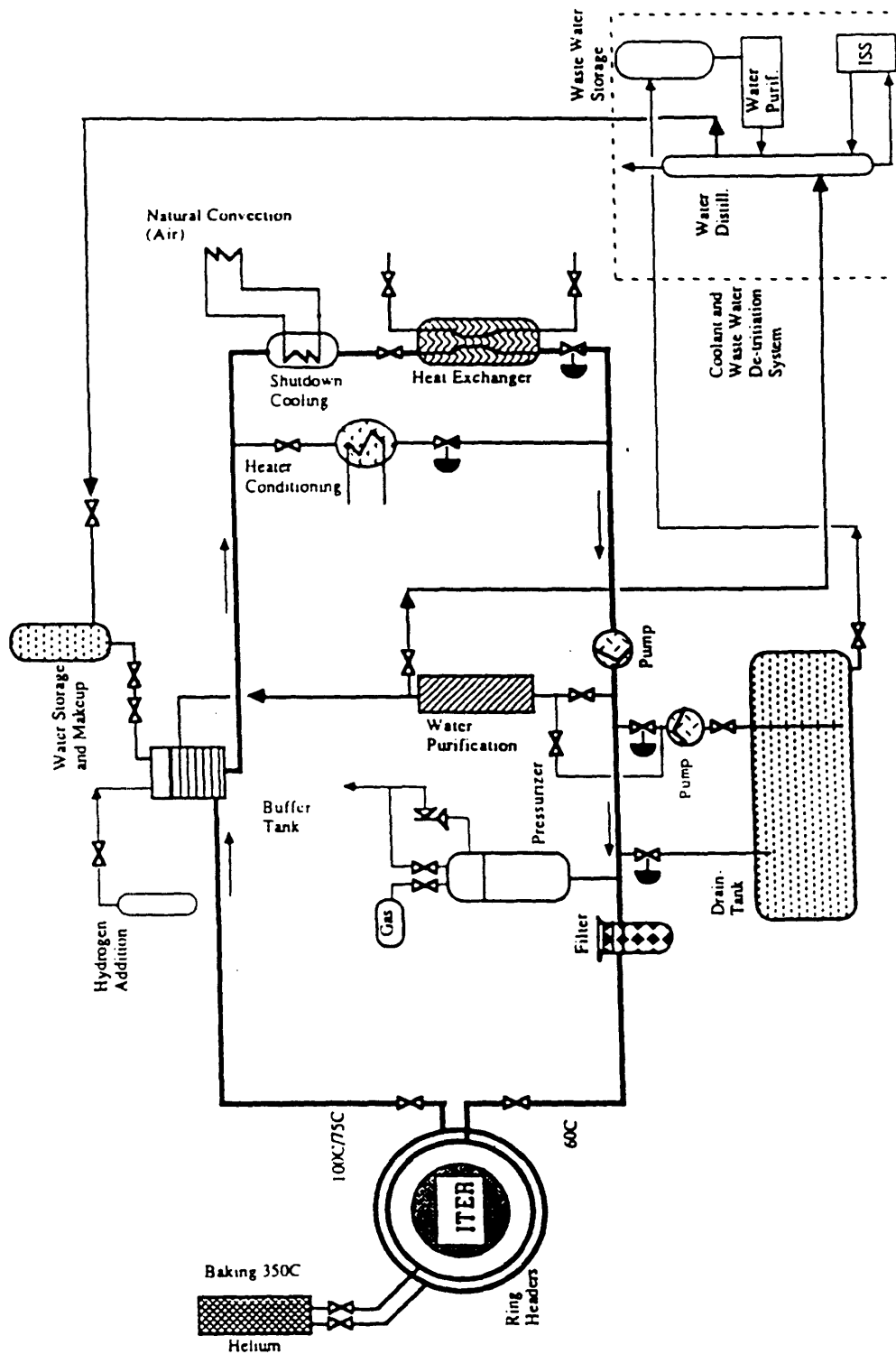


Figure 3-6: Typical cooling loop configuration for divertor [15]

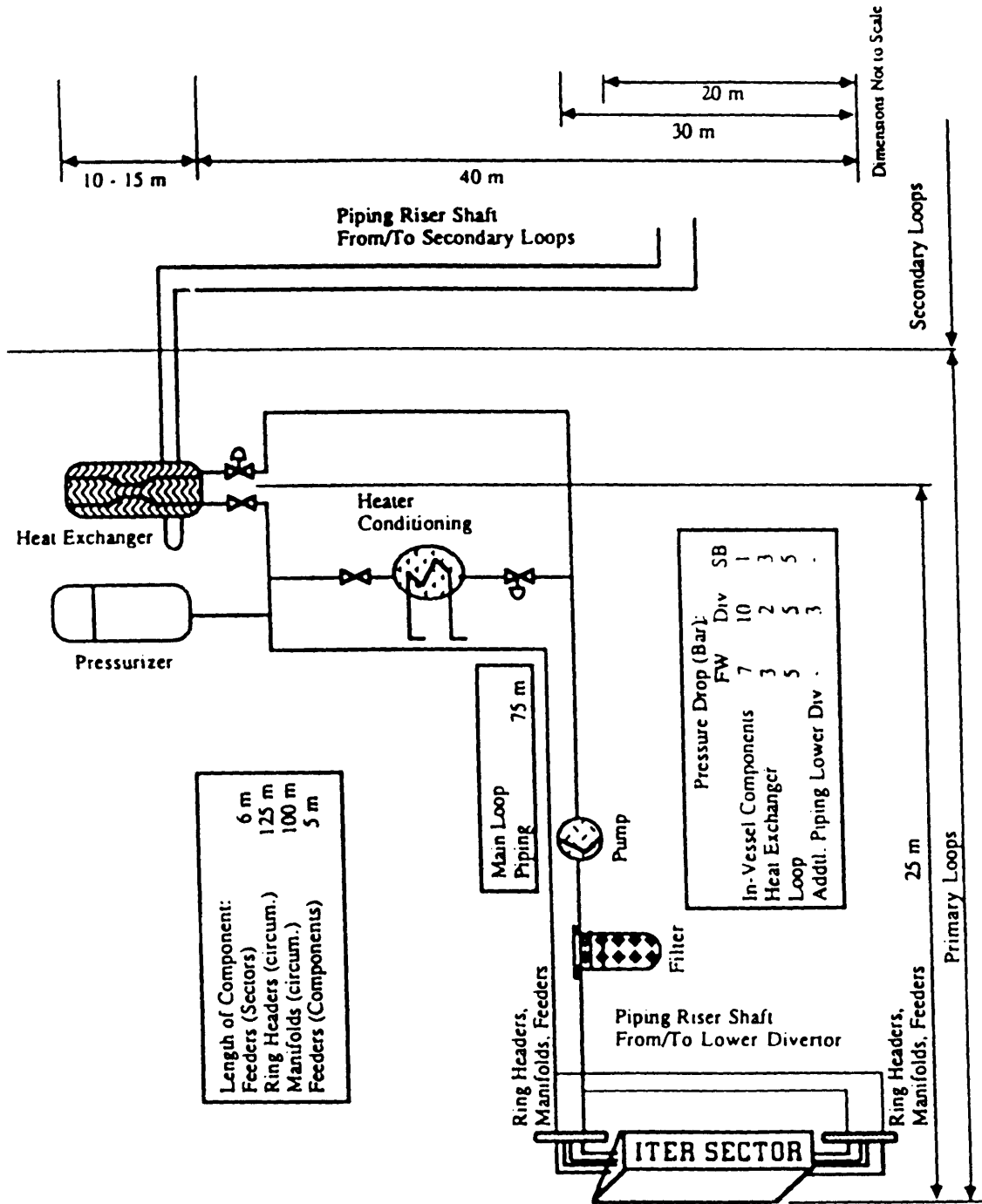


Figure 3-7: Primary loop for divertor [15]

<b>Parameter</b>	<b>Value</b>
Power	170 MW
Pressure	3.5 MPa
Divertor Inlet temperature	60°C
Divertor Outlet temperature	75°C
Total flow rate	3120 kg/s or 3.25 m <sup>3</sup> /s
Number of loops	4
Coolant velocity in divertor plates	10 m/s
Pressure drop:	
-in-vessel components	1 MPa
-heat exchanger	0.16 MPa
-loop	0.8 MPa
-total	2 MPa
Tritium concentration in the coolant	1 Ci/l or 40 TBq/m <sup>3</sup>
Total pump power	6.4 MW
Total coolant volume	356 m <sup>3</sup>

**Table 3.3: Major parameters of the primary cooling system of ITER divertor [15]**

Although an approximate analytical solution of the problem of melting and evaporation might lend insight into the parameters affecting the physics of the process, it is much more uncertain than a more sophisticated computer model mainly because of several approximations that have to be introduced; some examples are as follows:

1. the use of constant material properties instead of temperature dependent properties;
2. the use of a geometrical model (reference [1]: two finite slabs for the coating and substrate) instead of the real configuration of the divertor;
3. the use of a normal distribution to describe the material loss, instead of obtaining a distribution by propagating the variable uncertainties.

Sanzo [1] notes that comparing results of the analytical model with those of a more sophisticated computer model shows a maximum potential error for melt thickness predictions in the range +50 percent to -10 percent, and for the material vaporized  $\pm 10$  percent.

The HEATING 7.2 program allows for resolving this succession of problems and storing the output data of a first problem and reusing it to obtain restart information for a second problem. HEATING 7.2 is the most recent version of HEATING, which is a conduction heat transfer program. It can solve steady-state and/or transient problems in one-, two-, or three-dimensional Cartesian, cylindrical, or spherical coordinates. A model may include multiple materials, and the thermal conductivity, density, and specific heat of each material may be both time- and temperature-dependent. Materials may undergo change of phase. The boundary conditions may be specified temperatures or any combination of prescribed flux, forced convection, natural convection, and radiation.

Our geometry is best represented in the two-dimensional Cartesian plane; the section of interest is perpendicular to the divertor length (of 3.41 meters), and is at the critical location on the divertor where the highest heat flux load occurs. As Figure 3-4 shows, the surface heat flux is a function of the distance along the divertor. Along the length of the DP, there are two regions where the plasma strikes with the highest density and thus the heat flux reaches its peak values. As recommended for the technology phase, the highest peak is  $11 \text{ MW/m}^2$ , and that is the limiting steady-state heat flux that we use for this work. We note that it seems reasonable to perform a two-dimensional analysis as opposed to a three-dimensional one,

since the temperature change of the coolant (water) is about 30 °C/m while the temperature gradient through the divertor is approximately 100 °C/mm. Thus the axial conduction of heat is negligible compared to the conduction through the divertor.

The melt and vaporized material is estimated from the output of the disruption transient case (problem 3); this problem uses as input the temperature distribution at the end of the initial transient (recall the category 2 transients; category 1 transients do not affect divertor temperature before a disruption) (problem 2), which in turn has the steady-state temperature distribution as input (problem 1). Problem 1 is the scope of the current section. We assume that the reactor has on-off cycle durations such that the temperature distributions through the divertor can be considered to have reached a steady-state condition (this is true for any reactor with a pulse period longer than several component thermal time constants).

For normal operation and category 1 transients, the input file for HEATING 7.2 program is given in Appendix A. The analysis has been performed for half of a divertor submodule, as it appears in Figure 3.3, which contains equal height cooling channels. Figure 3-8 represents half of the submodule, the other half being symmetric against the dotted line in the figure; translating the symmetry into zero heat flux allows for simplification of the problem.

In Figure 3-8, regions 1 and 2 form the divertor tungsten coating, and regions 3 to 25 are made from niobium alloy. The material properties are also part of the input file, as they are described in Section 3.2. The operational power density in the divertor from neutron interactions is also included. This volumetric heat source tends to be small compared to the surface heat flux, but the effect is included for completeness. The boundary conditions refer to the heat flux on the plasma side and the heat transfer coefficients at the coolant channel walls. The heat transfer coefficients are calculated using the appropriate correlations with the help of MATHCAD.

From geometrical considerations, it turns out that the highest heat load is applied at about 80 cm distance from the end of DP where the water enters the divertor cooling channel. Before calculating the heat transfer coefficients, one has to check the nature of the flow at this location. Reference [21] gives the turbulent developing flow length as follows:

$$\frac{z}{D} = 25 \text{ to } 40 \quad (3.1)$$

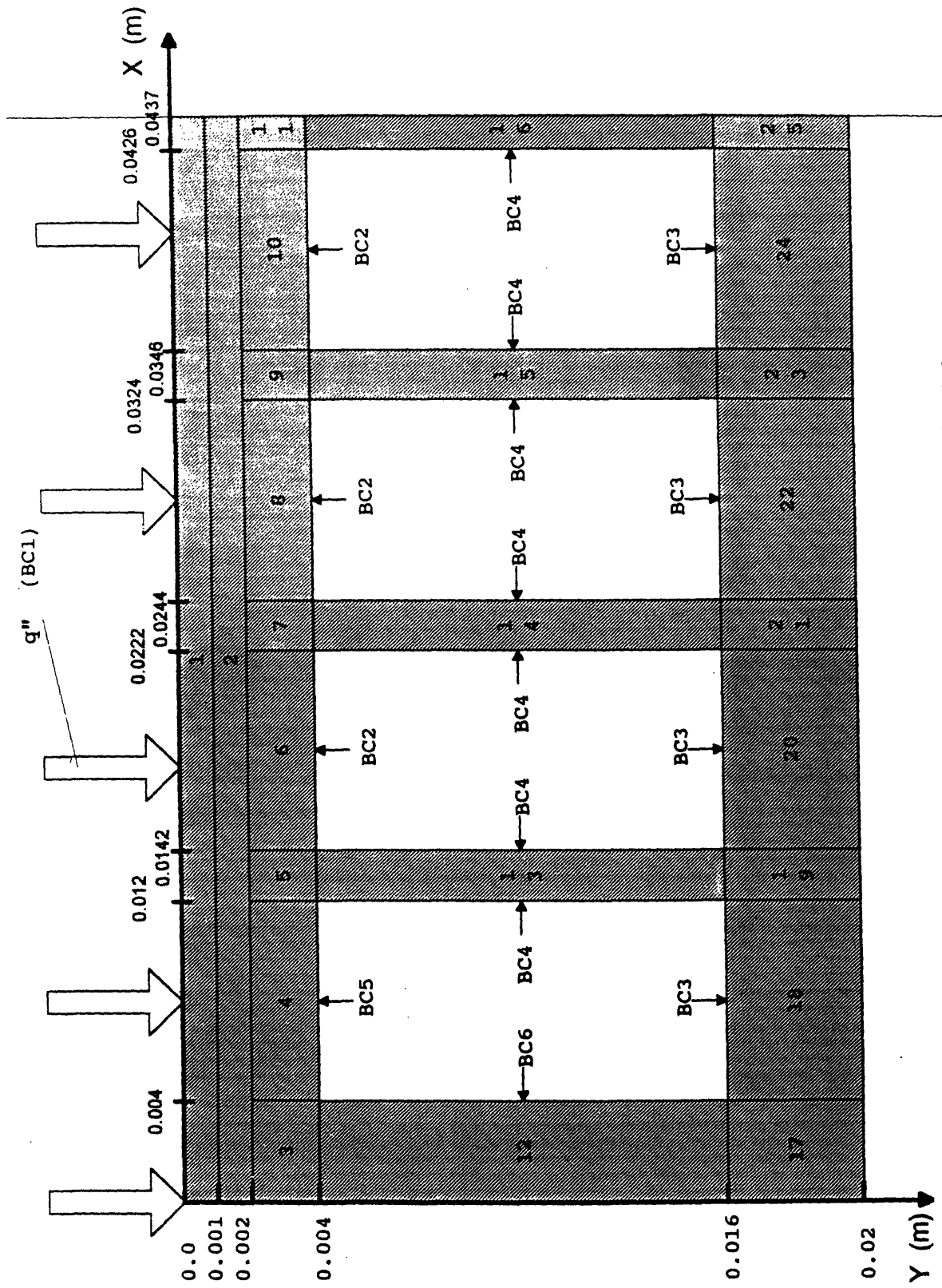


Figure 3-8. Divertor submodule regions as used for the thermal analysis

where  $z$  is the axial distance, and  $D$  is the equivalent hydraulic diameter of the divertor sub-module (17.3 mm). That gives a  $z$  in the range 43 to 69 cm, which is smaller than 80 cm. This result shows that in the section of interest the flow is fully developed turbulent (Reynolds number is  $3.4 \cdot 10^5$  for a coolant velocity of 10 m/s).

Reference [22] presents the results of an assessment of a thermal-hydraulics correlation package recently developed for ITER by AECL, for use in the analysis of heat transfer within the divertor cooling channels. Three single-phase heat transfer correlations were assessed, and these are: Dittus-Boelter, Petukhov, and Sieder-Tate. The predictions of the last two correlations agree closely with each other, and they are presently recommended for divertor plate analysis. We choose to use the Petukhov correlation, after we concluded that the coolant has not reached the Onset of Nucleate Boiling (ONB). The experimental results of Yin et al. [23], performed under conditions similar to ITER's ( $p = 3.5$  MPa,  $G = 10$  Mg/m<sup>2</sup>·s,  $T_{in} = 50$  °C), show that ONB does not occur as long as the wall temperature is not about 45 degrees higher than the saturation temperature (242.6 °C at 3.5 Mpa).

The Petukhov correlation (equations 3.2 and 3.3) takes into account the wall region viscosity changes. The properties of  $c_p$  (specific heat at constant pressure),  $k_b$  (thermal conductivity),  $\mu_b$  (dynamic viscosity) are to be evaluated at bulk temperature, and  $\mu_w$  at wall temperature. Therefore, we perform several iterations with HEATING 7.2 by introducing new heat transfer coefficients calculated for the viscosity at the walls for the temperatures of the previous HEATING 7.2 run. The friction factor,  $f$ , is obtained from the Moody diagram or from equation 3.4.

$$Nu = \frac{Re \cdot Pr \cdot f}{X \cdot 8} \left( \frac{\mu_w}{\mu_b} \right)^{0.11} \quad (3.2)$$

$$X = 1.07 + 12.7 \left( (Pr)^{\frac{2}{3}} - 1 \right) \left( \frac{f}{8} \right)^{0.5} \quad (3.3)$$

$$f = (1.82 \log(Re_b) - 1.64)^{-2} \quad (3.4)$$

The MATHCAD calculations are presented in Appendix B.

## **Chapter 4**

# **Effects of Transients and Associated Uncertainties**

### **4.1 Identification of transients and their frequencies of occurrence**

This section presents a detailed description of the transients, and a point estimate for their frequency of occurrence.

Data analysis is an integral part of PRA. It is the process by which the information available to us is incorporated into our models. In general, there are three sources of such information available:

1. general engineering knowledge of the design and manufacturing of the equipment in question and the frequency to be expected on this basis;
2. the historical performance in other plants similar to the one in question;
3. the past experience in the specific plant being studied.

Since there are no previous large fusion reactors from which data can be drawn for the divertor, assessing the frequencies of occurrence of some of the initiating events causing transients which involve subsystems that are fusion reactor specific must be done through extrapolation of the existing component failure rate data base. This extrapolation may involve the use of



<b>Transient</b>	<b>Mean frequency of occurrence (per year)</b>
1. Auxiliary Heating System Disturbances	6.4
2. Magnet Systems Disturbances	1.3
3. Main coolant Disturbances	1.7
4. Balance of Plant Disturbances	5.5
5. Internal Plasma Disturbances	760.0

Table 4.1: Mean frequencies of occurrence of category 1 transients [1]

expert opinion. Where similarities exist between fusion power plant components and fission plant components, the available fission power plant data base is exploited [10].

The transient events have already been classified in Table 2.1. All those transients affect the lifetime of the divertor, although the category 2 transients may have a higher effect because of the higher temperature at the start of disruption. On the other hand, we expect the frequency of occurrence of category 1 transients to be higher, so their effect may be higher from this point of view.

#### 4.1.1 Category 1 Transients

The transients listed in category 1 include those assumed due to initiating events in the reactor subsystems. In addition to those transients identified in reference [4] via a MLD, Sanzo [1] has introduced another transient group, Balance of Plant Disturbances, which includes those systems common to both fission and fusion reactors (e. g., turbines).

The mean frequencies of occurrence for category 1 transients are listed in Table 4-1. It should be noted that there is state-of-knowledge uncertainty surrounding transient frequencies.

<b>Transient</b>	<b>Transient frequencies of occurrence (per year)</b>
1. Loss of Flow	1.75E-2
2. Loss of Heat Sink	8.76E-3
3. Loss of Coolant	1.E-2
4. Overpower Transient	2.0

Table 4.2: Mean frequencies of occurrence of category 2 transients

#### **4.1.2 Category 2 Transients**

The frequencies of occurrence of Category 2 transients are assessed via a fault tree analysis of the ITER divertor coolant loop, as it is presented in Figure 3-7. The main cooling circuit consists of a hot leg, a heat exchanger, a primary pump, a filter, and a cold leg. The pressurizer is connected to the hot leg of the main circuit via the surge line. The pressurizer contains steam and water at saturated conditions. Up to now, no emergency cooling systems are foreseen in the design. So, according to the information we have, there is no redundancy neither for the heat exchanger nor for the pump, and there is no redundant coolant loop. Therefore, we assume there are no common causes that could contribute to the system failure except one: a common cause that would produce the simultaneous failure of all divertor cooling circuits.

The frequencies of occurrence for category 2 transients are listed in Table 4-2, and the way they have been obtained is presented below.

#### **Loss of Flow Accident (LOFA)**

LOFA represents the loss of the forced coolant flow, and may be induced by one of the following transient events:

1. loss of electrical power for the primary pump;
2. inadvertent valve closure;
3. mechanical blockage of a primary pump;

4. clogging of a single cooling tube.

Pump inertia and natural convection may provide further cooling capacity, if the design of the systems supports this mode of operation. In that case, the temperature increase during the transient is quite mild.

In order to minimize this transient consequences, some recommendations for the design are:

1. coolant loop should have adequate inertia;
2. the cooling system should be designed to enhance natural coolant circulation;
3. very quickly actuated (less than 1 second scale) active plasma shutdown together with quick (1 to 5 seconds scale) passive plasma shutdown mechanisms should be provided for accidents entailing a quick divertor temperature rise.

The fault tree constructed for LOFA transient is presented in Figure 4-1 with the top event "Insufficient flow to DP's due to LOFA". The fault tree is a deductive analysis that begins with the undesired state of the system and goes down to the basic events that contribute to this top event. The basic events are those events for which frequencies of occurrence (Table 4-3) have to be provided in order to calculate the frequency of occurrence of the top event. Once the fault tree has been drawn, an equivalent Boolean equation can be obtained as follows:

$$\begin{aligned}
 Q &= GO_1 \vee GO_2 \\
 GO_1 &= CCF \vee A \\
 A &= A_1 \wedge A_2 \wedge \dots \wedge A_{48} \\
 GO_2 &= B \vee C \vee GO_3 \\
 GO_3 &= GO_4 \vee GO_5 \vee H \\
 GO_4 &= D \vee E \\
 GO_5 &= F \vee G
 \end{aligned}
 \tag{4.1}$$

so the resultant equation is composed of nine single-order minimal cut sets:

$$Q = CCF \vee A \vee B \vee C \vee D \vee E \vee F \vee G \vee H
 \tag{4.2}$$

where the events are defined as follows:

Q: loss of flow

CCF; common cause failure that causes all the divertor cooling sectors to fail simultaneously

$A_i$ ,  $i = 1$  to 48: failure of divertor cooling circuit  $i$

B: filter plugged

C: motor driven pump fails to run

D: valve 1 fails to remain open

E: catastrophic internal leakage at valve 1

F: valve 2 fails to remain open

G: catastrophic internal leakage at valve 2

H: heat exchanger tube leak

Now we can develop an algebraic equation for the probability of the top event in terms of the probabilities of the basic events:

$$p(Q) = p(CCF + A + B + C + D + E + F + G + H) \quad (4.3)$$

$$p(Q) = p(CCF) + p(A) + p(B) + p(C) + p(D) + p(E) + p(F) + p(G) + p(H) \quad (4.4)$$

Equation 4.4 is exact only if the events are mutually exclusive; otherwise, it might be a good approximation for the case when the probabilities of the events are very small. This is particularly true for nuclear power plants, where the frequencies of occurrence are very small. That is called "the rare event approximation".

If  $A_i$  are independent events, then the probability that all of them will happen simultaneously, known as their joint probability, is:

$$p(A) = p(\prod A_i) = p(A_1) \cdot p(A_2) \cdot \dots \cdot p(A_{48}) \quad (4.5)$$

which is vanishingly small.

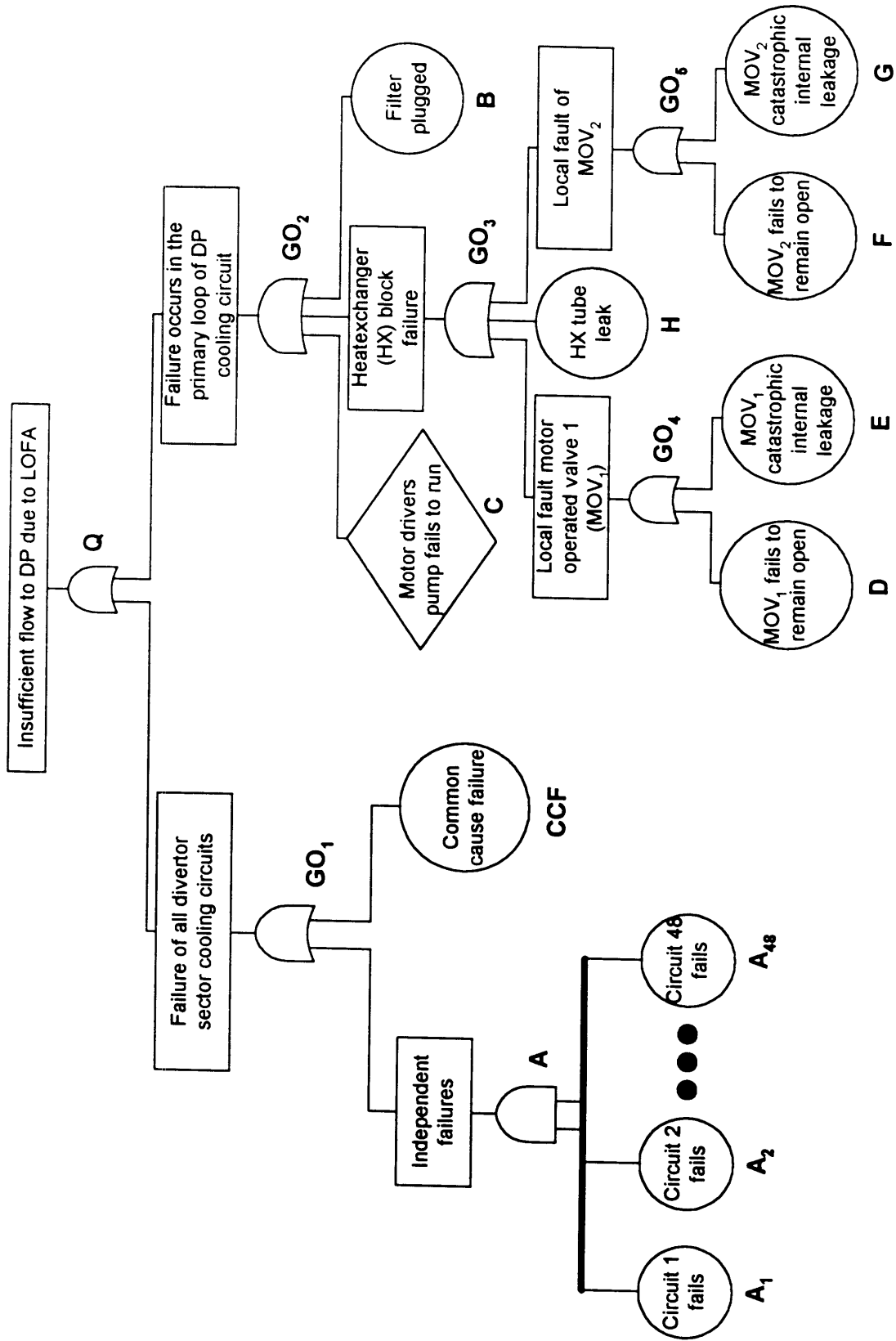


Figure 4-1: Fault Tree for Loss of Flow in divertor coolant loop

It is further assumed that all failures are purely random, so that the failure rate is constant over time. Since the divertor coolant system is operating continuously, this gives rise to exponential distributions (reference [31]) for the component failure frequencies. That is the probability that the component X fails with a failure rate  $\lambda_x$  at a moment of time between zero and time t is as follows:

$$p_x(t) = 1 - e^{-\lambda_x t} \quad (4.6)$$

For small failure rates, the probability can be approximated by  $(\lambda_x t)$ .

Operating experience in the fission industry has shown that some component failures occur essentially simultaneously due to lack of total independence of failure modes among components. These dependent failures are referred to as common cause failures (CCF). Some CCF modes, such as fires and floods, must be dealt with separately and are not considered here. What we consider here are those CCF's which are the result of design errors, construction errors, procedural deficiencies, and unforeseen environmental variations. All of these possible dependencies are analyzed via the beta factor method. The beta factor model considers the total constant failure rate  $\lambda$  of each component to be composed of independent and CCF failure rates:

$$\lambda = \lambda_i + \lambda_c \quad (4.7)$$

where  $\lambda_i$  is the component failure rate for independent failures, and  $\lambda_c$  is the dependent contribution to the component failure rate. When dependent failure occurs, the redundant components are assumed to fail. A parameter  $\beta$  is defined as the fraction of the total component failure rate attributable to CCF.

$$\beta = \frac{\lambda_c}{\lambda_c + \lambda_i} = \frac{\lambda_c}{\lambda} \quad (4.8)$$

so that  $\lambda_c = \beta\lambda$  and  $\lambda_i = (1 - \beta)\lambda$  and  $0 \leq \beta \leq 1$ .

The definition 4.8 can be now used to derive p(CCF):

$$p(CCF) = 1 - e^{-(\beta\lambda_{A_i})t} \quad (4.9)$$

Component	Failure mode	Mean failure rate
Divertor cooling sector	rupture/excessive leakage during operation	1.5E-7/h
Filter	plugging	1.E-5/h
Motor driven pump	fail during operation	1.E-5/h
Motor operating valve	transfer open/close during operation	1.E-7/h
	catastrophic internal leakage	1.E-8/h
Heat exchanger	tube leak	1.E-9/h
	shell leak	1.E-6/h
Fuel pellet injection system	variable injection rate	1.E-3/h
Pipes	small breaks	1.E-2/yr
Beta	common cause	0.13

Table 4.3: Mean failure rates of components and mean beata factor [9]

where  $\beta$  is the beta factor for the divertor coolant sectors.

Now equation 4.4 can be written as:

$$p(Q) = \left[1 - e^{-(\beta\lambda_{A_i})t}\right] + \left[1 - e^{-\lambda_B t}\right] + \left[1 - e^{-\lambda_C t}\right] + \left[1 - e^{-\lambda_D t}\right] + \left[1 - e^{-\lambda_E t}\right] + \left[1 - e^{-\lambda_F t}\right] + \left[1 - e^{-\lambda_G t}\right] + \left[1 - e^{-\lambda_H t}\right] \quad (4.10)$$

An inspection of Table 4.1 reveals that the pump and the filter have the highest failure rates (by at least two orders of magnitude higher than the other components). That is we can approximate equation 4.10 by

$$p(Q) = \left[1 - e^{-\lambda_B t}\right] + \left[1 - e^{-\lambda_C t}\right] = 2 \left[1 - e^{-\lambda_B t}\right] \approx 2\lambda_B t \quad (4.11)$$

since  $\lambda_B$  and  $\lambda_C$  are equal and small.

To obtain the frequency of occurrence of LOFA, and of the other transients, use is made of the definition of the hazard rate (reference [30] page 271):

$$\lambda_i(t) = -\frac{1}{1 - p(Q_i)} \frac{d(1 - p(Q_i))}{dt} \quad (4.12)$$

where the subscript  $i$  is used to denote the transients of category 2; we should note that  $p(Q_i)$  is a function of time.

Using equations 4.11 and 4.12 for LOFA, we get the result:

$$\lambda_{LOFA} \approx 2\lambda_B \quad (4.13)$$

### **Loss of Heat Sink Accident (LHS)**

LHS refers to the loss of the heat exchanger due to a shell leak. Given the failure rate in Table 4-3, the probability that the transient occurs between zero and  $t$  time is given by the equation 4.6 where  $\lambda_x$  is the failure rate of the heat exchanger due to a shell leak  $\lambda_{HX}$ . According to equation 4.13, we get the frequency of LHS accident as:

$$\lambda_{LHS} = \lambda_{HX} \quad (4.14)$$

### **Loss of Coolant Accident (LOCA)**

LOCA refers to a pipe break in the divertor cooling system. The consequences of this transient depend on the break location, and they could be:

1. total or partial loss of heat removal from divertor resulting in temperature transients;
2. implications of the ejected water/steam, i.e. jet forces, pipe whip, splashing water and flooding;
3. pressurization of external structures;
4. mobilization and dispersion of radioactivity.

The LOCA frequency of occurrence may be taken the same as for a fission reactor (reference [10]). This is plausible, since fusion reactors will be constructed with at least the same quality standards as fission reactors. We choose the failure rate for a pipe break equal to the small LOCA (< 51 mm break diameter) frequency of occurrence. As a consequence:



$$\lambda_{LOCA} = \lambda_{small\_LOCA} \quad (4.15)$$

### Overpower Transient (OP)

The overpower transient is the result of an excessive energy production on the plasma side of the divertor, by contrast with the other three category 2 transients which are the result of a deficiency in heat removal on the coolant side of the divertor. OP could be caused by a change in the external delivery rate of the fuel pellets to the plasma. The hourly rate of failure of the fuel injection system is given in Table 4-3; it applies to hours of system operation. Considering the ITER overall availability goal of 25% [15], the frequency of occurrence of an OP transient will then be:

$$\lambda_{OP} = \lambda_{fuel\_inj\_sys} T \quad (4.16)$$

where  $T = 2000 \text{ h/yr}$

## 4.2 Thermal Analysis of the Transients

As we have already mentioned, a disruption is assumed to be induced via the shutdown mechanism after a certain length of time that we will call 'the shutdown mechanism response time' ( $t_r$ ). The values of this time period are taken from current nuclear safety systems figures (reference [32]).

HEATING 7.2 program is used to perform the thermal analysis during the transients by making the appropriate changes in the input file, according to a particular model for each transient. Recall that category 1 transients do not affect the divertor temperature prior to a disruption, so the temperature distribution given as input for the disruption case (problem 3) is the steady-state one. By contrast, the category 2 transients, caused by power balance disturbances, will increase the temperature throughout the divertor plate, therefore they have to be studied separately in problem 2; this can be done by developing models for each transient which consist of different boundary conditions.

A LOCA in the divertor coolant loop is potentially severe, and a conservative thermal model is needed. The blowdown following a LOCA causes the pressure in the coolant loop to

drop rapidly. This causes vapor to form in the cooling channels, which has an insulating effect. The divertor, no longer able to transfer heat to the coolant, begins to heat up rapidly. The conservative assumptions in the model would be:

- the insulated behavior of the divertor starts at the beginning of the transient, that is for problem 2 associated with LOCA the heat transfer coefficients at the cooling channel walls are zero;
- the surface heat flux remains constant (equal to the nominal heat flux) until shutdown occurs.

The only heat transfer mechanism allowed is radiation, in the cooling channels and from the divertor plate to the first wall and the inner vacuum vessel. Reference [33] is a thermal analysis of a tokamak divertor plate after a sudden coolant dry-out; their conclusion is that the extremely high temperature reached makes the heat radiation to be a non negligible heat transfer mechanism.

Relatively to the **overpower transient**, we should note that no detailed analysis, assumptions or discussions appear to exist in literature other than the mention of a generic overpower transient with the exception of references [1] and [41]. Reference [1] develops a scenario in which the normal tritium and deuterium external delivery rate to the plasma is doubled. Our scenario is even simpler: due to some fuel injection abnormalities, the power produced in the plasma increases linearly from the start of the transient until the plasma shutdown, and so does the surface heat flux. This model is similar to the one developed in reference [41]: plasma heat flux increases well above the nominal level with no corresponding increase in the cooling rate.

For the **LHS** scenario, it can be assumed that the heat exchanger is far enough away from the DP's that any temperature increase in the coolant has no effect on the divertor before the shutdown system is activated [1].

The **LOFA** refers to a decrease of the coolant flow rate, which could be modeled as a linear drop to zero during the time  $t_r$  [34], or as a drop to half of the steady-state value throughout the  $t_r$  time period until shutdown [1]. Furthermore, the heat transfer coefficient depends on the flow rate in a power law fashion, i.e.  $h \propto (\dot{m})^n$ , where  $n < 1$ . Though, reference [1] takes the heat transfer coefficient as half of their steady-state values throughout the  $t_r$  time period until

shutdown, and the surface heat flux equal to the nominal value until the shutdown is activated.

Samples of the input files for the LOCA and overpower transient (problem 2) are included in Appendix C, as well as an output file for the overpower transient. The output file can be further used to obtain the detailed temperature distribution.

The problem 2 temperature distribution output represents the input for the **plasma disruption transient** (problem 3). Intense energy fluxes to the in-vessel components are expected to occur during this transient. This high energy deposition in short times may cause severe surface erosion resulting from melting and vaporization. The coating (tungsten in our case) is proposed to protect and maintain the integrity of the underneath structural material from both erosion losses as well as from high thermal stresses encountered during a disruption. The coating thickness should be large enough to withstand both erosion losses and to reduce the temperature rise in the substrate material. Yet the coating thickness should be minimized to reduce the potential problems from radioactivity, toxicity, and plasma contamination.

A disruption scenario is composed of two phases [43]. A thermal quench phase followed by a current quench phase. The duration of the thermal quench is usually short as it ranges from 0.1 to 3.0 ms. The duration of the current quench phase is of the order of 10-50 ms. The energy densities deposited on the divertor plates during the thermal quench are much higher than during the current quench (order of 12 MJ/m<sup>2</sup> as compared to 2 MJ/m<sup>2</sup>). Therefore, in this work, we consider only the thermal phase of the disruption.

The disruption transient model is used to determine the amount of material melted and vaporized that occurs at the coating surface. Appendix C also contains the input file for problem 3 following an overpower transient; we assume that the heat transfer coefficients on the coolant side are not affected, since the surface heat flux will be very high (equal to  $\frac{E_d}{t_d}$ , where  $E_d$  and  $t_d$  are the energy and the time of disruption during) over a short period of time  $t_d$  (of the order of milliseconds).

## 4.3 Uncertainties in the Frequencies of Occurrence of Transients

The point estimate values of the frequencies of occurrence of the transients were presented in the first section of this chapter. This current section evaluates the uncertainties of these values; the objective is to develop distributions that are to be used in the reliability function.

As we will soon see, the uncertainties are very large, which justifies the use of lognormal distributions, as the Reactor Safety Study (RSM) suggests [35]. We assume that our state of knowledge of the frequency of occurrence of a transient is expressed by a lognormal with the 5th and 95th percentiles equal to respectively the lower and upper values of the assessed range, which reflects our belief that there is a 0.90 probability that the frequencies of occurrence are to be found within this assessed range.

### 4.3.1 Category 1 Transients

Estimates for the category 1 transient frequencies of occurrence taken from Sanzo's work (Reference [1]) are shown in Table 4.4. The lognormal distributions shown in Table 4.5 are derived associating the maximum estimate for the event to the 95th percentile, and the minimum estimate for the event to the 5th percentile of the distribution. We use these two values to calculate the parameters  $\mu$  and  $\sigma$  of the lognormal distribution (reference [30]). If  $\lambda_0$  is the midpoint reference value (i.e. the median), and  $K$  is an error factor constant ( $K > 1$ ), then  $\lambda_L = \frac{\lambda_0}{K}$  and  $\lambda_U = \lambda_0 K$ , where  $\lambda_L$  and  $\lambda_U$  are respectively the lower and the upper values of the assessed range. When  $\lambda$  falls in the range  $[\frac{\lambda_0}{K}, \lambda_0 K]$  with a  $100(1 - 2\alpha)$  percentile certainty ( $\alpha$  is 5% in our case), then the lognormal distribution has parameters  $\mu = \log \lambda_0$  and  $\sigma = \frac{\log K}{L}$ , where  $L$  is the  $100(1 - \alpha)$  percentile of the normal distribution with the mean of zero and variance of unity. As a consequence, the median, the mean and the variance can be calculated using the equations:

$$\begin{aligned}
 \text{Median} : \lambda_0 &= e^\mu \text{ or } \lambda_0 = \sqrt{\lambda_L \lambda_U} \\
 \text{Mean} : \lambda_{mean} &= e^{\mu + 0.5\sigma^2} \\
 \text{Variance} : V &= e^{2\mu + \sigma^2} (e^{\sigma^2} - 1)
 \end{aligned}
 \tag{4.17}$$

<b>Transient</b>	<b>Transient frequency [per year]</b>
1. Auxiliary heating system disturbances	0.5 - 22.0
2. Magnet system disturbances	0.2 - 3.9
3. Main coolant disturbances	0.9 - 3.0
4. Balance of plant disturbances	0.7 - 17.2
5. Internal plasma disturbances	122.0 - 2200.0

Table 4.4: Estimates of frequencies of occurrence of category 1 transients [1]

<b>Transient</b>	<b>5th % (/yr)</b>	<b>Median (/yr) <math>\lambda_0</math></b>	<b>95th % (/yr)</b>	<b>Mean (/yr) <math>\lambda_{\text{mean}}</math></b>	<b>Variance (/yr<sup>2</sup>) V</b>
1. Auxiliary heating system disturbances	0.5	3.3	22.0	6.42	113.65
2. Magnet systems disturbances	0.2	0.88	3.9	1.32	2.22
3. Main coolant disturbances	0.9	1.6	3.0	1.76	0.44
4. Balance of plant disturbances	0.7	3.5	17.0	5.52	47.61
5. Internal plasma disturbances	122.0	510.0	2200.0	759.55	6.834·10 <sup>5</sup>

Table 4.5: Probability distributions for frequencies of occurrence of category 1 transients

### 4.3.2 Category 2 Transients

We calculated the point estimates of the frequencies of occurrence based on the failure rates of relevant component groups [36]. These component groups were structured from individual components, with their associated failure rates. This implies uncertainties in the frequencies of occurrence of category 2 transients derived from uncertainties in failure rates of components involved in a particular transient.

The median values ( $\lambda_0$ ) of the different components failure rates and their associated error factors ( $K$ ) as taken from references [9] and [15] are presented in Table 4.6. We calculate the parameters  $\mu$  and  $\sigma$ , and then the mean and the variance of the lognormal distributions for each component by using the equations in the previous section.

Since LHS, LOCA and OP transients are basically the results of a single component failure, the estimation of their distributions is straightforward. For LOFA, the calculation is more elaborate: we obtain the probability distribution function of the transient frequency of occurrence by adding the different component failure rates distributions. That is done by conforming to the following rules [31]:

1. the mean of the resultant distribution is the sum of the means of the component distributions;
2. the variance of the resultant distribution is the sum of the individual variances of the component distributions.

The resulting lognormal distributions are presented in Table 4.7.

### 4.3.3 Catastrophic and non-catastrophic transients

In order to derive an analytical expression for the reliability, the category 1 and 2 transients are divided into catastrophic and non-catastrophic groups.

LOCA is considered the only catastrophic transient in this work, as there may be no coolant in the divertor cooling loop during disruption; this would make impossible the beginning of a new on-cycle. The frequency of occurrence of the catastrophic transient group will be then given by:

<b>Component</b>	<b>Failure mode</b>	<b>Median (/h) <math>\lambda_0</math></b>	<b>Error factor K</b>	<b>Mean (/h) <math>\lambda_{mean}</math></b>	<b>Variance (/h<sup>2</sup>) V</b>
Divertor cooling sector	rupture/excessive leakage	1.5E-7	10	4.0E-7	9.7E-13
Filter	plugging	1.E-5	10	2.7E-5	4.3E-9
Motor driven pump	fail during operation	1.E-5	10	2.7E-5	4.3E-9
Motor operated valve	transfer open/close	1.E-7	3	1.25E-7	8.8E-15
	internal leakage	1.E-8	100	5.0E-7	6.4E-10
Heat exchanger	tube leak	1.E-9	10	2.7E-9	0
	shell leak	1.E-6	10	2.7E-6	4.3E-11
Fuel gas inj. sys.	variable inj. rate	1.E-3	10	0.003	4.3E-5
Pipe	small break	1.E-2/yr	10	0.027/yr	0.004/yr <sup>2</sup>

Table 4.6: Component failure rates [9,15]

<b>Transient</b>	<b>Median (/yr)</b>	<b>Mean (/yr)</b>	<b>Variance (/yr<sup>2</sup>)</b>
1. Loss of Flow Accident	1.75E-2	0.486	0.762
2. Loss of Heat Sink	8.76E-3	0.023	0.003
3. Loss of Coolant Accident	1.E-2	0.027	4.0E-3
4. Overpower Transient	2.0	5.3	173.0

Table 4.7: Probability distributions for frequencies of occurrence of category 2 transients

$$\lambda_c = \lambda_{LOCA} \quad (4.18)$$

The category 1 transients together with the all remaining category 2 transients are considered non-catastrophic transients. It is assumed that the divertor can recover from a heat transfer point of view for these transients, and the beginning of a new cycle is not precluded. The frequency of occurrence of the non-catastrophic transient group will be:

$$\lambda_{nc} = \sum_{i=1}^5 \lambda_{cat1,i} + \lambda_{OP} + \lambda_{LHS} + \lambda_{LOFA} \quad (4.19)$$

Using the fact that the mean and variance of a sum of random variables are given by the sum of the individual means and variances (reference [31]), we generate lognormal distributions for  $\lambda_c$  and  $\lambda_{nc}$ . This results in the lognormal distributions with the parameters  $\mu$  and  $\sigma$  shown in Table 4.8.

Appendix D contains the calculations performed with MATHCAD for the uncertainties in the frequencies of occurrence of the transients.

#### 4.4 Parameters affecting Material Loss

In Section 4.2, we presented the deterministic models for the transients that could be used to determine the material loss by running HEATING 7.2 program.



Parameter	Mean (/yr)	Variance (/yr <sup>2</sup> )	$\mu$	$\sigma$
Frequency of occurrence of catastrophic transients	0.027	4.0E-3	-4.605	1.4
Frequency of occurrence of non-catastrophic transients	780.4	6.84E5	6.3	0.87

Table 4.8: Probability distributions of the frequencies of occurrence for catastrophic and non-catastrophic transients

The reliability function depends on the material loss due to melting and vaporization during the transients, which is an uncertain parameter. The material loss ( $Y$ ) depends on several parameters with uncertainties. In the present work, only three of these parameters are considered, the first of them appearing in problem 2, and the last two appearing in problem 3:

- the response time of the shutdown mechanism ( $t_r$ );
- the surface heat flux at the divertor plate during a disruption ( $H$ );
- the duration of a disruption ( $t_d$ ).

This section presents the probability distribution functions associated with these parameters, and a method to propagate these distributions through the transient model to obtain a probability distribution function of the material loss during the transients.

#### 4.4.1 Uncertainties in the parameters affecting the material loss

Since the uncertainty in the  $t_r$  parameter is not as large as the uncertainties in  $H$  and  $t_d$  (based on the existent experience in the fission power plants), we associate to it a normal distribution with the 5th percentile equal to the lower limit of the range and the 95th percentile equal to the upper limit of the range; as estimated in reference [32], the range is 1 to 3 seconds.

The parameters  $\mu$  and  $\sigma$  of the normal distribution are equal to the mean and respectively variance of the normal distribution, and are calculated as follows:

$$\begin{aligned}
t_r &= \frac{t_{r,L} + t_{r,U}}{2} \\
\sigma &= \frac{t_{r,U} - \mu}{T_{r,U}}
\end{aligned}
\tag{4.20}$$

where  $t_{r,L} = 1s$ ,  $t_{r,U} = 3s$ , and  $T_{r,U}$  is the standard substitution of the form  $T_{r,U} = \frac{t_{r,U} - \mu}{\sigma}$ ;  $T_{r,U}$  value is found in the table of the cumulative normal distribution function (reference [31]).

The disruption parameter ranges are those considered for the ITER divertor technology phase:

- disruption time:  $t_d = 0.1$  to  $3$  ms;
- disruption energy:  $E_d = 5$  to  $20$  MJ/m<sup>2</sup>.

We associate lognormal distributions to these parameters by taking the maximum estimate for the event equal to the 95th percentile, and the minimum estimate for the event equal to the 5th percentile of the distribution. We use equation 4.17 to determine the  $\mu$  and  $\sigma$  parameters of the distributions.

The material loss does not depend explicitly on the  $E_d$ , but on the surface heat flux  $H$ , where  $H = \frac{E_d}{t_d}$ . Hence, the distribution of  $H$  is also lognormal and its parameters are (reference[31]):

$$\begin{aligned}
\mu_H &= \mu_{E_d} - \mu_{t_d} \\
\sigma_H^2 &= \sigma_{E_d}^2 + \sigma_{t_d}^2
\end{aligned}
\tag{4.21}$$

Table 4.9 contains the  $\mu$  and  $\sigma$  values of the parameters affecting the material loss, as calculated with MATHCAD (Appendix D).

#### 4.4.2 Uncertainty of the Material Loss

The problem now is to find the distribution of a random variable (material loss during transients,  $Y$ ) that is a function of three random variables with known distributions of varying degrees of precision. An analytic form for the propagation of the input probability distribution functions (pdf's) through the finite-difference heat conduction code (HEATING 7.2) may be difficult to derive, if not impossible.

One alternative to the analytic approach is to approximate the output pdf by finding the moments of the distribution. These moments can be found by use of a Monte Carlo sampling

Parameter	5th %	95th %	$\mu$	$\sigma$
Response time (s)	1	3	2	0.608
Disruption energy (MJ/m <sup>2</sup> )	5	20	2.303	0.421
Disruption time (ms)	0.1	3	- 0.602	1.034
Disruption heat flux (10 <sup>9</sup> W/m <sup>2</sup> )	3	115	2.905	1.116

Table 4.9: Probability distributions for the parameters affecting the material loss

technique. By sampling the input pdf's and finding the resultant consequence (Y) for each sample set, the moments of the pdf for the output consequence can be obtained. Each Monte Carlo sample of the input parameters requires a separate expensive computer run, and the Monte Carlo approach will often require thousands of runs to determine a statistically meaningful output pdf. The combination of a finite-difference heat conduction code with Monte Carlo sampling is too expensive and too time consuming to be practical.

To minimize computer time, a simplified but accurate approximation to the output of the HEATING finite-difference code is required. Fortunately, methods have been devised to model the output of complex codes by simplified equations, usually polynomials of either first or second order. These methods are called Response Surface Methodology (RSM).

The basic RSM approach [37, 38, 39] is to model a complex problem which has a consequence ( $\varepsilon$ ) dependent on n input parameters ( $x_i$ ) with a function of the following form:

$$\varepsilon = a_0 + \sum_{i=1}^n b_i \cdot x_i + \sum_{i=1}^n c_i \cdot x_i^2 + \sum_{i=1}^n \sum_{j=1}^n d_{ij} \cdot x_i \cdot x_j \quad (4.22)$$

where  $a_0$ ,  $b_i$ ,  $c_i$ , and  $d_{ij}$  are constant coefficients determined by matching  $\varepsilon$  at various values of  $x_i$ .

Such a simplified model requires only a relatively few runs of the complex code to obtain sufficient information to establish all the coefficients. Then, input parameters with uncertainties can be varied in a proper statistical manner (such as Monte Carlo) to provide adequate statistics

for the moments of the pdf of the consequence of interest. This approach can be accomplished with relatively modest computational expense. In addition, the sensitivity of the various input parameters can be easily found.

A second-order response surface for the approximation of a given consequence,  $\zeta(\bar{z})$ , as a function of the accident parameters,  $z_1, \dots, z_n$ , has the following form:

$$\tilde{\zeta}(\bar{z}) = A + \sum_{j=1}^n \left[ \left[ B_j + C_j (z_j - z_{j0}) + \sum_{k=j+1}^n D_{jk} (z_k - z_{k0}) \right] (z_j - z_{j0}) \right] \quad (4.23)$$

where  $z_j$  is the  $j^{\text{th}}$  parameter of  $\bar{z}$  and the vector  $\bar{z}_0 = (z_{10}, z_{20}, \dots, z_{n0})$  is a reference point, usually the mean of the individual parameters.

For determining all coefficients, several methods can be used; one of them is the Lagrange interpolation technique extended to a multivariate case. Algebraic expressions are obtained for coefficients, thereby avoiding the need for a matrix inversion:

$$\begin{aligned} A &= \zeta_0 \\ B_j &= R_{j1} (z_{j0} - z_{j2}) + R_{j2} (z_{j0} - z_{j1}) \\ C_j &= R_{j1} + R_{j2} \end{aligned}$$

where

$$\begin{aligned} R_{j1} &= \frac{\zeta_1(j) - \zeta_0}{(z_{j1} - z_{j0})(z_{j1} - z_{j2})} \\ R_{j2} &= \frac{\zeta_2(j) - \zeta_0}{(z_{j2} - z_{j0})(z_{j2} - z_{j1})} \\ D_{jk} &= \frac{\zeta_0 + \zeta_{11}(j,k) - \zeta_1(j) - \zeta_1(k)}{(z_{j1} - z_{j0})(z_{k1} - z_{k0})} \end{aligned} \quad (4.24)$$

for all  $j = 1, \dots, n$  and selected pairs  $j, k$ . The vector  $\bar{z}_0$  is defined for equation 4.23, and  $\zeta_0 = \zeta(\bar{z}_0)$ . In addition,  $z_{j1}$  and  $z_{j2}$  are two other values of  $z_j$  which give

$$\begin{aligned} \zeta_1(j) &= \zeta(z_j = z_{j1}) \\ \zeta_2(j) &= \zeta(z_j = z_{j2}) \\ \zeta_{11}(j, k) &= \zeta(z_j = z_{j1}, z_k = z_{k1}) \end{aligned} \quad (4.25)$$

The other components of  $\bar{z}$  not given as arguments of  $\zeta$  above have as their values  $z_l = z_{l0}$ , i.e.

$$\zeta_1(j) = \zeta(z_{10}, z_{20}, \dots, z_{j-1,0}, z_{j1}, z_{j+1,0}, \dots, z_{n0}) \quad (4.26)$$

The values of  $z_{j0}$ ,  $z_{j1}$ , and  $z_{j2}$  are taken so that  $z_{j0}$  is the mean value of  $z_j$ , and  $z_{j1}$  and  $z_{j2}$  are calculated from:

$$\int_{z_{j1}}^{\infty} f_j(z_j) dz_j = \int_{-\infty}^{z_{j2}} f_j(z_j) dz_j = p \quad (4.27)$$

where  $f_j(z_j)$  is the probability density function of  $z_j$  and  $p$  is a probability truncation limit. If a 90% confidence level is desired, this would lead to a choice of  $p = 0.05$ .

The resultant points  $z_{j0}$ ,  $z_{j1}$ , and  $z_{j2}$ , called knot-points, are illustrated in Figure 4-2. This selection of points provides values of  $\zeta$  at the high and low truncation values of  $z_j$  ( $z_{j1}$  and  $z_{j2}$ ), the center (mean,  $z_{j0}$ ) value, and a single interaction point,  $\zeta_{11}$ , in the quadrant where  $(z_j - z_{j0})$  and  $(z_k - z_{k0})$  are both positive. Solving the second order response surface by this method gives a solution with a minimum number of required values of  $\zeta$ . However, this method has two disadvantages:

1. the interaction term,  $\zeta_{11}(j, k)$ , is determined only in one quadrant;
2. using a single response surface over the entire parameter range may not adequately model complex shapes (i.e., the effect of the higher terms).

A different knot-point selection scheme (Figure 4-3) could be used for a better model of  $\zeta$  over the entire range. Here the new points:

$$\begin{aligned} z_{j3} &= z_{j0} + \frac{z_{j1} - z_{j0}}{\sqrt{2}} \\ z_{j4} &= z_{j0} + \frac{z_{j2} - z_{j0}}{\sqrt{2}} \end{aligned} \quad (4.28)$$

are used to generate separate response surfaces in each quadrant. By subdividing the parameter range, a more accurate prediction of the main and interaction effects results. When calculating the consequence,  $\zeta$ , the coefficients used for particular  $z_j$  and combinations of  $z_j$  and  $z_k$  depend on the quadrant in which they fall. This improved knot-point selection scheme requires  $1 + 4 \cdot n + 2 \cdot n \cdot (n - 1)$  values of  $\zeta$  (versus  $1 + 2 \cdot n + \frac{n \cdot (n-1)}{2}$  for a single response surface).

For the problem at hand, the second-order response surface for the approximation of the

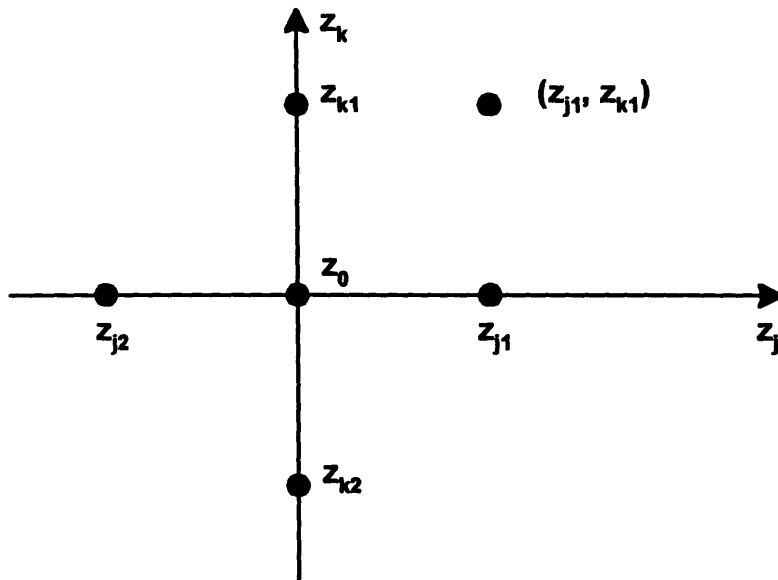


Figure 4-2: Knot-points for single quadrant response surface

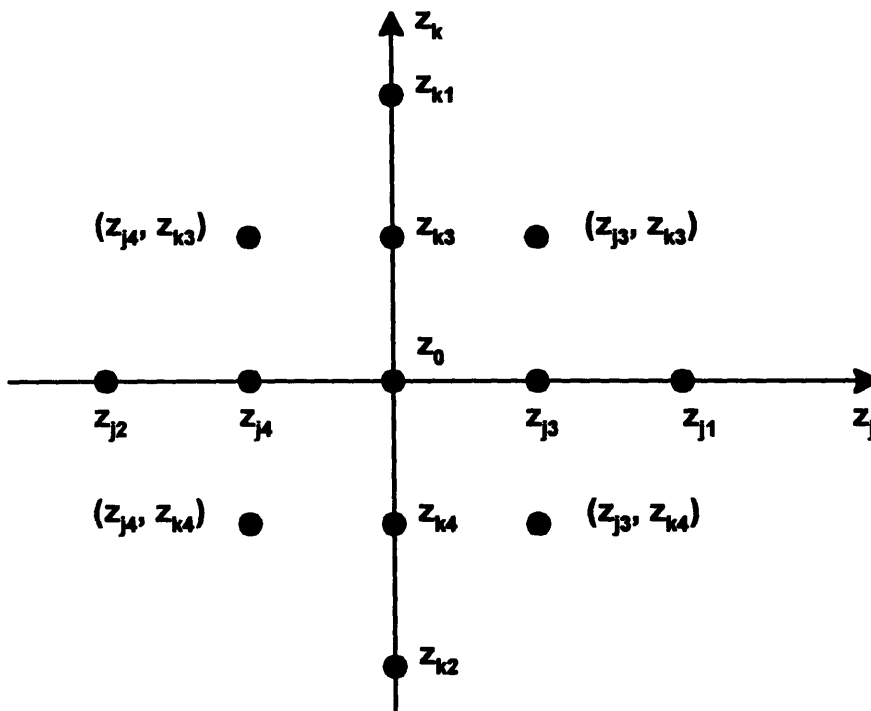


Figure 4-3: Knot-points for multi quadrant response surface

material loss,  $\tilde{Y}$ , as a function of the parameters  $t_r$ ,  $t_d$  and  $H$  has the following functional form:

$$\begin{aligned} \tilde{Y}(t_r, t_d, H) = & A_0 + B_r + C_r(t_r - \bar{t}_r) + B_d + C_d(t_d - \bar{t}_d) + B_H + C_H(H - \bar{H}) + \\ & + D_{rd}(t_r - \bar{t}_r)(t_d - \bar{t}_d) + D_{rH}(t_r - \bar{t}_r)(H - \bar{H}) + D_{dH}(t_d - \bar{t}_d)(H - \bar{H}) \end{aligned} \quad (4.29)$$

where  $\bar{t}_r$ ,  $\bar{t}_d$ , and  $\bar{H}$  are mean values, and the coefficients are derived using a multi quadrant response surface. Knot-points as those defined in equation 4.28 are used for the three parameters. The calculation of the coefficients is presented in Appendix E.

Additional points at which the material loss  $Y$  is found with HEATING 7.2 have been used to check for fit of the second order response surface  $\tilde{Y}$  to the original material loss  $Y$ . Error factors of the order of -20% and +20% have been found; exceptions are the material losses calculated for values of the parameters  $t_r$ ,  $t_d$  and  $H$  close to the margins of their estimated ranges, which generate higher error factors.

The measure  $I_j = |Y_{1j} - Y_o| + |Y_{2j} - Y_o|$ , where  $j = r, d, \text{ or } H$ ,  $Y_o = Y(\bar{t}_r, \bar{t}_d, \bar{H})$ , and for example  $Y_{1r} = Y(t_{r1}, \bar{t}_d, \bar{H})$ ,  $Y_{2r} = Y(t_{r2}, \bar{t}_d, \bar{H})$ , gives an indication about the sensitivity/importance of the individual parameters. As a result, we observe that the material loss is the most sensitive to the disruption time  $t_d$  variations, and the least sensitive to the variations of response time  $t_r$ .

Although a response surface for the material loss that fits better to the HEATING 7.2 program results could be evaluated, we consider the function from equation 4.29 with the coefficients from Appendix E as being acceptable for our purposes.

## Chapter 5

# Generation of Reliability Function

In the previous chapters, we have defined all the parameters with their associated uncertainties that are needed to calculate the divertor reliability. In this chapter, we develop an analytical reliability function, and explain the methodology used to propagate the uncertainties of the parameters through this function.

### 5.1 Development of a stochastic reliability function

We should now recall some important concepts:

- **reliability** means the frequency (fraction of times) with which the component performs its intended function without failure for a specified period of time;
- **failure** refers to a component becoming non-functional under a given set of Failure Criteria (FC) corresponding to a postulated set of Failure Modes (FM's);
- **quantifying reliability** involves calculating the minimum time to failure under the FC corresponding to all the FM's of interest. It also involves choosing a particular set of values for the variables. The reliability at a given point in time actually has a probability distribution associated with it due to the uncertainties in variables. As an example, in Figure 2-2,  $R_{10}(t_0)$  expresses our belief that there is a probability of 0.1 that the reliability is less than or equal to 0.5 at  $t_0$ .

We have used the following assumptions in developing the reliability function:



1. Occurrence of transients is Poisson distributed in time (reference [40]), and the only statistical uncertainty. Therefore, the time between transients is distributed exponentially (reference [40], example 5d, page 135).
2. The frequency of occurrence of a transient is not changed by the occurrence of another transient.
3. All the transient events require plasma shutdown performed by an induced disruption, in order to minimize potential reactor damages; therefore, it is impossible to have more than one non-catastrophic transient per cycle. Recall that ITER is a pulsed machine. We use the following notations:  $n$  is the number of cycles that have occurred,  $k$  is the number of non-catastrophic transients that have occurred,  $t_p$  is the "on" time of each cycle. As a consequence, we can translate this assumption into a mathematical form:

$$k \leq n \quad (5.1)$$

4. Even when the shutdown occurs before the end of a normal cycle, we still take the duration of that "on" cycle equal to  $t_p = 2000$  seconds.
5. Using assumption (1), we define the probability that a non-catastrophic transient occurs in time  $t_p$  as:

$$p = 1 - e^{-\lambda_{nc} t_p} \quad (5.2)$$

where  $\lambda_{nc}$  is the frequency of occurrence of non-catastrophic transients.

6. Using assumption (3), the frequency of  $k$  non-catastrophic transients in  $n$  cycles is binomial [40] and given by:

$$fr(k \text{ non-catastrophic transients in } n \text{ cycles}) = \binom{n}{k} p^k (1 - p)^{n-k} \quad (5.3)$$

where:  $\binom{n}{k} = \frac{n!}{k!(n-k)!}$

7. Since the primary objective of this work is to develop a methodology to calculate the divertor reliability, we can afford to use only one failure mode, the material loss, although

this might not be accurate when calculating a component reliability (especially if this failure mode is not the dominant one for the type of machine considered). Once the methodology is completed, other failure modes can be easily included in the model. In order to balance this non-conservative assumption, we consider that all the material melted and vaporized during disruption is lost, so we do not account for redeposition of melted material. In addition to these material loss sources, there is an erosion of the coating during normal operation. We use the following model to account for these effects, and determine when failure occurs:

$$\varepsilon \cdot t_p \cdot n + \sum_{\substack{\# \text{ of non-catastrophic} \\ \text{transients in } n \text{ cycles}}} Y_i \leq \Delta \quad (5.4)$$

where:

$\varepsilon$  = material erosion rate during normal operation;

$Y_i$  = amount of material lost during a transient;

$\Delta$  = some predetermined limit (e.g., coating thickness; to be more conservative, we take half of the coating thickness).

8.  $Y_i$  is constant for all transients. This is justified by the fact that the material loss is much more sensitive to the disruption parameters than to the nature of the transient. With more knowledge about the nature of transients,  $Y_i$  may become transient dependent or characterized as statistical uncertainty. As a consequence, we can write:

$$\sum_{\substack{\# \text{ of non-catastrophic} \\ \text{transients in } n \text{ cycles}}} Y_i = k \cdot Y \quad (5.5)$$

where  $Y$  is the material loss following an overpower transient. We choose the overpower transient as generic for the non-catastrophic transients since the material loss is expected to be higher due to a higher temperature at the beginning of disruption. Recall that the non-catastrophic transient group contains the category 1 transients and the following category 2 transients: LHS, LOFA, and overpower transient. By combining equations 5.4 and 5.5, we obtain:

$$\varepsilon \cdot t_p \cdot n + k \cdot Y \leq \Delta \quad (5.6)$$

At this point we can write the reliability at time  $t$  after  $n$  cycles as:

$$R(t|\bar{\Phi}) = fr \left[ \begin{array}{l} \text{(no catastrophic transients in } n \text{ cycles)} \wedge \\ \text{(\# of cycles to failure due to material loss } \geq n) \end{array} \right] \quad (5.7)$$

where  $t = nt_p$ , and  $\bar{\Phi}$  is a vector whose elements are the uncertain parameters used to define the reliability function;  $\bar{\Phi} = (\lambda_c, \lambda_{nc}, Y(t_r, t_d, H))$ . That is:

$$R(t|\bar{\Phi}) = fr(\text{no catastrophic transients in } n \text{ cycles}) \cdot \sum_{k=0}^n [fr(k \text{ non-catastrophic transients in } n \text{ cycles}) \cdot fr(\text{FC has not been reached})] \quad (5.8)$$

If  $k_{\max}$  is the maximum number of the non-catastrophic transients that the divertor plate can survive without having reached the FC, equation 5.8 becomes:

$$R(t|\bar{\Phi}) = fr(\text{no catastrophic transients in } n \text{ cycles}) \cdot \sum_{k=0}^{k_{\max}} fr(k \text{ non-catastrophic transients in } n \text{ cycles}) \quad (5.9)$$

$k_{\max}$  is determined by two simultaneous conditions given by the equations 5.1 and 5.6. Figure 5-1 explains the way  $k_{\max}$  is calculated for a given amount of the material loss in order to calculate the divertor reliability after  $n^*$  cycles:  $k_{\max}$  is limited by two lines: (1)  $k = n$ , (2)  $k \cdot Y + \varepsilon \cdot t_p \cdot n = \Delta$ . That is failure does not occur as long as the points  $(k, n)$  are in the hatched area in Figure 5-1.  $n_{\max}$  is the maximum number of cycles that DP could survive in case no transients have occurred.

We assume the frequency of occurrence of catastrophic transients is exponentially distributed; then, the frequency of no catastrophic transients in  $n$  cycles is given by:

$$fr(\text{no catastrophic transients in } n \text{ cycles}) = e^{-\lambda_c n t_p} \quad (5.10)$$

By combining equations 5.3, 5.9, and 5.10, we obtain the stochastic reliability function:

$$R(t|\Phi) = e^{-\lambda_c n t p} \cdot \sum_{k=0}^{k_{\max}} \left( \frac{n!}{k! (n-k)!} p^k (1-p)^{n-k} \right) \quad (5.11)$$

## 5.2 Propagation of Uncertainties

At this point, we have developed an analytical function for reliability, which depends on a set of uncertain parameters. The uncertainties of all these parameters have already been evaluated in the previous chapter by expressing them as probability distributions characterized by the parameters  $\mu$  and  $\sigma$ .

We choose to propagate the uncertainties through the reliability function using MATHCAD, because it is a very interactive program. Steps in the calculations are performed one at a time, so one can easily notice when an error occurs. The algorithm is presented in Appendix F.

A normal distribution function has been related to the time of response of the shutdown mechanism as follows:

$$f(t_r) = \frac{1}{\sigma_r \sqrt{2\pi}} \cdot e^{-\frac{(t_r - \mu_r)^2}{2\sigma_r^2}} \quad (5.12)$$

So, in order to propagate uncertainties in the parameter  $t_r$ , we need to generate  $t_r$  values that follow this probability distribution function (pdf), that is we want to obtain the inverse function of  $f(t_r)$ :

$$t_{r_i} = \mu_r + \sigma_r \sqrt{-2 \ln(\text{rnd}(1))} \cdot \cos(2\pi \cdot \text{rnd}(1)) \quad (5.13)$$

where  $\text{rnd}(1)$  is a function that returns a uniformly distributed random number between 0 and 1. If  $i$  takes values from 0 to 2000 for example,  $\text{rnd}$  function generates 2001 different random numbers; by plotting a histogram with  $t_{r_i}$  values, we obtain a normal distribution. Note that the function given in equation 5.12 is not bijective (two values of  $t_r$  correspond to the same value of  $f(t_r)$ ), but since it is symmetric, we first obtain the inverse for half of the  $t_r$  values ( $t_r \in (0, \text{mean } mt_r)$ ), then we multiply the inverse function obtained by the factor  $\cos(2\pi \cdot \text{rnd}(1))$ .

Lognormal distribution functions have been associated to all the other uncertain parameters

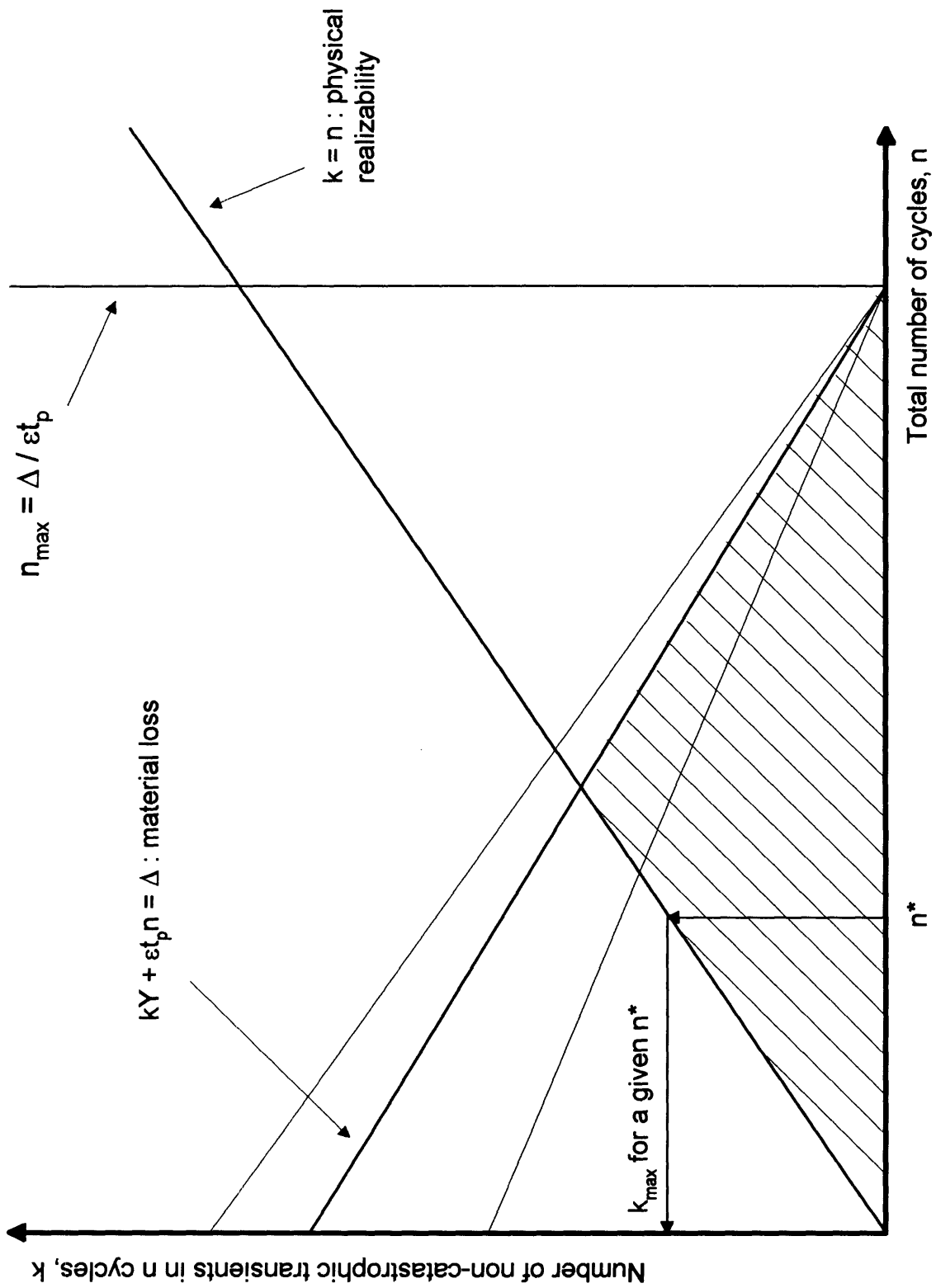


Figure 5-1:  $(k, n)$  plane

considered here:  $t_d, H, \lambda_c, \lambda_{nc}$  :

$$g(x) = \frac{1}{x\sigma\sqrt{2\pi}} \cdot e^{-\frac{(\ln(x)-\mu)^2}{2\sigma^2}} \quad (5.14)$$

where  $x$  is one of the four parameters, and  $\mu$  and  $\sigma$  are the characteristic parameters of the associated lognormal distribution. Using a similar approach as for the normal distribution, we obtain the inverse function of the lognormal distribution:

$$x = e^{\mu - \sigma^2 + \sqrt{-2\sigma^2 \ln(\text{rnd}(1))} \cdot \cos(2\pi \cdot \text{rnd}(1))} \quad (5.15)$$

As a result, for each random number between 0 and 1 generated by the rnd function we obtain one value for each of the functions:  $\lambda_{c_i}, \lambda_{nc_i}, t_{r_i}, t_{d_i}, H$ ; the last three of these values are used to calculate one value of the material loss  $\tilde{Y}_i$ , according to equation 4.29, which in turn generates a value for  $k_{\max_i}$ , as explained in Figure 5-1. The reliability after  $n^*$  cycles for this particular value of rnd function is calculated:

$$R_i(n^* t_p | \Phi_i) = e^{-\lambda_{c_i} n^* t_p} \cdot \sum_{k=0}^{k_{\max_i}} \left( \frac{n^*!}{k! (n^* - k)!} p_i^k (1 - p_i)^{n^* - k} \right) \quad (5.16)$$

where

$$p_i = 1 - e^{-\lambda_{nc_i} t_p}$$

So, for each value of  $n$ , taking  $i$  from 0 to 2000, we obtain a pdf,  $h(R)$ , for reliability. This function is used to generate the following three reliability values:  $R_{10\%}, R_{50\%}, R_{90\%}$ , as follows:

$$\begin{aligned} \int_0^{R_{10\%}} h(R) dR &= 0.10 \\ \int_0^{R_{50\%}} h(R) dR &= 0.50 \\ \int_0^{R_{90\%}} h(R) dR &= 0.90 \end{aligned} \quad (5.17)$$

where  $R_q\%$  (with  $q = 10\%, 50\%, 90\%$ ) expresses our belief that there is a  $q\%$  probability that the reliability after  $n$  cycles is less than or equal to this value.

By obtaining, for example, 10 reliability pdf's corresponding to 10 values of  $n^*$ 's, we can now draw the reliability curves as initially shown in Figure 2-2.

When using MATHCAD to develop this algorithm several difficulties have been encountered:

- Calculating  $k_{\max}$  as shown above does not necessarily results in an integer value, as it is required to calculate the reliability since  $k_{\max}$  is the upper limit of a sum. However, MATHCAD version 4.0 has a logical operator which returns only a zero or a one; by multiplying the expression under the sum in equation 5.16 with the expression  $(k_{\max_i} \geq k)$ , MATHCAD adds only those terms of the sum for which the expression returns a one; in other words, for the terms of the sum with  $k > k_{\max_i}$ , MATHCAD returns a zero, so that they are not actually added to the sum.
- Equation 5.16 contains the factorial operator (!), but MATHCAD can only calculate the factorial for values up to 170 (170!); our problem implies values of n of the order of thousands. We have resolved this problem by calculating the terms of the binomial distribution using an iteration:

$$\begin{aligned}
 D_0 &= (1 - p)^n \\
 D_{q+1} &= D_q \cdot \frac{n-q}{q+1} \cdot \frac{p}{1-p}
 \end{aligned}
 \tag{5.18}$$

Figures 5-2 and 5-3 contain the reliability curves as obtained from the calculations in Appendix F. The two figures basically show the same reliability results as a function of time (in years) and as a function of the number of cycles respectively.

Figure 5-2 shows that there is a 90% probability that the reliability is zero after 0.34 year, and a 10% probability that the reliability is zero after 0.05 year. In other words, there is a probability of failure of divertor plates of 90% after 0.34 year, and 10% after 0.05 year. That is basically due to the high heat loads during disruption transients. If the ITER reactor could be designed such that no transients of any type occurred, the divertor reliability would be perfect until erosion of material during normal operation resulted in failure. Moreover, if transients occurred, but the shutdown mechanism did not induce any disruption, divertor reliability could be significantly improved.

$i := 0..10$

$t_i :=$	$R10\%_i :=$	$R50\%_i :=$	$R90\%_i :=$	$n_i :=$
0.001	1.	1	1	0
0.0482	$2.193 \cdot 10^{-5}$	0.958	1	760
0.0723	$7.166 \cdot 10^{-11}$	0.232	1	1140
0.0964	0	0.052	1	1520
0.1446	0	$3.098 \cdot 10^{-5}$	0.999	2280
0.193	0	$6.016 \cdot 10^{-10}$	0.925	3040
0.241	0	0	0.317	3800
0.2892	0	0	0.013	4560
0.3374	0	0	$5.917 \cdot 10^{-6}$	5320
0.3856	0	0	$3.456 \cdot 10^{-10}$	6080
0.488	0	0	0	7692

[years]

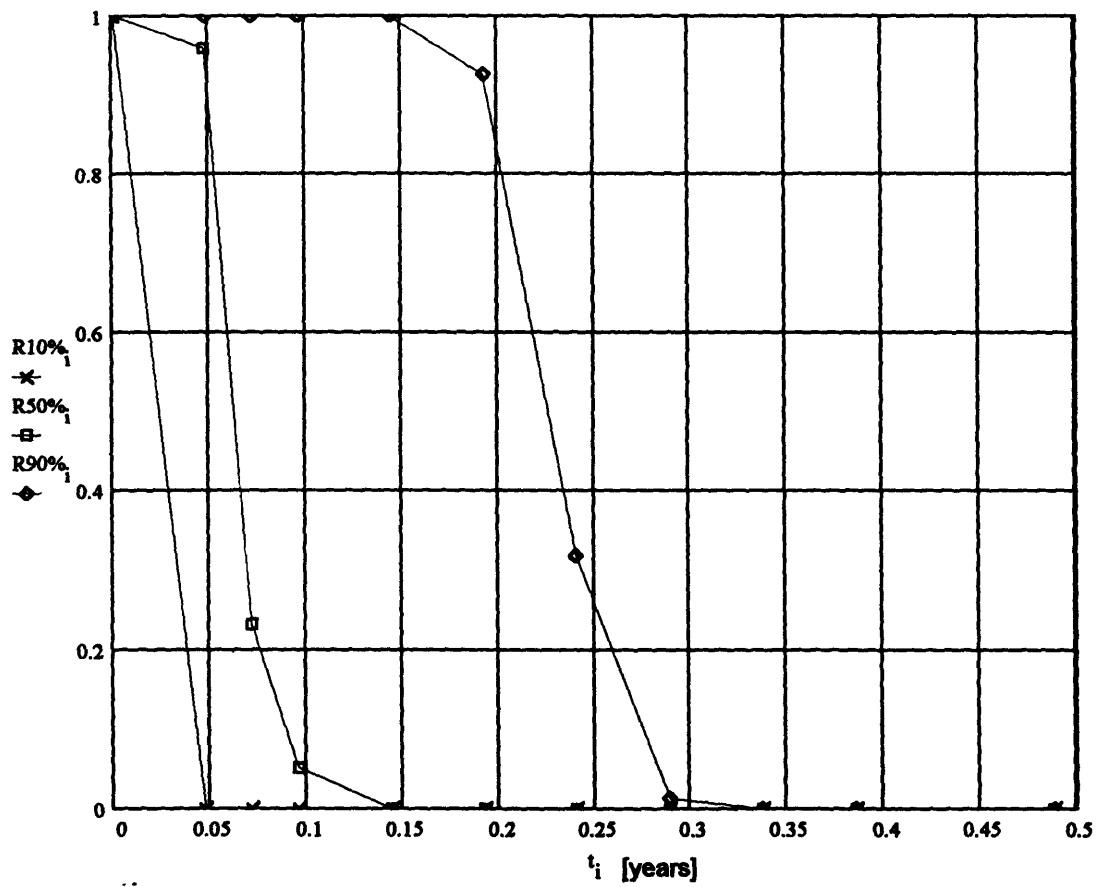


Figure 5-2: Divertor reliability versus time



$i = 0..10$

$t_i :=$	$R10\%_i :=$	$R50\%_i :=$	$R90\%_i :=$	$n_i :=$
0.001	1.	1	1	0
0.0482	$2.193 \cdot 10^{-5}$	0.958	1	760
0.0723	$7.166 \cdot 10^{-11}$	0.232	1	1140
0.0964	0	0.052	1	1520
0.1446	0	$3.098 \cdot 10^{-5}$	0.999	2280
0.193	0	$6.016 \cdot 10^{-10}$	0.925	3040
0.241	0	0	0.317	3800
0.2892	0	0	0.013	4560
0.3374	0	0	$5.917 \cdot 10^{-6}$	5320
0.3856	0	0	$3.456 \cdot 10^{-10}$	6080
0.488	0	0	0	7692

[years]

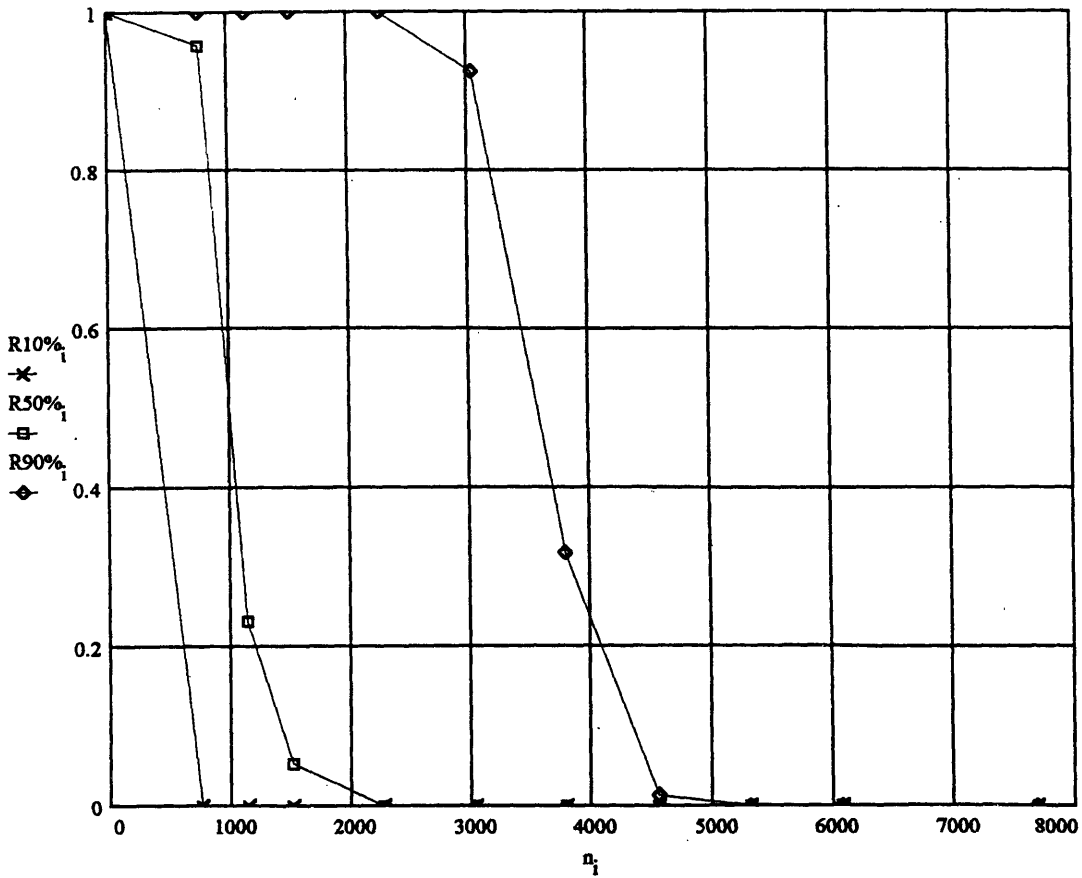


Figure 5-3: Divertor reliability versus the number of cycles

## Chapter 6

# Summary, Conclusions and Recommendations for Future Work

### 6.1 Summary

A methodology for assessing ITER divertor plates reliability has been developed. It includes:

- the identification and classification of the transient events;
- thermal analysis for normal operation and transient events;
- estimation of probability distributions for state-of-knowledge uncertainties surrounding the important parameters;
- definition of an analytical reliability function and propagation of uncertainties through this function.

The  $R_{50\%}$  curve in Figure 5-2 shows that there is a 50% probability that the divertor plate reliability is less than the values on the curve at the corresponding time.

The FC used to obtain the reliability curves in Figures 5-2 and 5-3 is that the material loss during normal operation and transients is smaller than half of the coating. If no transients occur, the number of cycles during which half of the coating is eroded due only to sputtering during normal operation is  $n_{\max} \cong 7692$ . However, the reliability curve corresponding to 90%

probability goes to zero at  $n \cong 5300$ . The conclusion is that the occurrence of transients is the dominant contributor to decreased reliability.

## **6.2 Recommendations**

### **6.2.1 Extension to other failure modes**

We should recall that only one failure mode (material loss) has been taken into consideration, as the main objective of the present work was to obtain a methodology for a probabilistic evaluation of the reliability. Therefore, the reliability curves resulted might not reflect the real divertor reliability values. As a consequence, a first required improvement of the method should be the introduction of other failure modes like:

- cumulative cyclic damage due to fatigue and creep;
- limits on the amounts of swelling strain and creep irradiation strain.

### **6.2.2 Improvement in the limiting rules**

Furthermore, it is not clear that the limiting value of the thickness is truly one half of the original thickness. It might be possible to better assess the required thickness by providing a statistical analysis of the uniformity of the disruptions.

### **6.2.3 Providing the appropriate model geometry selection**

In terms of thermal analysis, HEATING 7.2 is a heat transfer program that allows a three-dimensional (3-D) analysis. Since the heat flux on the divertor is very non-uniform in the axial direction, a 3-D analysis using the tools developed in the present study may result in a better characterization of the divertor operation.

### **6.2.4 Modeling of the material losses**

In addition to the uncertainties that have already accounted for, other parameter uncertainties could be included, as the heat flux in steady-state or the erosion rate, and last but not least the

amount of material loss should be made dependent of transient and considered as a statistical uncertain parameter.

### **6.2.5 Improving the calculational tools**

MATCAD program has been very useful to check the possibility of obtaining pertinent results when using the methods developed in this work. However, the high volume of calculations would much easier be resolved with a short code in C or FORTRAN computer languages. This would also make the method much less time expensive.

In closing, our opinion is that the methodology presented in this work could be successfully used in comparing different ITER divertor candidate designs. We believe that a probabilistic approach reflects much better the depth of knowledge than a deterministic one could do alone; however, probabilistic methods do not preclude the use of deterministic ones, they both are needed together to accurately model the physical processes and their uncertainties.

## **Appendix A**

# **HEATING 7.2 input file for steady-state problem**

```

* problem 1
* nb alloy structure, tungsten coating, water coolant
* units: J, kg, s, m, C
* steady-state
1.E3 7 0 1
REGIONS
1 1 0.0 0.0437 0.0 0.001
1 1 0 0 1 0
2 1 0.0 0.0437 0.001 0.002
1 1 0 0 0 0
3 2 0.0 0.004 0.002 0.004
1 1 0 0 0 0
4 2 0.004 0.012 0.002 0.004
1 1 0 0 0 5
5 2 0.012 0.0142 0.002 0.004
1 1 0 0 0 0
6 2 0.0142 0.0222 0.002 0.004
1 1 0 0 0 2
7 2 0.0222 0.0244 0.002 0.004
1 1 0 0 0 0
8 2 0.0244 0.0324 0.002 0.004
1 1 0 0 0 2
9 2 0.0324 0.0346 0.002 0.004
1 1 0 0 0 0
10 2 0.0346 0.0426 0.002 0.004
1 1 0 0 0 2
11 2 0.0426 0.0437 0.002 0.004
1 1 0 0 0 0
12 2 0.0 0.004 0.004 0.016
1 1 0 6 0 0
13 2 0.012 0.0142 0.004 0.016
1 1 4 4 0 0
14 2 0.0222 0.0244 0.004 0.016
1 1 4 4 0 0
15 2 0.0324 0.0346 0.004 0.016
1 1 4 4 0 0
16 2 0.0426 0.0437 0.004 0.016
1 1 4 0 0 0
17 2 0.0 0.004 0.016 0.02
1 1 0 0 0 0
18 2 0.004 0.012 0.016 0.02
1 1 0 0 3 0
19 2 0.012 0.0142 0.016 0.02
1 1 0 0 0 0
20 2 0.0142 0.0222 0.016 0.02
1 1 0 0 3 0
21 2 0.0222 0.0244 0.016 0.02
1 1 0 0 0 0
22 2 0.0244 0.0324 0.016 0.02
1 1 0 0 3 0
23 2 0.0324 0.0346 0.016 0.02
1 1 0 0 0 0
24 2 0.0346 0.0426 0.016 0.02
1 1 0 0 3 0
25 2 0.0426 0.0437 0.016 0.02
1 1 0 0 0 0

```

MATERIALS

1 tungsten 1. 19300. 1. -1 0 -2 1  
3410. 2.51E5,5660. 4.81E6  
2 nb-1zr 1. 8590. 270. -3

INITIAL TEMPERATURES

1 30.

HEAT GENERATIONS

1 4.0E6

BOUNDARY CONDITIONS

1 1 900.

0 1.701E-8 0 0 11.E6

2 1 64.

55890.

3 1 64.

49690.

4 1 64.

47240.

5 1 64.

57810.

6 1 64.

50690.

XGRID

0.0,0.004,0.012,0.0142,0.0222,0.0244,0.0324,0.0346,0.0426,0.0437

4,4,4,4,4,4,4,4,4

YGRID

0.0,0.001,0.002,0.004,0.016,0.02

40,10,4,4,4

TABULAR FUNCTIONS

1

27. 174.,77. 167.,127. 159.,227. 146.,327. 137.,527. 125.,727. 118.,  
@927. 112.,1127. 108.,1327. 104.,1527. 101.,1727. 98.,2027. 94.,  
@2127. 92.5,2227. 91.5,2327. 90.5,2427. 90.,2527. 89.5

2

25. 132.1,127. 135.6, 527. 140.06, 1027. 157.3, 1527. 170.16,  
@2027. 183.5,2327. 191.7,2527. 203.7,2727. 223.,2927. 250.3,  
@3127. 284.5,3327. 335.7,3409. 359.8,3410. 193.44,5727. 193.44

3

27. 48.,227. 52.,527. 56.,627. 58.,727. 60.,927. 60.

STEADY-STATE

2

8

## **Appendix B**

# **MATHCAD heat transfer coefficient calculations**



**Water properties at 3.5 MPa :**

$$\sigma := 27.98 \cdot 10^{-3} \cdot \frac{\text{newton}}{\text{m}} \quad \text{Hfg} := 1753.2806 \cdot 10^3 \cdot \frac{\text{joule}}{\text{kg}} \quad \rho_g := 17.436 \cdot \frac{\text{kg}}{\text{m}^3}$$

$$k_f := .6251 \cdot \frac{\text{watt}}{\text{m} \cdot \text{K}} \quad T_{\text{sat}} := 515.75 \cdot \text{K} \quad F := 11 \cdot 10^6 \cdot \frac{\text{watt}}{\text{m}^2}$$

The bulk temperature at the section of interest where the flux is 11MW/m2 is 63.52 degrees Celsius.

$$T_b := 336.67 \cdot \text{K}$$

**Water properties at 3.5 MPa and  $T_b$ :**

$$\mu_b := 5.0010105 \cdot 10^{-4} \cdot \frac{\text{newton} \cdot \text{sec}}{\text{m}^2} \quad c_{pb} := 4184.668 \cdot \frac{\text{joule}}{\text{kg} \cdot \text{K}} \quad k_b := .65617 \cdot \frac{\text{watt}}{\text{m} \cdot \text{K}} \quad \rho_b := 982.64 \cdot \frac{\text{kg}}{\text{m}^3}$$

The velocity of the coolant in the channel is:  $v := 10 \cdot \frac{\text{m}}{\text{sec}}$

The equivalent diameter of the divertor submodule is calculated with the formula  $D = 4 \cdot A_{\text{flow}} / P_{\text{wetted}}$ ; a submodule has 8 channels of 10 mm height and 8 mm width each.

$$D := 17.3 \cdot 10^{-3} \cdot \text{m}$$

Re and Pr numbers at the bulk temperature are:

$$\text{Re}_b := \frac{\rho_b \cdot v \cdot D}{\mu_b} \quad \text{Pr}_b := \frac{\mu_b \cdot c_{pb}}{k_b} \quad \text{Re}_b = 3.399 \cdot 10^5 \quad \text{Pr}_b = 3.189$$

For a flux of 11 MW/m2, Yin and Abdelmessih correlation gives the following result for the wall temperature at the onset of nucleate boiling:

$$T_{w\text{ONB}} := \left( \frac{1800 \cdot F \cdot \sigma \cdot T_{\text{sat}}}{\text{Hfg} \cdot \rho_g \cdot k_f} \right)^{-.5} + T_{\text{sat}} \quad T_{w\text{ONB}} = 638.029 \cdot \text{K}$$

$$\Delta T_{\text{satONB}} := T_{w\text{ONB}} - T_{\text{sat}} \quad \Delta T_{\text{satONB}} = 122.279 \cdot \text{K}$$

This means that at 11 MW/m2 ONB will appear if the wall temperature is more than 122.3 degrees higher than the saturation temperature at 3.5 MPa which is 242.6 degrees Celsius, as predicted by Yin and Abdelmessih correlation.

Considering that the flux (y) and the wall temperature (x) at ONB are both unknowns, they can be obtained by solving simultaneously from Yin and Abdelmessih correlation and the heat transfer equation (reference 25, page 154). In order to be able to use the heat transfer equation, we have to calculate the heat transfer coefficient as follows:

Dittus-Boelter correlation:  $Nu_{DB} := .023 \cdot Re_b^8 \cdot Pr_b^4$

$$h_{DB} := Nu_{DB} \cdot \frac{kb}{D}$$

$$Tw1 := Tb + \frac{F}{h_{DB}}$$

(from tables)

$$Nu_{DB} = 973.453 \quad h_{DB} = 3.692 \cdot 10^4 \cdot \frac{\text{watt}}{\text{m}^2 \cdot \text{K}} \quad Tw1 = 634.595 \cdot \text{K} \quad \mu1 := 2.3195 \cdot 10^{-5} \cdot \frac{\text{newton} \cdot \text{sec}}{\text{m}^2}$$

Pethukov correlation can be now used since we have an estimation for the wall temperature, so that the viscosity can be evaluated:

$$ff := .014 \quad (\text{from Moody diagram}) \quad \text{or} \quad ff := (1.82 \cdot \log(Re_b) - 1.64)^{-2} \quad ff = 0.014$$

$$X := 1.07 + 12.7 \cdot \left( Pr_b^{\frac{2}{3}} - 1 \right) \cdot \left( \frac{ff}{8} \right)^{-.5}$$

First iteration:

$$Nu_{P1} := \frac{Re_b \cdot Pr_b}{X} \cdot \frac{ff}{8} \cdot \left( \frac{\mu_b}{\mu1} \right)^{.11} \quad h_{P1} := Nu_{P1} \cdot \frac{kb}{D} \quad Nu_{P1} = 1.581 \cdot 10^3 \quad h_{P1} = 5.998 \cdot 10^4 \cdot \frac{\text{watt}}{\text{m}^2 \cdot \text{K}}$$

Second iteration:

$$Tw2 := Tb + \frac{F}{h_{P1}} \quad Tw2 = 520.067 \cdot \text{K} \quad \mu2 := 6.366 \cdot 10^{-5} \cdot \frac{\text{newton} \cdot \text{sec}}{\text{m}^2}$$

$$Nu_{P2} := \frac{Re_b \cdot Pr_b}{X} \cdot \frac{ff}{8} \cdot \left( \frac{\mu_b}{\mu2} \right)^{.11} \quad h_{P2} := Nu_{P2} \cdot \frac{kb}{D} \quad Nu_{P2} = 1.415 \cdot 10^3 \quad h_{P2} = 5.367 \cdot 10^4 \cdot \frac{\text{watt}}{\text{m}^2 \cdot \text{K}}$$

Third iteration:

$$Tw3 := Tb + \frac{F}{h_{P2}} \quad Tw3 = 541.609 \cdot \text{K} \quad \mu3 := 3.14732 \cdot 10^{-5} \cdot \frac{\text{newton} \cdot \text{sec}}{\text{m}^2}$$

$$Nu_{P3} := \frac{Re_b \cdot Pr_b}{X} \cdot \frac{ff}{8} \cdot \left( \frac{\mu_b}{\mu3} \right)^{.11} \quad h_{P3} := Nu_{P3} \cdot \frac{kb}{D} \quad Nu_{P3} = 1.529 \cdot 10^3 \quad h_{P3} = 5.8 \cdot 10^4 \cdot \frac{\text{watt}}{\text{m}^2 \cdot \text{K}}$$

Fourth iteration:

$$Tw4 := Tb + \frac{F}{h_{P3}} \quad Tw4 = 526.328 \cdot \text{K} \quad \mu4 := 5.42344 \cdot 10^{-5} \cdot \frac{\text{newton} \cdot \text{sec}}{\text{m}^2}$$

$$Nu_{P4} := \frac{Re_b \cdot Pr_b}{X} \cdot \frac{ff}{8} \cdot \left( \frac{\mu_b}{\mu4} \right)^{.11} \quad h_{P4} := Nu_{P4} \cdot \frac{kb}{D} \quad Nu_{P4} = 1.44 \cdot 10^3 \quad h_{P4} = 5.463 \cdot 10^4 \cdot \frac{\text{watt}}{\text{m}^2 \cdot \text{K}}$$

We use the last value of heat transfer coefficient to calculate FONB and TwONB.

The guess values are taken as from Yin's experimental results, since the experimental conditions are similar to the parameters in the present work (3.5 MPa, 10 Mg/m<sup>2</sup>\*s, Tin = 50C).

$$x := 285 \cdot \text{K} \quad y := 4 \cdot 10^6 \cdot \frac{\text{watt}}{\text{m}^2}$$

Given

$$x = \left( \frac{1800 \cdot y \cdot \sigma \cdot T_{\text{sat}}}{\text{Hfg} \cdot \rho_g \cdot k_f} \right)^{.5} + T_{\text{sat}}$$

$$y = \text{hhP4} \cdot (x - T_b)$$

$$\begin{pmatrix} x_{\text{val}} \\ y_{\text{val}} \end{pmatrix} := \text{Find}(x, y)$$

$$x_{\text{val}} = 674.024 \cdot \text{K} \quad y_{\text{val}} = 1.843 \cdot 10^7 \cdot \frac{\text{watt}}{\text{m}^2}$$

That is the ONB would occur for a wall temperature 158.3 degrees higher than the saturation temperature and a flux of 18.43 MW/m<sup>2</sup>, which is far from the Yin's experimental results.

If we use Bergles and Rohsenow correlation and the heat transfer equation, the results are:

The same guess values:

$$xx := 285.$$

$$yy := 4 \cdot 10^6$$

$$p := 35.$$

$$\text{hhP4} := 5.463 \cdot 10^4$$

$$TT_{\text{sat}} := 515.75$$

$$TT_b := 336.67$$

Given

$$xx = .556 \cdot \left( \frac{yy}{1082 \cdot p^{1.156}} \right)^{.463 \cdot p^{.0234}} + TT_{\text{sat}}$$

$$yy = \text{hhP4} \cdot (xx - TT_b)$$

$$\begin{pmatrix} xx_{\text{val}} \\ yy_{\text{val}} \end{pmatrix} := \text{Find}(xx, yy)$$

$$xx_{\text{val}} = 522.765$$

$$yy_{\text{val}} = 1.017 \cdot 10^7$$

That is the ONB would occur for a wall temperature 7 degrees higher than the saturation temperature and a flux of 10.2 MW/m<sup>2</sup>.

**CONCLUSION:** Taking into account that Yin's experiment has been performed for ITER divertor conditions, we consider the values from his experiments as reference for our case, even if his correlation does not seem to fit to our parameters. The wall temperatures predicted by Bergles and Rohsenow correlation are far below the experiment data.

As a consequence, as long as the wall temperature is not 45 degrees higher than the saturation temperature we consider that the ONB does not occur. In this case, Petukhov correlation is used to calculate the heat transfer coefficient. This is done by iterating with HEATING 7.2 program and recalculating the viscosity at the walls.

After running HEATING 7.2 with h4P value, the viscosity at different walls for the 5th iteration is:

-the plasma side wall (boundary condition 2)

$$\mu_{5p} := 1.948 \cdot 10^{-5} \cdot \frac{\text{newton} \cdot \text{sec}}{\text{m}^2}$$

$$\text{NuP5p} := \frac{\text{Reb} \cdot \text{Prb}}{\text{X}} \cdot \frac{\text{ff}}{8} \cdot \left( \frac{\mu_b}{\mu_{5p}} \right)^{.11}$$

$$hP5p := \text{NuP5p} \cdot \frac{\text{kb}}{\text{D}}$$

$$hP5p = 6.114 \cdot 10^4 \cdot \frac{\text{watt}}{\text{m}^2 \cdot \text{K}}$$

-the opposite wall parallel to the plasma side wall (BC 3)

$$\mu_{5c} := 3.672 \cdot 10^{-4} \cdot \frac{\text{newton} \cdot \text{sec}}{\text{m}^2}$$

$$\text{NuP5c} := \frac{\text{Reb} \cdot \text{Prb}}{\text{X}} \cdot \frac{\text{ff}}{8} \cdot \left( \frac{\mu_b}{\mu_{5c}} \right)^{.11}$$

$$hP5c := \text{NuP5c} \cdot \frac{\text{kb}}{\text{D}}$$

$$hP5c = 4.426 \cdot 10^4 \cdot \frac{\text{watt}}{\text{m}^2 \cdot \text{K}}$$

-the side walls of the channels (BC 4)

$$\mu_{5s} := 1.452 \cdot 10^{-4} \cdot \frac{\text{newton} \cdot \text{sec}}{\text{m}^2}$$

$$\text{NuP5s} := \frac{\text{Reb} \cdot \text{Prb}}{\text{X}} \cdot \frac{\text{ff}}{8} \cdot \left( \frac{\mu_b}{\mu_{5s}} \right)^{.11}$$

$$hP5s := \text{NuP5s} \cdot \frac{\text{kb}}{\text{D}}$$

$$hP5s = 4.902 \cdot 10^4 \cdot \frac{\text{watt}}{\text{m}^2 \cdot \text{K}}$$

**NOTE:** With these new BC's, HEATING 7.2 run gives new temperatures at the walls; these are used to evaluate new viscosities at the walls which are introduced in the equations above to give new BC values. After the process was repeated three times, the values changes from one iteration to the next were under 5%, which was considered satisfactory. The final values used as BC's in HEATING 7.2 in order to calculate the steady-state temperature distribution were as follows:

$$\text{BC2: } h = 55890 \text{ W/m}^2\text{K}$$

$$\text{BC3: } h = 49690 \text{ W/m}^2\text{K}$$

$$\text{BC4: } h = 47240 \text{ W/m}^2\text{K}$$

$$\text{BC5: } h = 57810 \text{ W/m}^2\text{K}$$

BC's 5 and 6 are respectively for the plasma side and the channel side for the end channels of the submodule.

$$\text{BC6: } h = 50690 \text{ W/m}^2\text{K}$$

In case ONB is reached, Thom correlation should be used to calculate the h's at the walls; a sample calculus is the following:

$$T_w := 573. \quad P := 3.5 \cdot 10^6 \quad T_{w\text{onb}} := 558. \quad H_c := 6.114 \cdot 10^4 \text{ ( the hP5p value)}$$

$$F_B := 10^6 \cdot \left( e^{\frac{P}{87 \cdot 10^5} \cdot \frac{T_w - T_{T\text{sat}}}{22.65}} \right)^2 \quad F_B = 1.428 \cdot 10^7$$

$$F_0 := 10^6 \cdot \left( e^{\frac{P}{87 \cdot 10^5} \cdot \frac{T_{w\text{onb}} - T_{T\text{sat}}}{22.65}} \right)^2 \quad F_0 = 3.48 \cdot 10^6$$

$$F_c := H_c \cdot (T_w - T_{Tb}) \quad F_c = 1.445 \cdot 10^7$$

$$F_w := \sqrt{F_c^2 + F_B^2} \cdot \left( 1 - \frac{F_0}{F_B} \right)^2 \quad F_w = 1.804 \cdot 10^7$$

$$h_w := \frac{F_w}{T_w - T_{Tb}} \quad h_w = 7.634 \cdot 10^4$$

**NOTE:** this algorithm can also be used iteratively with HEATING 7.2 in order to come up with acceptable values for the heat transfer coefficients in ONB case.

## Appendix C

**HEATING 7.2 input files for  
problems 2 (LOCA and OP) and 3  
(OP); output file for problem 2  
(OP)**

```

* problem 2
* Nb alloy structure, tungsten coating, water coolant
* units: J, kg, s, m, C
* LOCA transient
1.E5 7 0 1
REGIONS
1 1 0.0 0.0437 0.0 0.001
1 1 0 0 1 0
2 1 0.0 0.0437 0.001 0.002
1 1 0 0 0 0
3 2 0.0 0.004 0.002 0.004
1 1 0 0 0 0
4 2 0.004 0.012 0.002 0.004
1 1 0 0 0 5
5 2 0.012 0.0142 0.002 0.004
1 1 0 0 0 0
6 2 0.0142 0.0222 0.002 0.004
1 1 0 0 0 2
7 2 0.0222 0.0244 0.002 0.004
1 1 0 0 0 0
8 2 0.0244 0.0324 0.002 0.004
1 1 0 0 0 2
9 2 0.0324 0.0346 0.002 0.004
1 1 0 0 0 0
10 2 0.0346 0.0426 0.002 0.004
1 1 0 0 0 2
11 2 0.0426 0.0437 0.002 0.004
1 1 0 0 0 0
12 2 0.0 0.004 0.004 0.016
1 1 0 6 0 0
13 2 0.012 0.0142 0.004 0.016
1 1 4 4 0 0
14 2 0.0222 0.0244 0.004 0.016
1 1 4 4 0 0
15 2 0.0324 0.0346 0.004 0.016
1 1 4 4 0 0
16 2 0.0426 0.0437 0.004 0.016
1 1 4 0 0 0
17 2 0.0 0.004 0.016 0.02
1 1 0 0 0 0
18 2 0.004 0.012 0.016 0.02
1 1 0 0 3 0
19 2 0.012 0.0142 0.016 0.02
1 1 0 0 0 0
20 2 0.0142 0.0222 0.016 0.02
1 1 0 0 3 0
21 2 0.0222 0.0244 0.016 0.02
1 1 0 0 0 0
22 2 0.0244 0.0324 0.016 0.02
1 1 0 0 3 0
23 2 0.0324 0.0346 0.016 0.02
1 1 0 0 0 0
24 2 0.0346 0.0426 0.016 0.02
1 1 0 0 3 0
25 2 0.0426 0.0437 0.016 0.02
1 1 0 0 0 0

```

MATERIALS

1 tungsten 1. 19300. 1. -1 0 -2 1  
3410. 2.51E5,5660. 4.81E6  
2 nb-1zr 1. 8590. 270. -3

INITIAL TEMPERATURES

1 30.

HEAT GENERATIONS

1 4.0E6

BOUNDARY CONDITIONS

1 1 900.

0 1.701E-8 0 0 11.E6

0 0 0 0 1

2 1 64.

0 6.652E-9

3 1 64.

0 6.652E-9

4 1 64.

0 6.652E-9

5 1 64.

0 6.652E-9

6 1 64.

0 6.652E-9

XGRID

0.0,0.004,0.012,0.0142,0.0222,0.0244,0.0324,0.0346,0.0426,0.0437

4,4,4,4,4,4,4,4,4

YGRID

0.0,0.001,0.002,0.004,0.016,0.02

40,10,4,4,4

TABULAR FUNCTIONS

1

27. 174.,77. 167.,127. 159.,227. 146.,327. 137.,527. 125.,727. 118.,  
@927. 112.,1127. 108.,1327. 104.,1527. 101.,1727. 98.,2027. 94.,  
@2127. 92.5,2227. 91.5,2327. 90.5,2427. 90.,2527. 89.5

2

25. 132.1,127. 135.6, 527. 140.06, 1027. 157.3, 1527. 170.16,  
@2027. 183.5,2327. 191.7,2527. 203.7,2727. 223.,2927. 250.3,  
@3127. 284.5,3327. 335.7,3409. 359.8,3410. 193.44,5727. 193.44

3

27. 48.,227. 52.,527. 56.,627. 58.,727. 60.,927. 60.

TRANSIENT

1 3.

0 10

\*



```

* problem 2
* nb alloy structure, tungsten coating, water coolant
* units: J, kg, s, m, C
* overpower transient
1.E5 7 0 1
REGIONS
1 1 0.0 0.0437 0.0 0.001
1 1 0 0 1 0
2 1 0.0 0.0437 0.001 0.002
1 1 0 0 0 0
3 2 0.0 0.004 0.002 0.004
1 1 0 0 0 0
4 2 0.004 0.012 0.002 0.004
1 1 0 0 0 5
5 2 0.012 0.0142 0.002 0.004
1 1 0 0 0 0
6 2 0.0142 0.0222 0.002 0.004
1 1 0 0 0 2
7 2 0.0222 0.0244 0.002 0.004
1 1 0 0 0 0
8 2 0.0244 0.0324 0.002 0.004
1 1 0 0 0 2
9 2 0.0324 0.0346 0.002 0.004
1 1 0 0 0 0
10 2 0.0346 0.0426 0.002 0.004
1 1 0 0 0 2
11 2 0.0426 0.0437 0.002 0.004
1 1 0 0 0 0
12 2 0.0 0.004 0.004 0.016
1 1 0 6 0 0
13 2 0.012 0.0142 0.004 0.016
1 1 4 4 0 0
14 2 0.0222 0.0244 0.004 0.016
1 1 4 4 0 0
15 2 0.0324 0.0346 0.004 0.016
1 1 4 4 0 0
16 2 0.0426 0.0437 0.004 0.016
1 1 4 0 0 0
17 2 0.0 0.004 0.016 0.02
1 1 0 0 0 0
18 2 0.004 0.012 0.016 0.02
1 1 0 0 3 0
19 2 0.012 0.0142 0.016 0.02
1 1 0 0 0 0
20 2 0.0142 0.0222 0.016 0.02
1 1 0 0 3 0
21 2 0.0222 0.0244 0.016 0.02
1 1 0 0 0 0
22 2 0.0244 0.0324 0.016 0.02
1 1 0 0 3 0
23 2 0.0324 0.0346 0.016 0.02
1 1 0 0 0 0
24 2 0.0346 0.0426 0.016 0.02
1 1 0 0 3 0
25 2 0.0426 0.0437 0.016 0.02
1 1 0 0 0 0

```

MATERIALS

1 tungsten 1. 19300. 1. -1 0 -2 1  
3410. 2.51E5,5660. 4.81E6

2 nb-1zr 1. 8590. 270. -3

INITIAL TEMPERATURES

1 30.

HEAT GENERATIONS

1 4.0E6

BOUNDARY CONDITIONS

1 1 900.

0 1.701E-8 0 0 11.E6 1

0 0 0 0 1

2 1 64.

55890.

3 1 64.

49690.

4 1 64.

47240.

5 1 64.

57810.

6 1 64.

50690.

XGRID

0.0,0.004,0.012,0.0142,0.0222,0.0244,0.0324,0.0346,0.0426,0.0437

4,4,4,4,4,4,4,4,4

YGRID

0.0,0.001,0.002,0.004,0.016,0.02

40,10,4,4,4

ANALYTICAL FUNCTION

1

1 1.,2 0.22

TABULAR FUNCTIONS

1

27. 174.,77. 167.,127. 159.,227. 146.,327. 137.,527. 125.,727. 118.,  
@927. 112.,1127. 108.,1327. 104.,1527. 101.,1727. 98.,2027. 94.,  
@2127. 92.5,2227. 91.5,2327. 90.5,2427. 90.,2527. 89.5

2

25. 132.1,127. 135.6, 527. 140.06, 1027. 157.3, 1527. 170.16,  
@2027. 183.5,2327. 191.7,2527. 203.7,2727. 223.,2927. 250.3,  
@3127. 284.5,3327. 335.7,3409. 359.8,3410. 193.44,5727. 193.44

3

27. 48.,227. 52.,527. 56.,627. 58.,727. 60.,927. 60.

TRANSIENT

1 3.

0 10

8

```

* problem 3
* Nb alloy structure, tungsten coating, water coolant
* units: J, kg, s, m, C
* disruption transient following overpower transient
1.E4 7 0 1
REGIONS
1 1 0.0 0.0437 0.0 0.001
1 1 0 0 1 0
2 1 0.0 0.0437 0.001 0.002
1 1 0 0 0 0
3 2 0.0 0.004 0.002 0.004
1 1 0 0 0 0
4 2 0.004 0.012 0.002 0.004
1 1 0 0 0 5
5 2 0.012 0.0142 0.002 0.004
1 1 0 0 0 0
6 2 0.0142 0.0222 0.002 0.004
1 1 0 0 0 2
7 2 0.0222 0.0244 0.002 0.004
1 1 0 0 0 0
8 2 0.0244 0.0324 0.002 0.004
1 1 0 0 0 2
9 2 0.0324 0.0346 0.002 0.004
1 1 0 0 0 0
10 2 0.0346 0.0426 0.002 0.004
1 1 0 0 0 2
11 2 0.0426 0.0437 0.002 0.004
1 1 0 0 0 0
12 2 0.0 0.004 0.004 0.016
1 1 0 6 0 0
13 2 0.012 0.0142 0.004 0.016
1 1 4 4 0 0
14 2 0.0222 0.0244 0.004 0.016
1 1 4 4 0 0
15 2 0.0324 0.0346 0.004 0.016
1 1 4 4 0 0
16 2 0.0426 0.0437 0.004 0.016
1 1 4 0 0 0
17 2 0.0 0.004 0.016 0.02
1 1 0 0 0 0
18 2 0.004 0.012 0.016 0.02
1 1 0 0 3 0
19 2 0.012 0.0142 0.016 0.02
1 1 0 0 0 0
20 2 0.0142 0.0222 0.016 0.02
1 1 0 0 3 0
21 2 0.0222 0.0244 0.016 0.02
1 1 0 0 0 0
22 2 0.0244 0.0324 0.016 0.02
1 1 0 0 3 0
23 2 0.0324 0.0346 0.016 0.02
1 1 0 0 0 0
24 2 0.0346 0.0426 0.016 0.02
1 1 0 0 3 0
25 2 0.0426 0.0437 0.016 0.02
1 1 0 0 0 0

```

MATERIALS

1 tungsten 1. 19300. 1. -1 0 -2 1  
3410. 2.51E5,5660. 4.81E6  
2 nb-1zr 1. 8590. 270. -3

INITIAL TEMPERATURES

1 30.

HEAT GENERATIONS

1 4.0E6

BOUNDARY CONDITIONS

1 1 900.

0 1.701E-8 0 0 34.046E9

2 1 64.

55890.

3 1 64.

49690.

4 1 64.

47240.

5 1 64.

57810.

6 1 64.

50960.

XGRID

0.0,0.004,0.012,0.0142,0.0222,0.0244,0.0324,0.0346,0.0426,0.0437

4,4,4,4,4,4,4,4,4

YGRID

0.0,0.001,0.002,0.004,0.016,0.02

40,10,4,4,4

TABULAR FUNCTIONS

1

27. 174.,77. 167.,127. 159.,227. 146.,327. 137.,527. 125.,727. 118.,  
@927. 112.,1127. 108.,1327. 104.,1527. 101.,1727. 98.,2027. 94.,  
@2127. 92.5,2227. 91.5,2327. 90.5,2427. 90.,2527. 89.5

2

25. 132.1,127. 135.6, 527. 140.06, 1027. 157.3, 1527. 170.16,  
@2027. 183.5,2327. 191.7,2527. 203.7,2727. 223.,2927. 250.3,  
@3127. 284.5,3327. 335.7,3409. 359.8,3410. 193.44,5727. 193.44

3

27. 48.,227. 52.,527. 56.,627. 58.,727. 60.,927. 60.

TRANSIENT

1 3.0001

0

8

\*\*\*\*\* ECHO OF INPUT DATA \*\*\*\*\*

Record

1 \* probelm 2  
2 \* nb alloy structure, tungsten coating, water coolant  
3 \* units: J, kg, s, m, C  
4 \* trl overpower  
5 1.E5 7 0 1  
6 REGIONS  
7 1 1 0.0 0.0437 0.0 0.001  
8 1 1 0 0 1 0  
9 2 1 0.0 0.0437 0.001 0.002  
10 1 1 0 0 0 0  
11 3 2 0.0 0.004 0.002 0.004  
12 1 1 0 0 0 0  
13 4 2 0.004 0.012 0.002 0.004  
14 1 1 0 0 0 5  
15 5 2 0.012 0.0142 0.002 0.004  
16 1 1 0 0 0 0  
17 6 2 0.0142 0.0222 0.002 0.004  
18 1 1 0 0 0 2  
19 7 2 0.0222 0.0244 0.002 0.004  
20 1 1 0 0 0 0  
21 8 2 0.0244 0.0324 0.002 0.004  
22 1 1 0 0 0 2  
23 9 2 0.0324 0.0346 0.002 0.004  
24 1 1 0 0 0 0  
25 10 2 0.0346 0.0426 0.002 0.004  
26 1 1 0 0 0 2  
27 11 2 0.0426 0.0437 0.002 0.004  
28 1 1 0 0 0 0  
29 12 2 0.0 0.004 0.004 0.016  
30 1 1 0 6 0 0  
31 13 2 0.012 0.0142 0.004 0.016  
32 1 1 4 4 0 0  
33 14 2 0.0222 0.0244 0.004 0.016  
34 1 1 4 4 0 0  
35 15 2 0.0324 0.0346 0.004 0.016  
36 1 1 4 4 0 0  
37 16 2 0.0426 0.0437 0.004 0.016  
38 1 1 4 0 0 0  
39 17 2 0.0 0.004 0.016 0.02  
40 1 1 0 0 0 0  
41 18 2 0.004 0.012 0.016 0.02  
42 1 1 0 0 3 0  
43 19 2 0.012 0.0142 0.016 0.02  
44 1 1 0 0 0 0  
45 20 2 0.0142 0.0222 0.016 0.02  
46 1 1 0 0 3 0  
47 21 2 0.0222 0.0244 0.016 0.02  
48 1 1 0 0 0 0  
49 22 2 0.0244 0.0324 0.016 0.02  
50 1 1 0 0 3 0  
51 23 2 0.0324 0.0346 0.016 0.02  
52 1 1 0 0 0 0  
53 24 2 0.0346 0.0426 0.016 0.02  
54 1 1 0 0 3 0

```

55 25 2 0.0426 0.0437 0.016 0.02
56 1 1 0 0 0 0
57 MATERIALS
58 1 tungsten 1. 19300. 1. -1 0 -2 1
59 3410. 2.51E5,5660. 4.81E6
60 2 nb-1zr 1. 8590. 270. -3
61 INITIAL TEMPERATURES
62 1 30.
63 HEAT GENERATIONS
64 1 4.0E6
65 BOUNDARY CONDITIONS
66 1 1 900.
67 0 1.701E-8 0 0 11.E6 1
68 0 0 0 0 1
69 2 1 64.
70 55890.
71 3 1 64.
72 49690.
73 4 1 64.
74 47240.
75 5 1 64.
76 57810.
77 6 1 64.
78 50690.
79 XGRID
80 0.0,0.004,0.012,0.0142,0.0222,0.0244,0.0324,0.0346,0.0426,0.0437
81 4,4,4,4,4,4,4,4,4
82 YGRID
83 0.0,0.001,0.002,0.004,0.016,0.02
84 40,10,4,4,4
85 ANALYTICAL FUNCTION
86 1
87 1 1.,2 0.22
88 TABULAR FUNCTIONS
89 1
90 27. 174.,77. 167.,127. 159.,227. 146.,327. 137.,527. 125.,727. 118.,
@927. 112.,1127. 108.,1327. 104.,1527. 101.,1727. 98.,2027. 94.,
@2127. 92.5,2227. 91.5,2327. 90.5,2427. 90.,2527. 89.5
91 2
92 25. 132.1,127. 135.6, 527. 140.06, 1027. 157.3, 1527. 170.16,
@2027. 183.5,2327. 191.7,2527. 203.7,2727. 223.,2927. 250.3,
@3127. 284.5,3327. 335.7,3409. 359.8,3410. 193.44,5727. 193.44
93 3
94 27. 48.,227. 52.,527. 56.,627. 58.,727. 60.,927. 60.
95 TRANSIENT
96 1 3.
97 0 10
98 %

```

```

***** CASE DESCRIPTION *****
* problem 2
*****SUMMARY OF PARAMETER CARD DATA *****

```

```

Maximum cpu time - seconds
Geometry type number - 7 (or xy )
Initial time - 0.0000000D+00

```

Temperature units - Celcius (Significant only if radiation involved)  
 This is a restart of previous case - Yes  
 Read node-to-node connector data file - No  
 Redirect or suppress convergence information - Yes (Suppress)  
 Output selected information during calculations - No

\*\*\*\*\* SUMMARY OF REGION DATA \*\*\*\*\*

Region Number	Material Number	Initial Temp.	Heat Gen. No.	Heat Gen. Number
1	1	1	1	1
2	1	1	1	1
3	2	1	1	1
4	2	1	1	1
5	2	1	1	1
6	2	1	1	1
7	2	1	1	1
8	2	1	1	1
9	2	1	1	1
10	2	1	1	1
11	2	1	1	1
12	2	1	1	1
13	2	1	1	1
14	2	1	1	1
15	2	1	1	1
16	2	1	1	1
17	2	1	1	1
18	2	1	1	1
19	2	1	1	1
20	2	1	1	1
21	2	1	1	1
22	2	1	1	1
23	2	1	1	1
24	2	1	1	1
25	2	1	1	1

----- Dimensions / Boundary Numbers -----

Region Number	First Axis		Second Axis		Third Axis	
	Smaller	Larger	Smaller	Larger	Smaller	Larger
1	0.0000E+00	4.3700E-02	0.0000E+00	1.0000E-03	0.0000E+00	0.0000E+00
	0	0	1	0	0	0
2	0.0000E+00	4.3700E-02	1.0000E-03	2.0000E-03	0.0000E+00	0.0000E+00
	0	0	0	0	0	0
3	0.0000E+00	4.0000E-03	2.0000E-03	4.0000E-03	0.0000E+00	0.0000E+00
	0	0	0	0	0	0
4	4.0000E-03	1.2000E-02	2.0000E-03	4.0000E-03	0.0000E+00	0.0000E+00
	0	0	0	5	0	0
5	1.2000E-02	1.4200E-02	2.0000E-03	4.0000E-03	0.0000E+00	0.0000E+00
	0	0	0	0	0	0
6	1.4200E-02	2.2200E-02	2.0000E-03	4.0000E-03	0.0000E+00	0.0000E+00
	0	0	0	2	0	0
7	2.2200E-02	2.4400E-02	2.0000E-03	4.0000E-03	0.0000E+00	0.0000E+00
	0	0	0	0	0	0
8	2.4400E-02	3.2400E-02	2.0000E-03	4.0000E-03	0.0000E+00	0.0000E+00
	0	0	0	2	0	0
9	3.2400E-02	3.4600E-02	2.0000E-03	4.0000E-03	0.0000E+00	0.0000E+00
	0	0	0	0	0	0

10	3.4600E-02	4.2600E-02	2.0000E-03	4.0000E-03	0.0000E+00	0.0000E+00
	0	0	0	2	0	0
11	4.2600E-02	4.3700E-02	2.0000E-03	4.0000E-03	0.0000E+00	0.0000E+00
	0	0	0	0	0	0
12	0.0000E+00	4.0000E-03	4.0000E-03	1.6000E-02	0.0000E+00	0.0000E+00
	0	6	0	0	0	0
13	1.2000E-02	1.4200E-02	4.0000E-03	1.6000E-02	0.0000E+00	0.0000E+00
	4	4	0	0	0	0
14	2.2200E-02	2.4400E-02	4.0000E-03	1.6000E-02	0.0000E+00	0.0000E+00
	4	4	0	0	0	0
15	3.2400E-02	3.4600E-02	4.0000E-03	1.6000E-02	0.0000E+00	0.0000E+00
	4	4	0	0	0	0
16	4.2600E-02	4.3700E-02	4.0000E-03	1.6000E-02	0.0000E+00	0.0000E+00
	4	0	0	0	0	0
17	0.0000E+00	4.0000E-03	1.6000E-02	2.0000E-02	0.0000E+00	0.0000E+00
	0	0	0	0	0	0
18	4.0000E-03	1.2000E-02	1.6000E-02	2.0000E-02	0.0000E+00	0.0000E+00
	0	0	3	0	0	0
19	1.2000E-02	1.4200E-02	1.6000E-02	2.0000E-02	0.0000E+00	0.0000E+00
	0	0	0	0	0	0
20	1.4200E-02	2.2200E-02	1.6000E-02	2.0000E-02	0.0000E+00	0.0000E+00
	0	0	3	0	0	0
21	2.2200E-02	2.4400E-02	1.6000E-02	2.0000E-02	0.0000E+00	0.0000E+00
	0	0	0	0	0	0
22	2.4400E-02	3.2400E-02	1.6000E-02	2.0000E-02	0.0000E+00	0.0000E+00
	0	0	3	0	0	0
23	3.2400E-02	3.4600E-02	1.6000E-02	2.0000E-02	0.0000E+00	0.0000E+00
	0	0	0	0	0	0
24	3.4600E-02	4.2600E-02	1.6000E-02	2.0000E-02	0.0000E+00	0.0000E+00
	0	0	3	0	0	0
25	4.2600E-02	4.3700E-02	1.6000E-02	2.0000E-02	0.0000E+00	0.0000E+00
	0	0	0	0	0	0

\*\*\*\*\* SUMMARY OF MATERIAL DATA \*\*\*\*\*

Material Number	Material Name	----- Thermal Parameters -----			Phase Change
		-- Temperature-Dependent Function Numbers --			
		Conductivity	Density	Specific Heat	
1	tungsten	1.000000D+00	1.930000D+04	1.000000D+00	Yes
		-1	0	-2	
2	nb-lzr	1.000000D+00	8.590000D+03	2.700000D+02	No
		-3	0	0	

\*\*\*\*\* SUMMARY OF PHASE CHANGES \*\*\*\*\*

Phase Change	Material Number	Transition Temperature	Latent Heat
1	1	3.410000D+03	2.510000D+05
2	1	5.660000D+03	4.810000D+06

\*\*\*\*\* SUMMARY OF INITIAL TEMPERATURE DATA \*\*\*\*\*

Number	Initial Temperature	Position-Dependent Function Numbers		
		x or r	y or th	z or p
1	3.000000D+01	0	0	0



\*\*\*\*\* SUMMARY OF HEAT GENERATION RATE DATA \*\*\*\*\*

Number Power Time-, Temperature-, and Position-Dependent Function Numbers  
 Density Time Temperature X or R Y or Theta Z or Phi  
 1 4.00000D+06 0 0 0 0 0

\*\*\*\*\* SUMMARY OF BOUNDARY CONDITION DATA \*\*\*\*\*

Number: 1 Type: Surface-to-Environment  
 Temperature and Any Functions Used to Define Dependence:  
 Temperature : 9.000000E+02  
 Heat Transfer Coefficients and Any Functions Used to Define Dependence:  
 Radiation : 1.701000E-08  
 Specified Heat Flux : 1.100000E+07  
 Time Function : 1

Number: 2 Type: Surface-to-Environment  
 Temperature and Any Functions Used to Define Dependence:  
 Temperature : 6.400000E+01  
 Heat Transfer Coefficients and Any Functions Used to Define Dependence:  
 Forced Convection : 5.589000E+04

Number: 3 Type: Surface-to-Environment  
 Temperature and Any Functions Used to Define Dependence:  
 Temperature : 6.400000E+01  
 Heat Transfer Coefficients and Any Functions Used to Define Dependence:  
 Forced Convection : 4.969000E+04

Number: 4 Type: Surface-to-Environment  
 Temperature and Any Functions Used to Define Dependence:  
 Temperature : 6.400000E+01  
 Heat Transfer Coefficients and Any Functions Used to Define Dependence:  
 Forced Convection : 4.724000E+04

Number: 5 Type: Surface-to-Environment  
 Temperature and Any Functions Used to Define Dependence:  
 Temperature : 6.400000E+01  
 Heat Transfer Coefficients and Any Functions Used to Define Dependence:  
 Forced Convection : 5.781000E+04

Number: 6 Type: Surface-to-Environment  
 Temperature and Any Functions Used to Define Dependence:  
 Temperature : 6.400000E+01  
 Heat Transfer Coefficients and Any Functions Used to Define Dependence:  
 Forced Convection : 5.069000E+04

\*\*\*\*\* SUMMARY OF GRID STRUCTURE \*\*\*\*\*

X (or R) Gross Grid Lines and Number of Divisions  
 0.000000E+00 4.000000E-03 1.200000E-02 1.420000E-02 2.220000E-02  
 2.440000E-02 3.240000E-02 3.460000E-02 4.260000E-02 4.370000E-02  
 4 4 4 4 4  
 4 4 4 4 4

X (or R) Fine Grid Lines Generated by HEATING  
 1 0.00000E+00 2 1.00000E-03 3 2.00000E-03 4 3.00000E-03  
 5 4.00000E-03 6 6.00000E-03 7 8.00000E-03 8 1.00000E-02  
 9 1.20000E-02 10 1.25500E-02 11 1.31000E-02 12 1.36500E-02  
 13 1.42000E-02 14 1.62000E-02 15 1.82000E-02 16 2.02000E-02  
 17 2.22000E-02 18 2.27500E-02 19 2.33000E-02 20 2.38500E-02

21	2.44000E-02	22	2.64000E-02	23	2.84000E-02	24	3.04000E-02
25	3.24000E-02	26	3.29500E-02	27	3.35000E-02	28	3.40500E-02
29	3.46000E-02	30	3.66000E-02	31	3.86000E-02	32	4.06000E-02
33	4.26000E-02	34	4.28750E-02	35	4.31500E-02	36	4.34250E-02
37	4.37000E-02						

Y (or Theta) Gross Grid Lines and Number of Divisions

0.000000E+00	1.000000E-03	2.000000E-03	4.000000E-03	1.600000E-02
2.000000E-02				

Y (or Theta) Fine Grid Lines Generated by HEATING

	40	10	4	4	4		
1	0.00000E+00	2	2.50000E-05	3	5.00000E-05	4	7.50000E-05
5	1.00000E-04	6	1.25000E-04	7	1.50000E-04	8	1.75000E-04
9	2.00000E-04	10	2.25000E-04	11	2.50000E-04	12	2.75000E-04
13	3.00000E-04	14	3.25000E-04	15	3.50000E-04	16	3.75000E-04
17	4.00000E-04	18	4.25000E-04	19	4.50000E-04	20	4.75000E-04
21	5.00000E-04	22	5.25000E-04	23	5.50000E-04	24	5.75000E-04
25	6.00000E-04	26	6.25000E-04	27	6.50000E-04	28	6.75000E-04
29	7.00000E-04	30	7.25000E-04	31	7.50000E-04	32	7.75000E-04
33	8.00000E-04	34	8.25000E-04	35	8.50000E-04	36	8.75000E-04
37	9.00000E-04	38	9.25000E-04	39	9.50000E-04	40	9.75000E-04
41	1.00000E-03	42	1.10000E-03	43	1.20000E-03	44	1.30000E-03
45	1.40000E-03	46	1.50000E-03	47	1.60000E-03	48	1.70000E-03
49	1.80000E-03	50	1.90000E-03	51	2.00000E-03	52	2.50000E-03
53	3.00000E-03	54	3.50000E-03	55	4.00000E-03	56	7.00000E-03
57	1.00000E-02	58	1.30000E-02	59	1.60000E-02	60	1.70000E-02
61	1.80000E-02	62	1.90000E-02	63	2.00000E-02		

\*\*\*\*\* LISTING OF ANALYTICAL FUNCTIONS \*\*\*\*\*

f(v) = a(1) + a(2)\*v + a(3)\*v\*\*2 + a(4)\*cos(a(5)\*v) + a(6)\*exp(a(7)\*v)  
+ a(8)\*sin(a(9)\*v) + a(10)\*log(a(11)\*v)

Analytical Function Number: 1  
a( 1) = 1.00000E+00  
a( 2) = 2.20000E-01

\*\*\*\*\* LISTING OF TABULAR FUNCTIONS \*\*\*\*\*

Table number -	1	Number of pairs -	18
Argument	Value	(Min) <- Relative Value ->	(Max)
2.7000000D+01	1.74000000D+02	*****	
7.7000000D+01	1.67000000D+02	*****	
1.2700000D+02	1.59000000D+02	*****	
2.2700000D+02	1.46000000D+02	*****	
3.2700000D+02	1.37000000D+02	*****	
5.2700000D+02	1.25000000D+02	*****	
7.2700000D+02	1.18000000D+02	*****	
9.2700000D+02	1.12000000D+02	*****	
1.1270000D+03	1.08000000D+02	*****	
1.3270000D+03	1.04000000D+02	*****	
1.5270000D+03	1.01000000D+02	****	
1.7270000D+03	9.80000000D+01	***	
2.0270000D+03	9.40000000D+01	**	
2.1270000D+03	9.25000000D+01	*	
2.2270000D+03	9.15000000D+01	*	
2.3270000D+03	9.05000000D+01	*	
2.4270000D+03	9.00000000D+01	*	
2.5270000D+03	8.95000000D+01	*	

Table number -	2	Number of pairs -	15
Argument	Value	(Min) <- Relative Value ->	(Max)
2.5000000D+01	1.3210000D+02	*	
1.2700000D+02	1.3560000D+02	*	
5.2700000D+02	1.4006000D+02	*	
1.0270000D+03	1.5730000D+02	***	
1.5270000D+03	1.7016000D+02	*****	
2.0270000D+03	1.8350000D+02	*****	
2.3270000D+03	1.9170000D+02	*****	
2.5270000D+03	2.0370000D+02	*****	
2.7270000D+03	2.2300000D+02	*****	
2.9270000D+03	2.5030000D+02	*****	
3.1270000D+03	2.8450000D+02	*****	
3.3270000D+03	3.3570000D+02	*****	
3.4090000D+03	3.5980000D+02	*****	
3.4100000D+03	1.9344000D+02	*****	
5.7270000D+03	1.9344000D+02	*****	

Table number -	3	Number of pairs -	6
Argument	Value	(Min) <- Relative Value ->	(Max)
2.7000000D+01	4.8000000D+01	*	
2.2700000D+02	5.2000000D+01	*****	
5.2700000D+02	5.6000000D+01	*****	
6.2700000D+02	5.8000000D+01	*****	
7.2700000D+02	6.0000000D+01	*****	
9.2700000D+02	6.0000000D+01	*****	

\*\*\*\*\* SOURCES OF NON-LINEARITY IN THE MODEL \*\*\*\*\*

Time dependent flux (transient calculations)  
Radiation (in calculations 273.15 will be added to temperatures to  
convert them to absolute)  
Temperature dependent conductivity  
Temperature dependent density or specific heat (transient calculations)

\*\*\*\*\* NUMBER OF PARAMETERS SPECIFIED BY THE INPUT DATA \*\*\*\*\*

Regions	25
Materials	2
Phase changes	2
Initial temperatures	1
Heat generations	1
Boundary conditions	6
Gross grid lines along x or r axis	10
Fine grid lines along x or r axis	37
Gross grid lines along y or theta axis	6
Fine grid lines along y or theta axis	63
Gross grid lines along z or phi axis	1
Fine grid lines along z or phi axis	1
Analytic functions	1
Tabular functions	3
Node-to-node connectors	0
Transient printout times	0
Nodes for monitoring of temperatures	0
Number of nodes	2295
Number of specified-temperature nodes	0
Position-dependent boundary temperature nodes	0

\*\*\*\*\* MEMORY REQUIREMENTS FOR VARIABLY DIMENSIONED ARRAYS \*\*\*\*\*

Phase 1 12K  
Phase 2 332K  
Phase 3 665K  
Phase 4 756K

\*\*\*\*\* INITIAL CONDITIONS \*\*\*\*\*

Number of time steps completed = 0  
Current time step = 0.00000000D+00  
Current problem time = 0.00000000D+00  
Elapsed cpu time (hr:min:sec) = 00:00:04.75  
Minimum Temperature = 6.43307E+01 at node 2141  
Maximum Temperature = 9.95375E+02 at node 1

HEAT GENERATION

Number	Current Rate (energy/time) (Modeled)	(Neglected)
1	1.96000E+03	0.00000E+00

BOUNDARY HEAT FLOW

Number	Environment Temperature	Current Rate (energy/time) (Modeled)	(Neglected)
1	9.00000E+02	4.80870E+05	0.00000E+00
2	6.40000E+01	-2.49380E+05	0.00000E+00
3	6.40000E+01	-1.10102E+03	0.00000E+00
4	6.40000E+01	-1.03969E+05	0.00000E+00
5	6.40000E+01	-9.35893E+04	0.00000E+00
6	6.40000E+01	-3.47898E+04	0.00000E+00
---	---	---	---
Sum		-1.96000E+03	0.00000E+00

\*\*\*\*\*

BEGIN TRANSIENT CALCULATION - EXPLICIT TECHNIQUE

Temperature-dependent material properties and boundary conditions will be reevaluated every time step.  
Maximum of the stability criterion - 2.1219976D-02  
Median of the stability criterion - 7.9093425D-06  
Minimum of the stability criterion - 7.5154610D-06 for point 1480  
The input time step size is 0.0000000D+00.  
the time step size will be set to the stability criterion of 7.5154610D-06.  
Estimated time step size for levy technique - 7.5154610D-05

\*\*\*WARNING\*\*\* The time step chosen for the Levy modified explicit technique  
\*\*\*WARNING\*\*\* is larger than the median stability criterion (i.e. the time  
\*\*\*WARNING\*\*\* step does not satisfy the stability criterion for over half  
\*\*\*WARNING\*\*\* the nodes.) This may produce inaccurate results.

Levy's explicit method with a constant time increment equal to 7.5154610D-05 will now be used.

Number of stable time increments completed = 20  
Current time = 1.5030922D-04

\*\*\*WARNING\*\*\* Table 3 must be evaluated for 9.27007034D+02. The  
\*\*\*WARNING\*\*\* value of the function will be 6.00000000D+01 for all  
\*\*\*WARNING\*\*\* arguments greater than 9.27000000D+02

\*\*\*\*\* TRANSIENT SOLUTION OUTPUT \*\*\*\*\*

Number of time steps completed = 39936  
 Current time step = 7.51546097D-05  
 Current problem time = 3.00002171D+00  
 Elapsed cpu time (hr:min:sec) = 01:38:49.50  
 Minimum Temperature = 6.43337E+01 at node 2141  
 Maximum Temperature = 1.49127E+03 at node 1

HEAT GENERATION

Number	Current Rate (energy/time) (Modeled)	(Neglected)
1	1.96000E+03	0.00000E+00

BOUNDARY HEAT FLOW

Number	Environment Temperature	Current Rate (energy/time) (Modeled)	(Neglected)
1	9.00000E+02	7.94758E+05	0.00000E+00
2	6.40000E+01	-3.83657E+05	0.00000E+00
3	6.40000E+01	-1.24651E+03	0.00000E+00
4	6.40000E+01	-1.59413E+05	0.00000E+00
5	6.40000E+01	-1.42216E+05	0.00000E+00
6	6.40000E+01	-5.09246E+04	0.00000E+00
---		-----	-----
Sum		5.73016E+04	0.00000E+00

The transient calculations have been completed.  
 Final time is 3.00002D+00  
 Number of time steps completed = 39936

\*\*\*\*\* END OF HEATING EXECUTION \*\*\*\*\*

\* problem 2  
 \*\*\*\*\* Number of warnings -- 2  
 \*\*\*\*\* Number of errors -- 0

## **Appendix D**

# **MATHCAD calculations of the parameters uncertainties**

For category 1 transients, we take the range of variation for the transient frequency of occurrence (per year) as in reference [1], assuming that the lower and the upper values are respectively 5th and 95th percentile values of a lognormal distribution. According to reference [30] page 482, we can calculate the parameters  $\mu$  and  $\sigma$  as follows:

$\lambda_5 := 0.5$        $\lambda_{95} := 22$ .      (for tr1 of cat1; for the other 4 tr of cat1, we just plug in the appropriate 5th and 95th values)

$$\mu := \ln(\sqrt{\lambda_5 \cdot \lambda_{95}})$$

$$\sigma := \frac{\ln\left(\frac{\lambda_{95}}{\lambda_5}\right)}{1.645}$$

$\mu = 1.199$        $\sigma = 1.15$

$\mu_1 := 1.199$        $\mu_2 := -0.124$        $\mu_3 := 0.497$        $\mu_4 := 1.238$        $\mu_5 := 6.242$   
 $\sigma_1 := 1.15$        $\sigma_2 := 0.903$        $\sigma_3 := 0.366$        $\sigma_4 := 0.97$        $\sigma_5 := 0.884$

Then we calculate the mean and variance for the lambda of each tr of cat1:

$$\text{mean} := e^{\mu + .5 \cdot \sigma^2}$$

$$\text{var} := e^{2 \cdot \mu + \sigma^2} \cdot [e^{(\sigma^2)} - 1]$$

$\text{mean} = 6.425$        $\text{var} = 113.649$

$\text{mean}_1 := 6.425$        $\text{mean}_2 := 1.328$        $\text{mean}_3 := 1.758$        $\text{mean}_4 := 5.52$        $\text{mean}_5 := 759.551$   
 $\text{var}_1 := 113.649$        $\text{var}_2 := 2.222$        $\text{var}_3 := 0.443$        $\text{var}_4 := 47.61$        $\text{var}_5 := 6.834 \cdot 10^5$

Now, according to reference [31] page 279, we calculate the lambda for cat1 tr's:

$\text{meancat1} := \text{mean}_1 + \text{mean}_2 + \text{mean}_3 + \text{mean}_4 + \text{mean}_5$

$\text{varcat1} := \text{var}_1 + \text{var}_2 + \text{var}_3 + \text{var}_4 + \text{var}_5$

$\text{meancat1} = 774.582$        $\text{varcat1} = 6.836 \cdot 10^5$

For category 2 transients, we basically use the data from reference [9] to evaluate the frequencies of occurrence per year by a system analysis method. Ref. [9] usually gives a point estimate, which we consider is the median value of a lognormal distribution, and an error factor. According to ref. [30] page 482, these 2 values are used to estimate the parameters  $\mu$  and  $\sigma$ .

-overpower transient:

$\mu_{op} := \ln(8.76)$        $\sigma_{op} := \frac{\ln(10)}{1.645}$

$\mu_{op} = 2.17$        $\sigma_{op} = 1.4$

-loss of heat sink accident:

$\mu_{LHS} := \ln(2)$        $\sigma_{LHS} := \frac{\ln(10)}{1.645}$

$\mu_{LHS} = 0.693$        $\sigma_{LHS} = 1.4$

$$\text{mean}\lambda := e^{\mu\text{LHS} + .5 \cdot \sigma\text{LHS}^2} \quad \text{var}\lambda := e^{2 \cdot \mu\text{LHS} + \sigma\text{LHS}^2} \cdot \left[ e^{(\sigma\text{LHS}^2)} - 1 \right]$$

$$\text{mean}\lambda = 5.327$$

$$\text{var}\lambda = 172.94$$

$$\text{meanop} := 5.3$$

$$\text{meanLHS} := 0.023$$

$$\text{varop} := 173.$$

$$\text{varLHS} := 0.003$$

-loss of flow accident: a fault tree is used as explained in Chapter 4.

$$\mu\mu1 := \ln(.13 \cdot 1.5 \cdot 10^{-7} \cdot 8760) \quad \sigma\sigma1 := \frac{\ln(10)}{1.645}$$

$$\mu\mu2 := \ln(10^{-5} \cdot 8760) \quad \sigma\sigma2 := \frac{\ln(10)}{1.645}$$

$$\mu\mu3 := \ln(10^{-5} \cdot 8760) \quad \sigma\sigma3 := \frac{\ln(10)}{1.645}$$

$$\mu\mu4 := \ln(10^{-7} \cdot 8760) \quad \sigma\sigma4 := \frac{\ln(3)}{1.645}$$

$$\mu\mu5 := \ln(10^{-8} \cdot 8760) \quad \sigma\sigma5 := \frac{\ln(100)}{1.645}$$

$$\mu\mu6 := \ln(10^{-9} \cdot 8760) \quad \sigma\sigma6 := \frac{\ln(10)}{1.645}$$

$$\text{meanL} := e^{\mu\mu1 + .5 \cdot \sigma\sigma1^2} \quad \text{varL} := e^{2 \cdot \mu\mu1 + \sigma\sigma1^2} \cdot \left[ e^{(\sigma\sigma1^2)} - 1 \right]$$

$$\text{meanL} = 4.55 \cdot 10^{-4}$$

$$\text{varL} = 1.262 \cdot 10^{-6}$$

$$\text{meanL1} := 4.55 \cdot 10^{-4}$$

$$\text{meanL2} := .233$$

$$\text{meanL3} := .233$$

$$\text{meanL4} := .001$$

$$\text{varL1} := 1.262 \cdot 10^{-6}$$

$$\text{varL2} := .332$$

$$\text{varL3} := .332$$

$$\text{varL4} := 6.738 \cdot 10^{-7}$$

$$\text{meanL5} := .004$$

$$\text{meanL6} := 2.333 \cdot 10^{-5}$$

$$\text{varL5} := .049$$

$$\text{varL6} := 3.318 \cdot 10^{-9}$$

$$\text{meanLOFA} := \text{meanL1} + \text{meanL2} + \text{meanL3} + 2 \cdot \text{meanL4} + 2 \cdot \text{meanL5} + \text{meanL6}$$

$$\text{varLOFA} := \text{varL1} + \text{varL2} + \text{varL3} + 2 \cdot \text{varL4} + 2 \cdot \text{varL5} + \text{varL6}$$

$$\text{meanLOFA} = 0.476$$

$$\text{varLOFA} = 0.762$$



So the mean and variance of the frequency of occurrence of the noncatastrophic transients are:

$$\text{meannc} := \text{meancat1} + \text{meanop} + \text{meanLHS} + \text{meanLOFA}$$

$$\text{varnc} := \text{varcat1} + \text{varop} + \text{varLHS} + \text{varLOFA}$$

$$\text{meannc} = 780.381 \quad \text{varnc} = 6.837 \cdot 10^5$$

We calculate the parameters  $\mu$  and  $\sigma$  for the lognormal distribution associated with the freq. of occ. of the noncatastrophic accidents:

guess values:  $\mu_{nc} := 5.$        $\sigma_{nc} := 1.$

Given

$$e^{\mu_{nc} + .5 \cdot \sigma_{nc}^2} = 780.4$$

$$e^{2 \cdot \mu_{nc} + \sigma_{nc}^2} \cdot \left[ e^{\sigma_{nc}^2} - 1 \right] = 6.84 \cdot 10^5$$

$$\text{Find}(\mu_{nc}, \sigma_{nc}) = \begin{pmatrix} 6.283 \\ 0.868 \end{pmatrix}$$

Loss of coolant transient belongs to cat2, and is the only catastrophic transient considered here:

$$\mu_{LOCA} := \ln(10^{-2}) \quad \sigma_{LOCA} := \frac{\ln(10)}{1.645}$$

$$\mu_{LOCA} = -4.605 \quad \sigma_{LOCA} = 1.4$$

So the  $\mu$  and  $\sigma$  parameters for the lognormal distribution associated with the freq. of occ. of the catastrophic accidents are:

$$\mu_c := \mu_{LOCA} \quad \sigma_c := \sigma_{LOCA}$$

$$\mu_c = -4.605 \quad \sigma_c = 1.4$$

The three parameters considered uncertain in the present work when calculating the material loss are: the response time of the shutdown mechanism ( $t_r$ ), the time and energy of disruption ( $t_d$  and  $E_d$ ).  $E_d$  does not appear explicitly in the problem but implicitly through the heat flux  $H=E_d/t_d$ . If we associate lognormal distributions to both  $t_d$  and  $E_d$ , then  $H$  will also be a lognormal on  $e$ , as ref. [31] explains at page 297. We associate a normal distribution to  $t_r$ .

Once we have the range of each parameter, we assume that the limits are the 5th and the 95th percentile of the associated distribution, and we calculate the  $\mu$  and  $\sigma$  parameters of the distributions.

$$i := 0..10$$

$$tr5 := 1.$$

$$tr95 := 3.$$

$$\mu_r := \frac{tr5 + tr95}{2.}$$

$$\sigma_r := \frac{tr95 - \mu_r}{1.645}$$

$$\mu_r = 2$$

$$\sigma_r = 0.608$$

$$tr_i := \mu_r + \sigma_r \cdot \sqrt{-2 \cdot \ln(\text{md}(1))} \cdot \cos(2 \cdot \pi \cdot \text{md}(1))$$

We can verify that the parameters are correct as follows:

$$f1(x) := \frac{1}{\sigma_r \cdot \sqrt{2 \cdot \pi}} \cdot e^{-\frac{(x - \mu_r)^2}{2 \cdot \sigma_r^2}}$$

$$\int_{-1000.}^{tr5} f1(x) dx = 0.05$$

$$\int_{-100.}^{tr95} f1(x) dx = 0.95$$

$$\int_{\mu_r - \sigma_r}^{\mu_r + \sigma_r} f1(x) dx = 0.683$$

$$td5 := .1$$

$$td95 := 3.$$

$$\mu_{td} := \ln(\sqrt{td5 \cdot td95})$$

$$\sigma_{td} := \frac{\ln\left(\sqrt{\frac{td95}{td5}}\right)}{1.645}$$

$$\text{meantd} := e^{\mu_{td} + \frac{\sigma_{td}^2}{2}}$$

$$\mu_{td} = -0.602$$

$$\sigma_{td} = 1.034$$

$$\text{meantd} = 0.935$$

$$td_i := e^{\mu_{td} - \sigma_{td}^2 + \sqrt{-2 \cdot \sigma_{td}^2 \cdot \ln(\text{md}(1))} \cdot \cos(2 \cdot \pi \cdot \text{md}(1))}$$

$$f2(x) := \frac{1}{x \cdot \sigma_{td} \cdot \sqrt{2 \cdot \pi}} \cdot e^{-\frac{(\ln(x) - \mu_{td})^2}{2 \cdot \sigma_{td}^2}}$$

$$\int_{0.}^{td5} f2(x) dx = 0.05$$

$$\int_{0.}^{td95} f2(x) dx = 0.95$$

$$Ed5 := 5.$$

$$Ed95 := 20.$$

$$\mu Ed := \ln(\sqrt{Ed5 \cdot Ed95})$$

$$\sigma Ed := \frac{\ln\left(\sqrt{\frac{Ed95}{Ed5}}\right)}{1.645}$$

$$\text{meanEd} := e^{\mu Ed + \frac{\sigma Ed^2}{2}}$$

$$\mu Ed = 2.303$$

$$\sigma Ed = 0.421$$

$$\text{meanEd} = 10.928$$

$$H_1 := e^{\mu Ed - \sigma Ed^2 + \sqrt{-2 \cdot \sigma Ed^2 \cdot \ln(\text{md}(1))} \cdot \cos(2 \cdot \pi \cdot \text{md}(1))}$$

$$f3(x) := \frac{1}{x \cdot \sigma Ed \cdot \sqrt{2 \cdot \pi}} \cdot e^{-\frac{(\ln(x) - \mu Ed)^2}{2 \cdot \sigma Ed^2}}$$

$$\int_0^{Ed5} f3(x) dx = 0.05$$

$$\int_0^{Ed95} f3(x) dx = 0.95$$

$$\mu H := \mu Ed - \mu td$$

$$\sigma H := \sqrt{\sigma Ed^2 + \sigma td^2}$$

$$\text{meanH} := e^{\mu H + \frac{\sigma H^2}{2}}$$

$$\mu H = 2.905$$

$$\sigma H = 1.116$$

$$\text{meanH} = 34.046$$

$$H_1 := e^{\mu H - \sigma H^2 + \sqrt{-2 \cdot \sigma H^2 \cdot \ln(\text{md}(1))} \cdot \cos(2 \cdot \pi \cdot \text{md}(1))}$$

$$f4(x) := \frac{1}{x \cdot \sigma H \cdot \sqrt{2 \cdot \pi}} \cdot e^{-\frac{(\ln(x) - \mu H)^2}{2 \cdot \sigma H^2}}$$

$$P(x) := \int_{.01}^x f4(x) dx$$

**guess value:** H5 := 1.

Given

$$P(H5) = .05$$

$$\text{Find}(H5) = 2.91$$

**guess value:** H95 := 100.

Given

$$P(H95) = .95$$

$$\text{Find}(H95) = 114.538$$

## Appendix E

# MATHCAD program for response surface coefficients calculation

$$\begin{aligned}
& \text{tr1} := 3. & \text{tr2} := 1. & \text{mtr} := 2. & \text{(mean value)} \\
& \text{tr3} := \text{mtr} + \frac{\text{tr1} - \text{mtr}}{\sqrt{2}} & \text{tr4} := \text{mtr} + \frac{\text{tr2} - \text{mtr}}{\sqrt{2}} & \text{tr3} = 2.707 & \text{tr4} = 1.293 \\
& \text{td1} := 3. & \text{td2} := .1 & \text{mtd} := .935 & \text{(mean value)} \\
& \text{td3} := \text{mtd} + \frac{\text{td1} - \text{mtd}}{\sqrt{2}} & \text{td4} := \text{mtd} + \frac{\text{td2} - \text{mtd}}{\sqrt{2}} & \text{td3} = 2.395 & \text{td4} = 0.345 \\
& \text{H1} := 114.539 & \text{H2} := 2.91 & \text{mH} := 34.046 & \text{(mean value)} \\
& \text{H3} := \text{mH} + \frac{\text{H1} - \text{mH}}{\sqrt{2}} & \text{H4} := \text{mH} + \frac{\text{H2} - \text{mH}}{\sqrt{2}} & \text{H3} = 90.963 & \text{H4} = 12.03
\end{aligned}$$

Y values (melting + evaporation thickness) in micrometers as obtained from HEATING7.2:

$$\begin{aligned}
& \text{Y0} := 211.4 \\
& \text{Y1r} := 216.4 & \text{Y2r} := 205.6 & \text{Y3r} := 222.3 & \text{Y4r} := 200. \\
& \text{Y1d} := 419.4 & \text{Y2d} := 225. & \text{Y3d} := 372. & \text{Y4d} := 115.4 \\
& \text{Y1H} := 265.4 & \text{Y2H} := 99.1 & \text{Y3H} := 250. & \text{Y4H} := 150. \\
& \text{Y3r3d} := 375. & \text{Y4r3d} := 364.3 & \text{Y4r4d} := 100. & \text{Y3r4d} := 124. \\
& \text{Y3r3H} := 255.3 & \text{Y4r3H} := 250. & \text{Y4r4H} := 150. & \text{Y3r4H} := 157. \\
& \text{Y3d3H} := 423.2 & \text{Y4d3H} := 150. & \text{Y4d4H} := 75. & \text{Y3d4H} := 284.2
\end{aligned}$$

Calculate the coefficients for the approximation Y(tr,td,H):

$$\begin{aligned}
& \text{A0} := \text{Y0} & \text{A0} = 211.4 \\
& \text{Br} := (\text{Y3r} - \text{Y0}) \cdot \frac{\text{mtr} - \text{tr4}}{(\text{tr3} - \text{mtr}) \cdot (\text{tr3} - \text{tr4})} + (\text{Y4r} - \text{Y0}) \cdot \frac{\text{mtr} - \text{tr3}}{(\text{tr4} - \text{mtr}) \cdot (\text{tr4} - \text{tr3})} \\
& \text{Bd} := (\text{Y3d} - \text{Y0}) \cdot \frac{\text{mtd} - \text{td4}}{(\text{td3} - \text{mtd}) \cdot (\text{td3} - \text{td4})} + (\text{Y4d} - \text{Y0}) \cdot \frac{\text{mtd} - \text{td3}}{(\text{td4} - \text{mtd}) \cdot (\text{td4} - \text{td3})} \\
& \text{BH} := (\text{Y3H} - \text{Y0}) \cdot \frac{\text{mH} - \text{H4}}{(\text{H3} - \text{mH}) \cdot (\text{H3} - \text{H4})} + (\text{Y4H} - \text{Y0}) \cdot \frac{\text{mH} - \text{H3}}{(\text{H4} - \text{mH}) \cdot (\text{H4} - \text{H3})} \\
& \text{Br} = 15.768 & \text{Bd} = 147.445 & \text{BH} = 2.2 \\
& \text{Cr} := (\text{Y3r} - \text{Y0}) \cdot \frac{1.}{(\text{tr3} - \text{mtr}) \cdot (\text{tr3} - \text{tr4})} + (\text{Y4r} - \text{Y0}) \cdot \frac{1.}{(\text{tr4} - \text{mtr}) \cdot (\text{tr4} - \text{tr3})} \\
& \text{Cd} := (\text{Y3d} - \text{Y0}) \cdot \frac{1.}{(\text{td3} - \text{mtd}) \cdot (\text{td3} - \text{td4})} + (\text{Y4d} - \text{Y0}) \cdot \frac{1.}{(\text{td4} - \text{mtd}) \cdot (\text{td4} - \text{td3})} \\
& \text{CH} := (\text{Y3H} - \text{Y0}) \cdot \frac{1.}{(\text{H3} - \text{mH}) \cdot (\text{H3} - \text{H4})} + (\text{Y4H} - \text{Y0}) \cdot \frac{1.}{(\text{H4} - \text{mH}) \cdot (\text{H4} - \text{H3})} \\
& \text{Cr} = -0.5 & \text{Cd} = -25.654 & \text{CH} = -0.027
\end{aligned}$$

$$\text{DrdI} := \frac{Y0 + Y3r3d - Y3r - Y3d}{(tr3 - mtr) \cdot (td3 - mtd)}$$

$$\text{DrdII} := \frac{Y0 + Y4r3d - Y4r - Y3d}{(tr4 - mtr) \cdot (td3 - mtd)}$$

$$\text{DrdIII} := \frac{Y0 + Y4r4d - Y4r - Y4d}{(tr4 - mtr) \cdot (td4 - mtd)}$$

$$\text{DrdIV} := \frac{Y0 + Y3r4d - Y3r - Y4d}{(tr3 - mtr) \cdot (td4 - mtd)}$$

$$\text{DrdI} = -7.651 \quad \text{DrdII} = -3.584$$

$$\text{DrdIII} = -9.581 \quad \text{DrdIV} = 5.509$$

$$\text{DrHI} := \frac{Y0 + Y3r3H - Y3r - Y3H}{(tr3 - mtr) \cdot (H3 - mH)}$$

$$\text{DrHII} := \frac{Y0 + Y4r3H - Y4r - Y3H}{(tr4 - mtr) \cdot (H3 - mH)}$$

$$\text{DrHIII} := \frac{Y0 + Y4r4H - Y4r - Y4H}{(tr4 - mtr) \cdot (H4 - mH)}$$

$$\text{DrHIV} := \frac{Y0 + Y3r4H - Y3r - Y4H}{(tr3 - mtr) \cdot (H4 - mH)}$$

$$\text{DrHI} = -0.139 \quad \text{DrHII} = -0.283$$

$$\text{DrHIII} = 0.732 \quad \text{DrHIV} = 0.251$$

$$\text{DdHI} := \frac{Y0 + Y3d3H - Y3d - Y3H}{(td3 - mtd) \cdot (H3 - mH)}$$

$$\text{DdHII} := \frac{Y0 + Y4d3H - Y4d - Y3H}{(td4 - mtd) \cdot (H3 - mH)}$$

$$\text{DdHIII} := \frac{Y0 + Y4d4H - Y4d - Y4H}{(td4 - mtd) \cdot (H4 - mH)}$$

$$\text{DdHIV} := \frac{Y0 + Y3d4H - Y3d - Y4H}{(td3 - mtd) \cdot (H4 - mH)}$$

$$\text{DdHI} = 0.152 \quad \text{DdHII} = 0.119 \quad \text{DdHIII} = 1.615 \quad \text{DdHIV} = 0.821$$

$$\text{Drd}(tr, td) := \text{if}(tr > mtr, \text{if}(td > mtd, \text{DrdI}, \text{DrdIV}), \text{if}(td > mtd, \text{DrdII}, \text{DrdIII}))$$

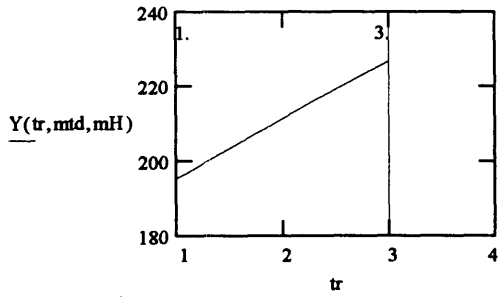
$$\text{DrH}(tr, H) := \text{if}(tr > mtr, \text{if}(H > mH, \text{DrHI}, \text{DrHIV}), \text{if}(H > mH, \text{DrHII}, \text{DrHIII}))$$

$$\text{DdH}(td, H) := \text{if}(td > mtd, \text{if}(H > mH, \text{DdHI}, \text{DdHIV}), \text{if}(H > mH, \text{DdHII}, \text{DdHIII}))$$

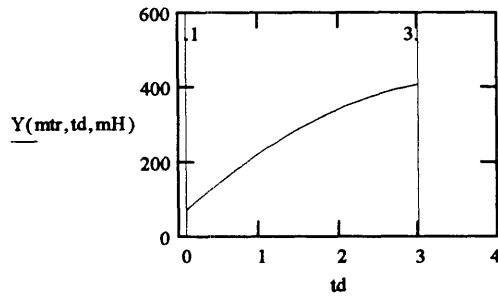
$$\begin{aligned} Y(tr, td, H) := & A0 + (Br + Cr \cdot (tr - mtr) + \text{Drd}(tr, td) \cdot (td - mtd) + \text{DrH}(tr, H) \cdot (H - mH)) \cdot (tr - mtr) \dots \\ & + (Bd + Cd \cdot (td - mtd) + \text{DdH}(td, H) \cdot (H - mH)) \cdot (td - mtd) \dots \\ & + (BH + CH \cdot (H - mH)) \cdot (H - mH) \end{aligned}$$

**NOTE:** The measure units of the coefficients are as following: A0[microm]; Br[microm/s]; Bd[microm/ms]; BH[microm/(E9\*W/m2)]; Cr[microm/s2]; Cd[microm/ms2]; CH[microm/(E9\*W/m2)2]; Drd[microm/(s\*ms)]; DrH[microm/(s\*(E9\*W/m2))]; DdH[microm/(ms\*(E9\*W/m2))]; and finally the estimated value of Y in [microm], tr[s], td[ms], H[E9\*W/m2].

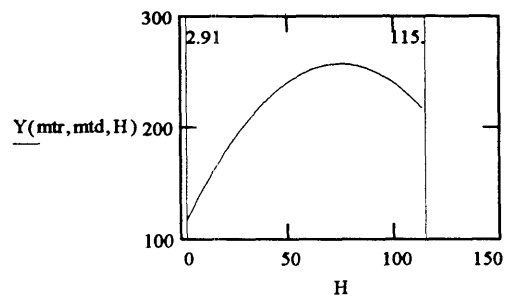
tr := 1, 1.1..3.



td := .1, .2..3.



H := 2.91..114.539



td := 1.

Given  $\frac{d}{dtd} Y(mtr, td, mH) = 0$ .

Find(td) = 3.809

H := 90.

Given  $\frac{d}{dH} Y(mtr, mtd, H) = 0$ .

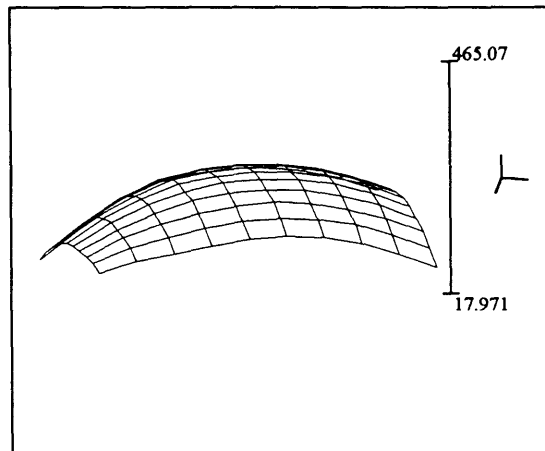
Find(H) = 75.186

i := 0..9

j := 0..9

$td_i := .1 + .322 \cdot i$      $H_j := 2.91 + 12.403 \cdot j$

$M1_{i,j} = Y(mtr, td_i, H_j)$



M1

## Appendix F

**MATHCAD program for  
propagation of the parameters  
uncertainties through the reliability  
function**



A0 = 211.4

Br = 15.768    Bd = 147.445    BH = 2.2    Cr = -0.5    Cd = -25.654    CH = -0.027

DrdI = -7.651    DrdII = -3.584    DrdIII = -9.581    DrdIV = 5.509

DrHI = -0.139    DrHII = -0.283    DrHIII = 0.732    DrHIV = 0.251

DdHI = 0.152    DdHII = 0.119    DdHIII = 1.615    DdHIV = 0.821

Mean values:    mtr = 2.    mtd = .935    mH = 34.046

Drd(tr, td) = if(tr > mtr, if(td > mtd, DrdI, DrdIV), if(td > mtd, DrdII, DrdIII))

DrH(tr, H) = if(tr > mtr, if(H > mH, DrHI, DrHIV), if(H > mH, DrHII, DrHIII))

DdH(td, H) = if(td > mtd, if(H > mH, DdHI, DdHIV), if(H > mH, DdHII, DdHIII))

I(tr, td, H) = A0 + (Br + Cr · (tr - mtr) + Drd(tr, td) · (td - mtd) + DrH(tr, H) · (H - mH)) · (tr - mtr) ...  
 + (Bd + Cd · (td - mtd) + DdH(td, H) · (H - mH)) · (td - mtd) ...  
 + (BH + CH · (H - mH)) · (H - mH)

μ = 2.    σ = .608    μd = -.602    σd = 1.034    μH = 2.905    σH = 1.116

Δ = 1 · 10<sup>-3</sup>    tp = 2000.    ε = 6.5 · 10<sup>-11</sup>    a = 365 · 24 · 3600

μc = -4.605    σc = 1.4    μnc = 6.317    σnc = 0.855

i = 0..99    n = 1140

r = 0..n    q = 0..n

$$X_i = I \left( \mu + \sigma \cdot \sqrt{-2 \ln(\text{rnd}(1))} \cdot \cos(2 \cdot \pi \cdot \text{rnd}(1)), e^{\mu d - \sigma d^2 + \sqrt{-2 \cdot \sigma d^2 \cdot \ln(\text{rnd}(1))} \cdot \cos(2 \cdot \pi \cdot \text{rnd}(1))}, e^{\mu H - \sigma H^2 + \sqrt{-2 \cdot \sigma H^2 \cdot \ln(\text{rnd}(1))} \cdot \cos(2 \cdot \pi \cdot \text{rnd}(1))} \right)$$

$$Y_i = \text{if}(X_i \geq 0, X_i, 0)$$

min(Y) = 6.028    max(Y) = 315.707

$$k_i = \text{if} \left( n \geq \frac{\Delta}{\varepsilon \cdot \text{tp} + Y_i \cdot 10^{-6}}, \frac{\Delta - \varepsilon \cdot \text{tp} \cdot n}{Y_i \cdot 10^{-6}}, n \right)$$

min(k) = 2.698    max(k) = 141.308

$$\lambda_{c_i} = e^{\mu c - \sigma c^2 + \sqrt{-2 \cdot \sigma c^2 \cdot \ln(\text{rnd}(1))} \cdot \cos(2 \cdot \pi \cdot \text{rnd}(1))}$$

min(λc) = 6.816 · 10<sup>-5</sup>    max(λc) = 0.027

$$\lambda_{nc_i} = e^{\mu nc - \sigma nc^2 + \sqrt{-2 \cdot \sigma nc^2 \cdot \ln(\text{rnd}(1))} \cdot \cos(2 \cdot \pi \cdot \text{rnd}(1))}$$

min(λnc) = 44.962    max(λnc) = 3.31 · 10<sup>3</sup>

$$p_i = 1 - e^{-\lambda_{nc_i} \cdot \frac{\text{tp}}{a}}$$

min(p) = 0.003    max(p) = 0.189

$$D_{0,i} = (1 - p_i)^n$$

$$D_{q+1,i} = D_{q,i} \cdot \frac{n - q}{q + 1} \cdot \frac{p_i}{1 - p_i} \cdot [k_i \geq (q + 1)]$$

$$R_i = e^{-\lambda_{c_i} \cdot \frac{\text{tp}}{a}} \cdot \sum_r D_{r,i} \cdot (k_i \geq r)$$

APPENDPRN(zum) = R

P = READPRN(zum)

rows(P) = 1 · 10<sup>3</sup>

S = sort(P)

S<sub>10%</sub> = 7.166 · 10<sup>-11</sup>

S<sub>50%</sub> = 0.424

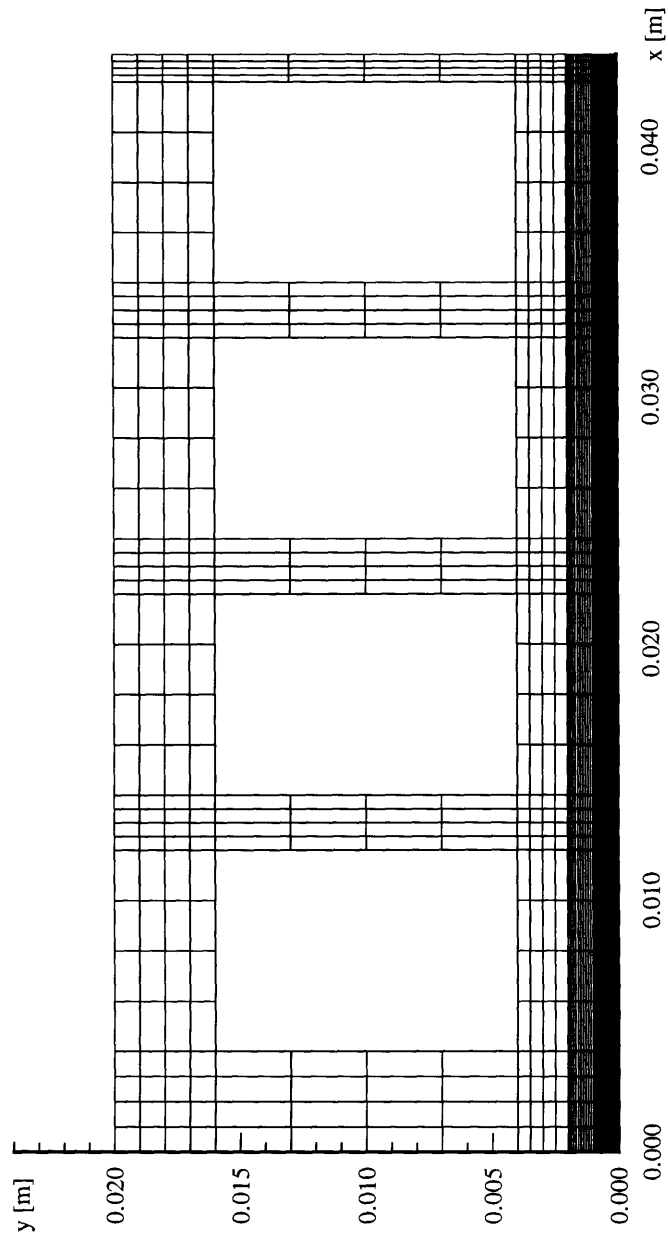
S<sub>90%</sub> = 1

## **Appendix G**

# **HEATING 7.2 thermal analyses results**

MESH OF CROSS-SECTION FROM FIG. 3.8

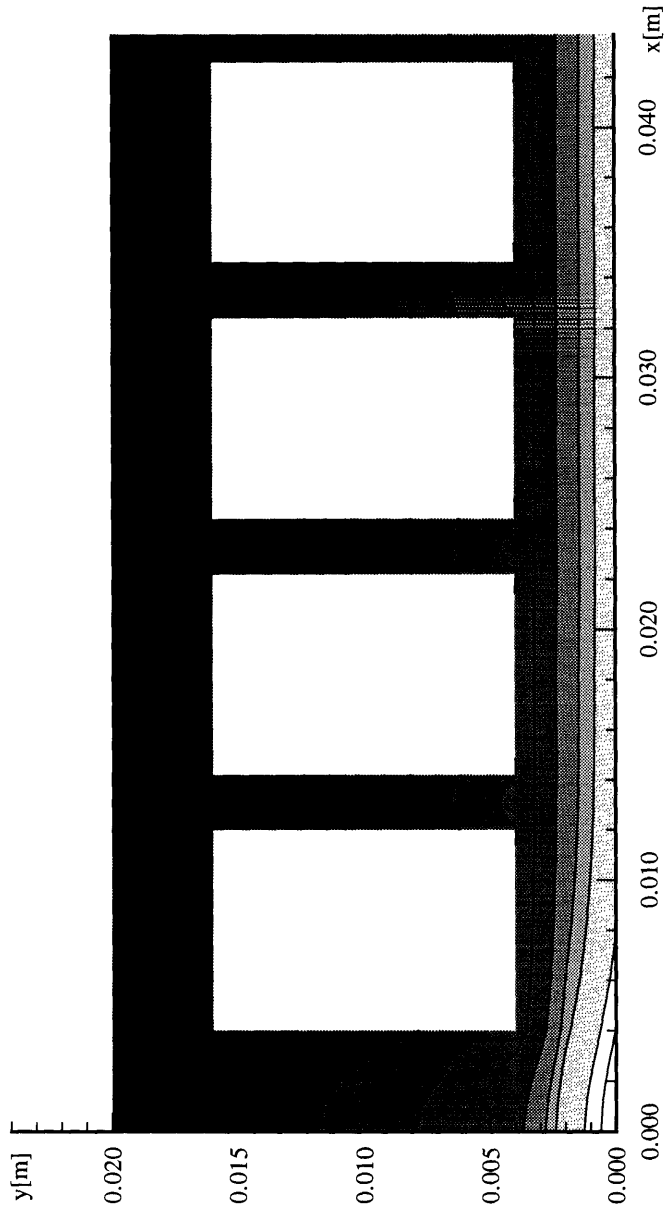
Note: It shows gross and fine grides as defined in the input files in App. A and C. Region 1 is black because of the high number of the fine grides.

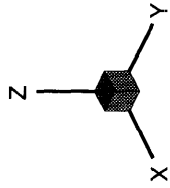


T001 [C]

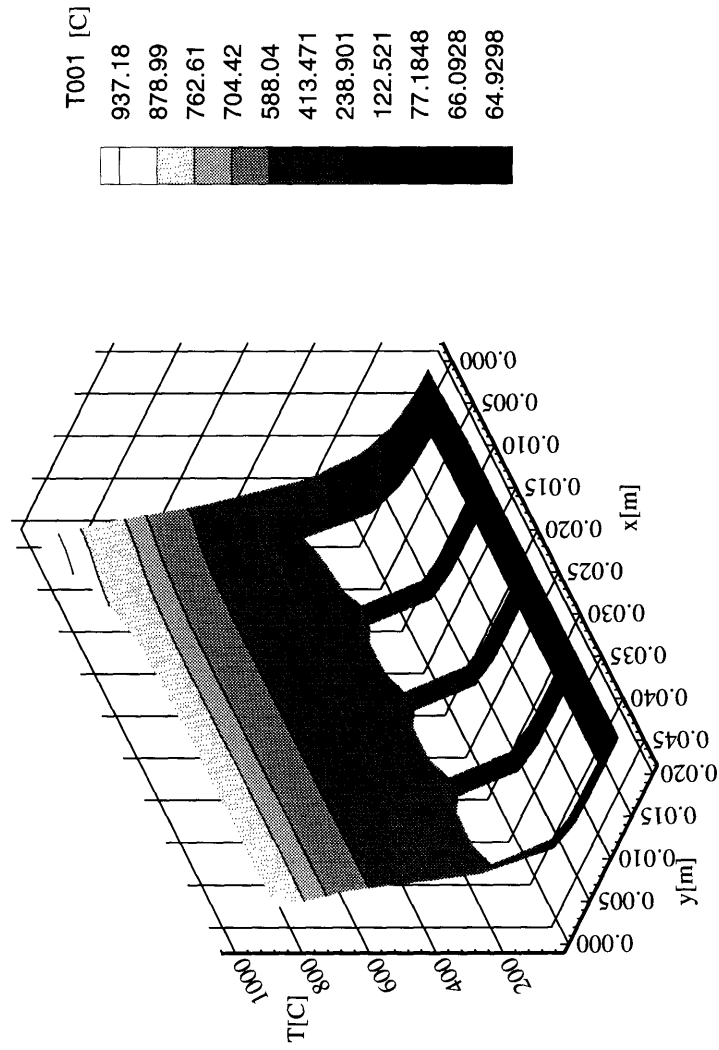
937.18
878.99
762.61
704.42
588.04
413.471
238.901
122.521
77.1848
66.0928
64.9298

STEADY-STATE TEMPERATURE DISTRIBUTION (PROBLEM 1)





STEADY-STATE TEMPERATURE DISTRIBUTION (PROBLEM 1)  
(3D-surface field plot)

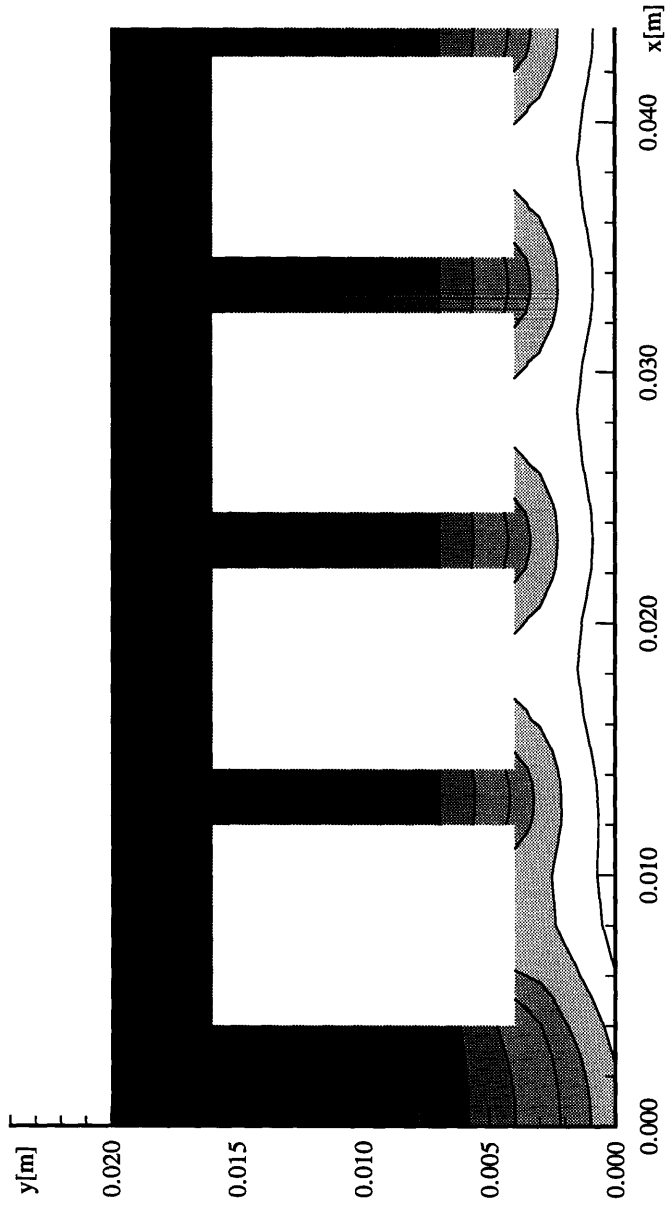


T002 [C]

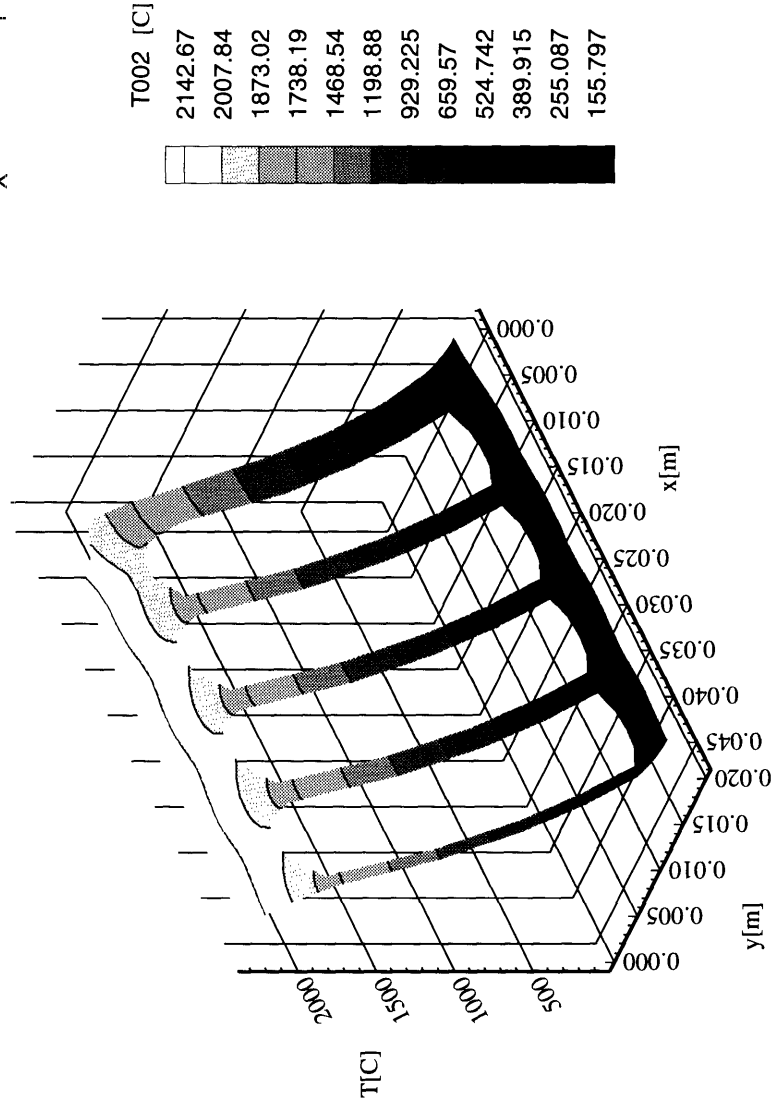
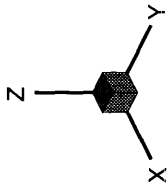
- 2142.67
- 2007.84
- 1873.02
- 1738.19
- 1468.54
- 1198.88
- 929.225
- 659.57
- 524.742
- 389.915
- 255.087
- 155.797



TEMPERATURE DISTRIBUTION FOLLOWING LOCA-PROBLEM 2 ( $t=2s$ )



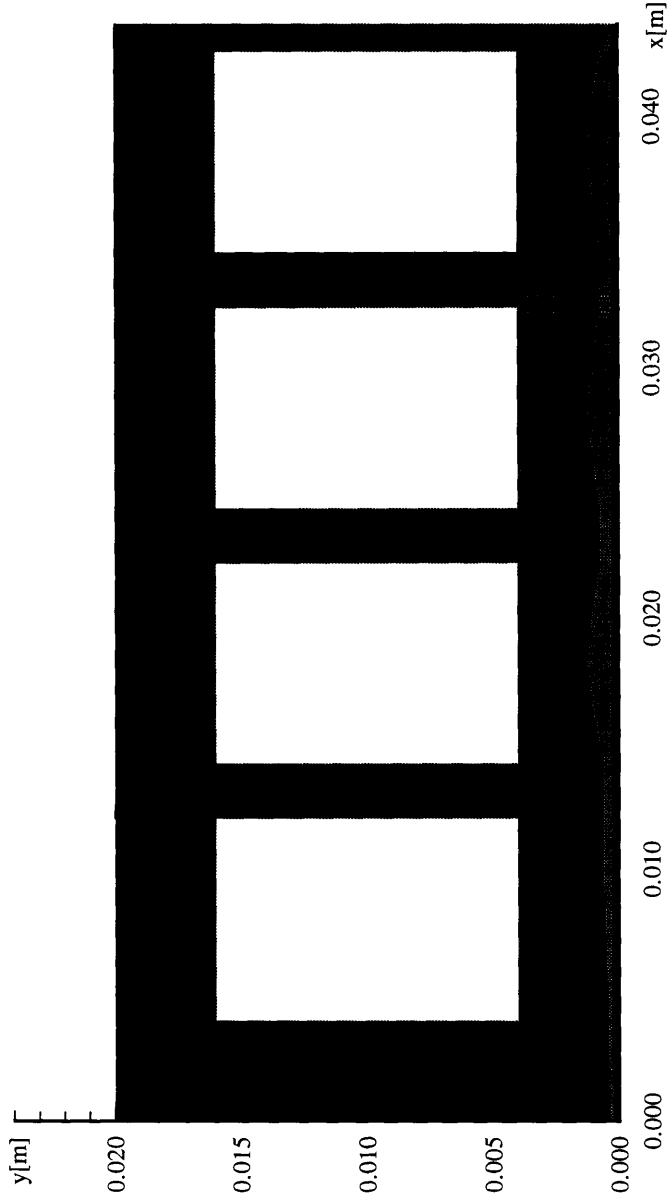
TEMPERATURE DISTRIBUTION FOLLOWING LOCA-PROBLEM 2 (tr=2s)  
 (3D-surface field plot)



T003 [C]

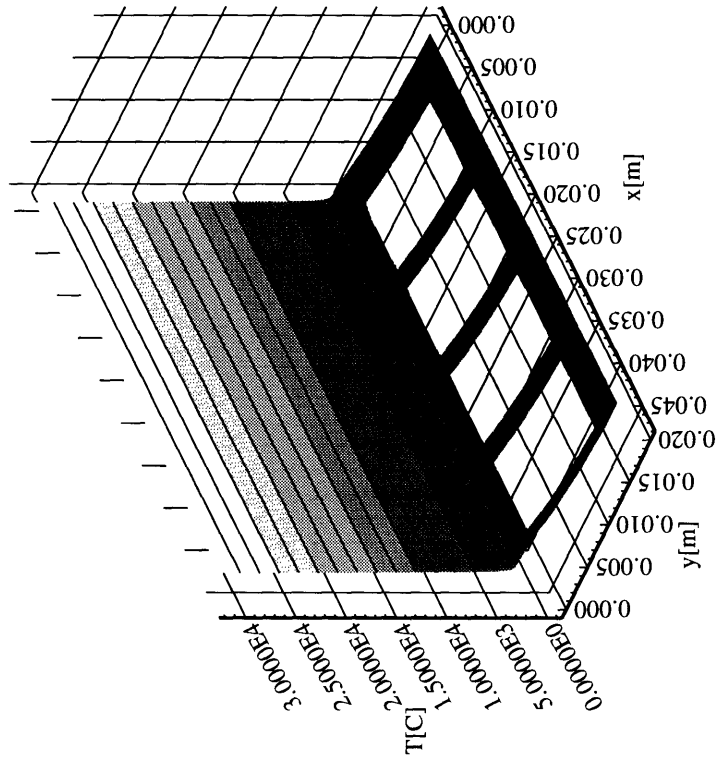
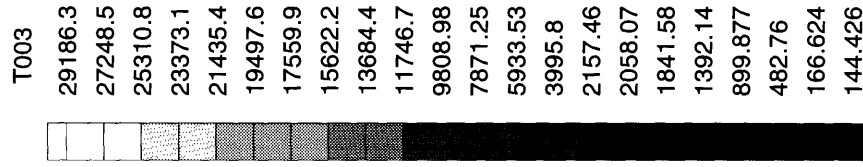
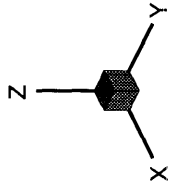
29186.3  
27248.5  
25310.8  
23373.1  
21435.4  
19497.6  
17559.9  
15622.2  
13684.4  
11746.7  
9808.98  
7871.25  
5933.53  
3995.8  
2157.46  
2058.07  
1841.58  
1392.14  
899.877  
482.76  
166.624  
144.426

TEMPERATURE DISTRIBUTION FOLLOWING LOCA-PROBLEM 3  
( $H=34E9W/m^2$ ,  $t_d=1$  ms)





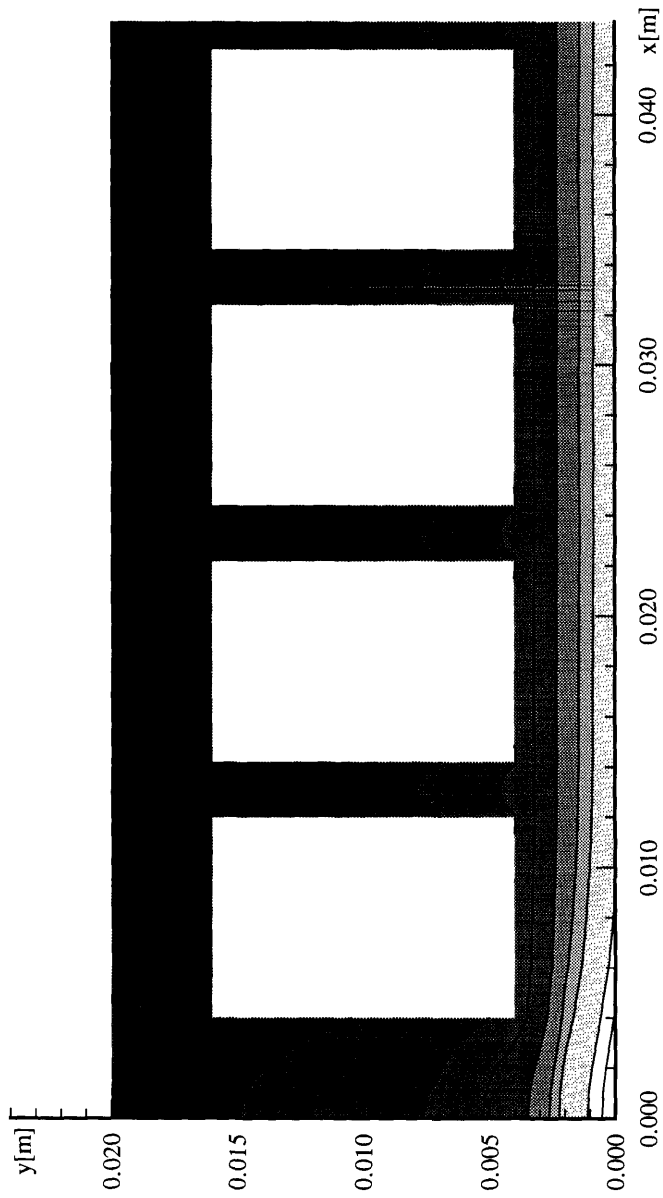
TEMPERATURE DISTRIBUTION FOLLOWING LOCA-PROBLEM 3  
 (H=34E9W/m<sup>2</sup>,td=1ms)  
 (3D-surface field plot)



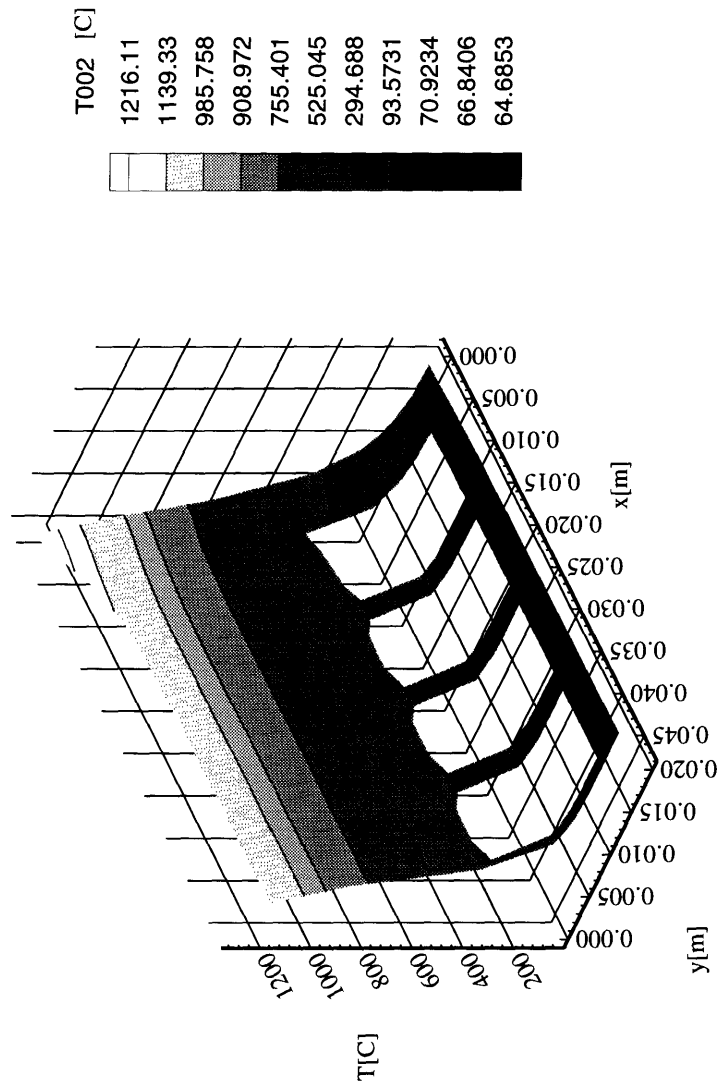
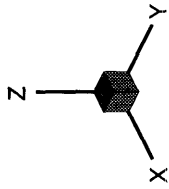
T002 [C]

- 1216.11
- 1139.33
- 985.758
- 908.972
- 755.401
- 525.045
- 294.688
- 93.5731
- 70.9234
- 66.8406
- 64.6853

TEMPERATURE DISTRIBUTION FOLLOWING  
OVERPOWER TRANSIENT-PROBLEM 2 (t=2s)



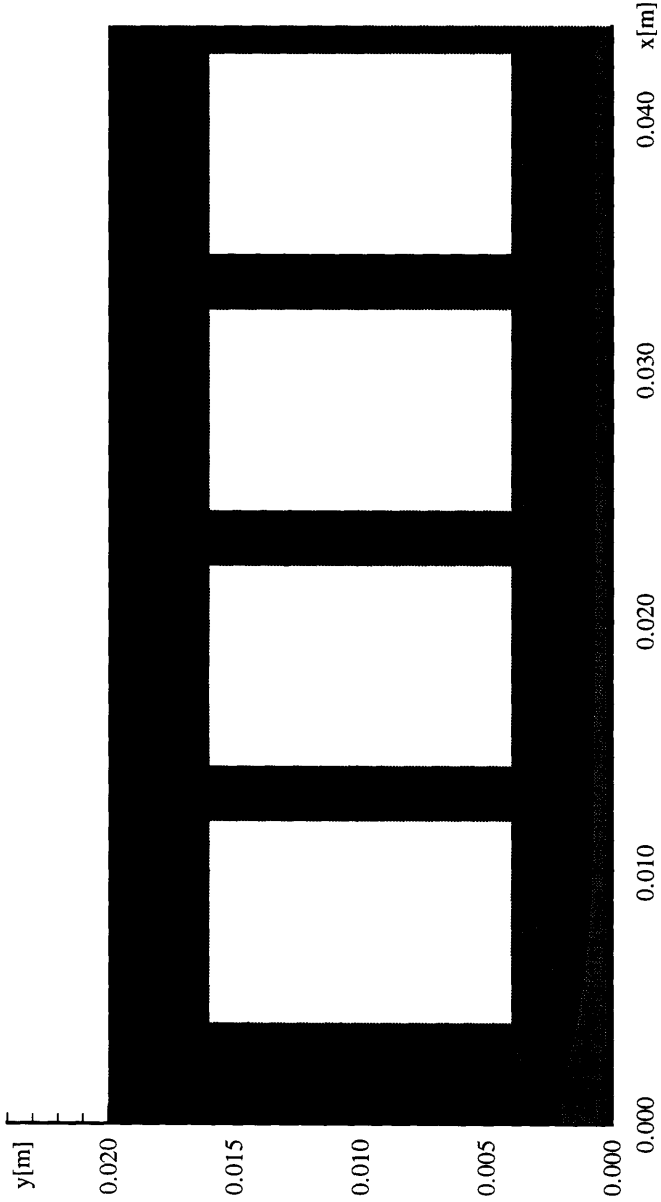
TEMPERATURE DISTRIBUTION FOLLOWING  
 OVERPOWER TRANSIENT-PROBLEM 2 (tr=2s)  
 (3D-surface field plot)



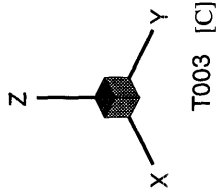
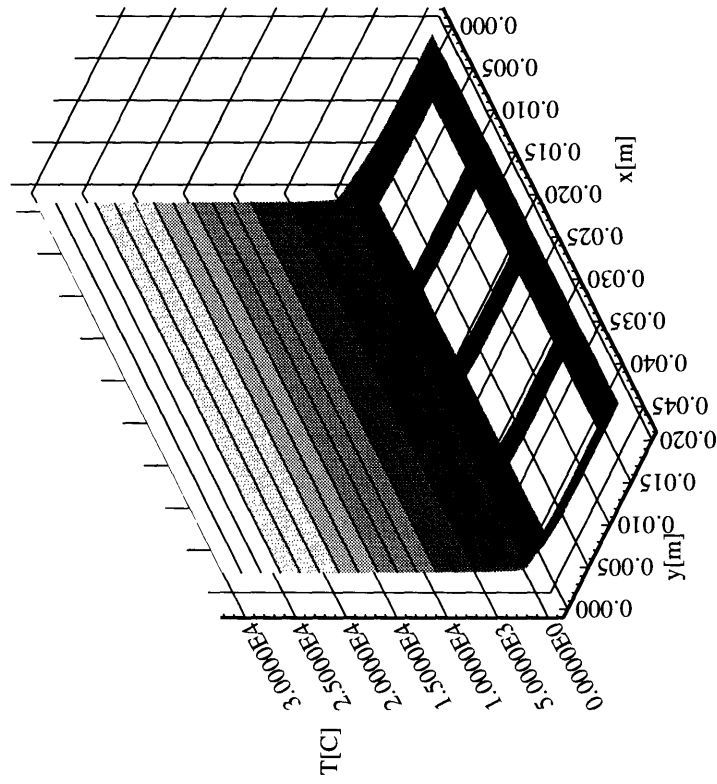
T003 [C]

28969
27042
25115.1
23188.1
21261.1
19334.1
17407.1
15480.2
13553.2
11626.2
9699.23
7772.25
5845.27
3918.29
1991.31
1018.33
729.057
405.128
185.441
91.6779
73.7948
67.2577
64.743

TEMPERATURE DISTRIBUTION FOLLOWING  
OVERPOWER TRANSIENT-PROBLEM 3  
( $H=34E9W/m^2, td=1ms$ )



TEMPERATURE DISTRIBUTION FOLLOWING  
 OVERPOWER TRANSIENT-PROBLEM 3  
 (H=34E9W/m<sup>2</sup>,td=1ms)  
 (3D-surface plot)



T003 [C]
28969
27042
25115.1
23188.1
21261.1
19334.1
17407.1
15480.2
13553.2
11626.2
9699.23
7772.25
5845.27
3918.29
1991.31
1018.33
729.057
405.128
185.441
91.6779
73.7948
67.2577
64.743

# Bibliography

- [1] Dean Lawrence Sanzo, "Probabilistic Lifetime Analysis of Tokamak In - Vessel Components", Ph.D. thesis, University of California at Los Angeles, 1988
- [2] P. H. Rebut, D. Boucher, D. J. Gambier, B. E. Keen, M. L. Watkins, "The key to ITER: the Divertor and the First Wall", JET-P(93)06, 1993
- [3] G. Vieider, A. Cardella, M. Akiba, R. Matera, and R. Watson, "ITER plasma facing components, design and development", Fusion Engineering and Design vol. 16, 1991
- [4] A. Madrid, G. Apostolakis, and R. W. Conn, "On the development of the accident sequences involving tokamak impurity control systems", Nuclear Technology/Fusion, vol. 4, September 1983
- [5] H. Th. Klippel and E. M. J. Komen, "Analysis of loss-of-coolant and loss-of-flow accidents in the divertor cooling system of NET/ITER", Fusion Engineering and Design vol. 17, 1991
- [6] D. Sanzo, G. Apostolakis, "A probabilistic description of overpower and loss of flow events and their impact on limiter temperature", Fusion Technology vol. 8, 1985
- [7] S. L. Thompson, et al., "Availability Program Phase I Report", Oak Ridge National Laboratory Report, ORNL/FEDC-84/10, 1985
- [8] Z. Musicki and C. W. Maynard, "The availability analysis of fusion power plants as applied to MARS", Nuclear Technology/Fusion vol. 4, 1983
- [9] L. C. Cadwallader and S. J. Piet, "1989 Failure Rate Screening Data for Fusion Reliability and Risk Analysis", EGG-FSP-8709, September 1989

- [10] Pickard, Lowe and Garrick, Inc., "Seabrook Station Probabilistic Safety Assessment", PLG-0300, 1983
- [11] G. Apostolakis, "Uncertainty in Probabilistic Risk Assessment", 9th International Conference on Structural Mechanics in Reactor Technology, M, pages 345-401, 1987
- [12] K. W. Childs, "HEATING 7.2 User's Manual", ORNL/TM-12262, February 1993
- [13] P.-H. Rebut, D. Boucher, D. J. Gambier, B. E. Keen, M. L. Watkins, "The Key to ITER", JET-P(93)06, January 1993
- [14] J. A. Koski, R. D. Watson, P. L. Goranson, A. M. Hassanein, J. C. Salmonson, "Thermal-hydraulic design issues and analysis for the ITER divertor", Fusion Technology vol. 19, May 1991
- [15] "ITER Concept Definition", vol. 2, IAEA, Vienna, 1989
- [16] R. F. Mattas, "First wall and divertor performance and lifetime analysis for the U. S. ITER design", Fusion Technology vol. 19, May 1991
- [17] Y. Hirooka, M. Bourham, J. N. Brooks, R. A. Causey, G. Chevalier, R. W. Conn, W. H. Eddy, J. Gilligan, M. Khandagle, Y. Ra, "Evaluation of Tungsten as Plasma-Facing Material for Steady-State Magnetic Fusion Devices", UCLA PPG#1430, May 1992
- [18] R. F. Mattas, "International Thermonuclear Experimental Reactor (ITER) Divertor Plate Performance and Lifetime Considerations", ANL/FPP/TM-246, March 1990
- [19] "CRC Handbook of Chemistry and Physics", 1993/1994, CRC Press, Cleveland, Ohio
- [20] "JANAF Thermochemical Tables", 3rd edition, part II (Cr-Zr), 1986
- [21] N. E. Todreas, M. S. Kazimi, "Nuclear Systems I, Thermal Hydraulic Fundamentals", Hemisphere Publishing Corporation, 1990
- [22] S. T. Yin, A. Cardella, A. H. Abdelmessih, "Assessment of a heat transfer correlations package for water-cooled plasma-facing components in fusion reactors", Proceedings of the 5th International Topical Meeting on reactor thermal-hydraulics", NURETH 5, September 21-24, vol. IV, 1992

- [23] S. T. Yin, J. W. Martin, A. J. Clark, "Measurement and analysis of single phase and subcooled nucleate boiling near divertor coolant operating conditions", AECL-2177, 1992
- [24] J. G. Collier, "Convective Boiling and Condensation", 2nd edition, McGRAW-HILL Book Company, 1981
- [25] S. T. Yin, A. H. Abdelmessih, "Prediction of incipient flow boiling from a uniformly heated surface", AIChE Symp. Series, vol. 73, No. 164, 1977
- [26] J. Schlosser, A. Cardella, P. Massmann, P. Chappuis, H. D. Falter, P. Deschamps, G. H. Deschamps, "Thermal-hydraulic tests on NET divertor targets using swirl tubes", 7th Proceedings of Nuclear Thermal Hydraulics, 1991 Winter Meeting, San Francisco CA, Nov. 10-14, 1991
- [27] M. N. Ozisik, "Heat Transfer - A Basic Approach", McGRAW-HILL Book Company, 1985
- [28] J. H. Lienhard, "A Heat Transfer Textbook", Prentice-Hall, 1981
- [29] E. J. Henley, H. Kumamoto, "Reliability Engineering and Risk Assessment", Prentice-Hall, 1981
- [30] A. E. Green, A. J. Bourne, "Reliability Technology", John Wiley & Sons Ltd., 1972
- [31] N. J. McCormick, "Reliability and Risk Analysis", Academic Press, New York, 1981
- [32] A. E. Green, "Safety Systems Reliability", John Wiley & Sons, New York, 1983
- [33] A. Soria, V. Renda, L. Papa, "Thermal analysis of a tokamak divertor plate after a sudden coolant dry-out", Fusion Engineering and Design vol. 13, 1991
- [34] C. C. Baker, M. A. Abdou, et al., "STARFIRE - A Commercial Tokamak Fusion Power Plant Study", ANL/FPP-80-1, 1980
- [35] US Nuclear Regulatory Commission, "Reactor Safety Study", WASH-1400, NUREG-75/014, October 1975
- [36] G. Apostolakis, "Data analysis in risk assessments", Nuclear Engineering and Design vol. 71, 1982



- [37] D. A. O'Brien, "Probabilistic Failure Analysis and its Application to Fusion Reactor First Wall Design", Ph.D. thesis, Rensselaer Polytechnic Institute, 1987
- [38] J. K. Vaurio, C. Mueller, "Probabilistic analysis of Liquid-Metal Fast Breeder Reactor accident consequences with response surface techniques", Nuclear Engineering and Design vol. 65, 1978
- [39] R. H. Myers, "Response Surface Methodology", Allyn and Bacon, Inc., 1971
- [40] S. Ross, "A First Course in Probability", 3rd edition, Macmillan Publishing Company, 1988
- [41] J. E. Massida, M. S. Kazimi, "Thermal Design Considerations for Passive Safety of Fusion Reactors, PFC/RR-87-18, 1987
- [42] A. Pages, M. Gondran, "System Reliability: Evaluation and Prediction in Engineering", North Oxford Academic, 1986
- [43] A. Hassanein, D. L. Smith, "Thermal Response of Substrate structural materials during a plasma disruption", Journal of Nuclear Materials, No. 191-194, 1992
- [44] E. Zolti, "Structural Lifetime of the NET / ITER divertor plates", Fusion Engineering and Design, vol. 18, 1991